BEHAVIOR OF CABLE STAYED BRIDGE: PARAMETRIC STUDY

A DISSERTATION

Submitted in partial fulfilment of the

requirements for the award of the degree

of

MASTER OF TECHNOLOGY

in

CIVIL ENGINEERING

(With Specialization in Structural Engineering)

By

JAYANSH GAUR

(17523010)

DEPARTMENT OF CIVIL ENGINEERING

INDIAN INSTITUTE OF TECHNOLOGY ROORKEE

ROORKEE – 247 667 (INDIA)

MAY, 2019

CANDIDATE'S DECLARATION

I hereby declare that work presented in this dissertation has been carried out by me in the Department of Civil Engineering at Indian Institute of Technology Roorkee under the supervision of **Dr. Akhil Upadhyay**, Professor, Department of Civil Engineering, IIT Roorkee. The matter embodied in this dissertation has not been submitted for the award of any other degree.

Date: (Jayansh Gaur)

Place: Roorkee 17523010

CERTIFICATE

This is to certify that the report entitled, **Behavior of Cable stayed bridge: Parametric study** submitted by **Jayansh Gaur**, embodies the work done by him under my supervision.

Date: (Dr. Akhil Upadhyay)

Professor,

Department of Civil Engineering,

Indian Institute of Technology Roorkee

ACKNOWLEDGEMENT

I would like to express my earnest gratitude and indebtedness to my supervisor **Dr. Akhil Upadhyay**, Professor, Department of Civil Engineering, Indian Institute of Technology, Roorkee, for his valuable suggestions, meticulous guidance, perpetual inspiration and support in completion of this dissertation submitted in partial fulfilment for the award of the degree of Master of Technology with specialization in Structural Engineering.

I would also like to thank all my seniors and batch-mates for their kindness and moral support during my study.

Last but not the least it is beyond my literary capabilities to express my gratitude to my family in absence of whom I could have never reached this position.

Jayansh Gaur

Date: 17523010

Place: Roorkee IIT Roorkee

CONTENTS

LIST OF FIGURES

LIST OF TABLES

CHAPTER 1

INTRODUCTION

1.1 General

The development of modern cable-stayed bridges has started with the completion of the Stromsund bridge in Sweden (Gimsing and Georgakis, 2012), which was opened to traffic in 1956. This may be viewed from the fact that Stromsund bridge had a main span of 183 m whereas Russky bridge in Russia (completed in the year 2012), which is currently the longest cable-stayed bridge in the world, has a main span of 1104 m.

1.2 Comparison of Cable-stayed and Suspension bridges

The fundamental difference between the two types of bridges is the manner in which the cables support the bridge deck. In suspension bridges, the deck is supported at relatively short intervals by vertical hanger cables which in turn are suspended from main cables. Main cables in these are relatively flexible and thus take a shape which is a function of position of load and magnitude of load. On the other hand, cable-stayed bridges have deck that is directly supported from the tower with the help of stay cables, thus providing a significantly stiffer structure. Also generally in cable stayed bridges the deflections are less, therefore the deck can be made lighter and more slender. This improves structurally the wind resistance and aesthetically the appearance (Troitsky, 1988).

1.3 Advantages of Cable-stayed bridges

Cable stayed bridges are structural system which are effectively composed of cables, deck and pylons. The cable stays provide intermediate supports for the girder so that it can cover a long distance.

As discussed in the previous section, because the deck in cable-stayed bridge is directly connected to the pylon with the help of cable-stays, thus they are stiffer as compared to suspension bridges. All the members are predominantly under the action of axial forces, the cables are under tension whereas the pylon and the deck is under compression, and so the members are efficiently utilised. And because of which relatively small size of bridge elements are required.

They can be constructed by free cantilevering on both sides of the pylon without the use of auxiliary piers. Thus the construction can be done speedily. And this is particularly advantageous in the case of deep rivers where placing auxiliary piers can be expensive, also in busy navigational channels. These bridges are aesthetically pleasing and are a landmark structure at the place where they are built.

1.4 Arrangement of stay cables

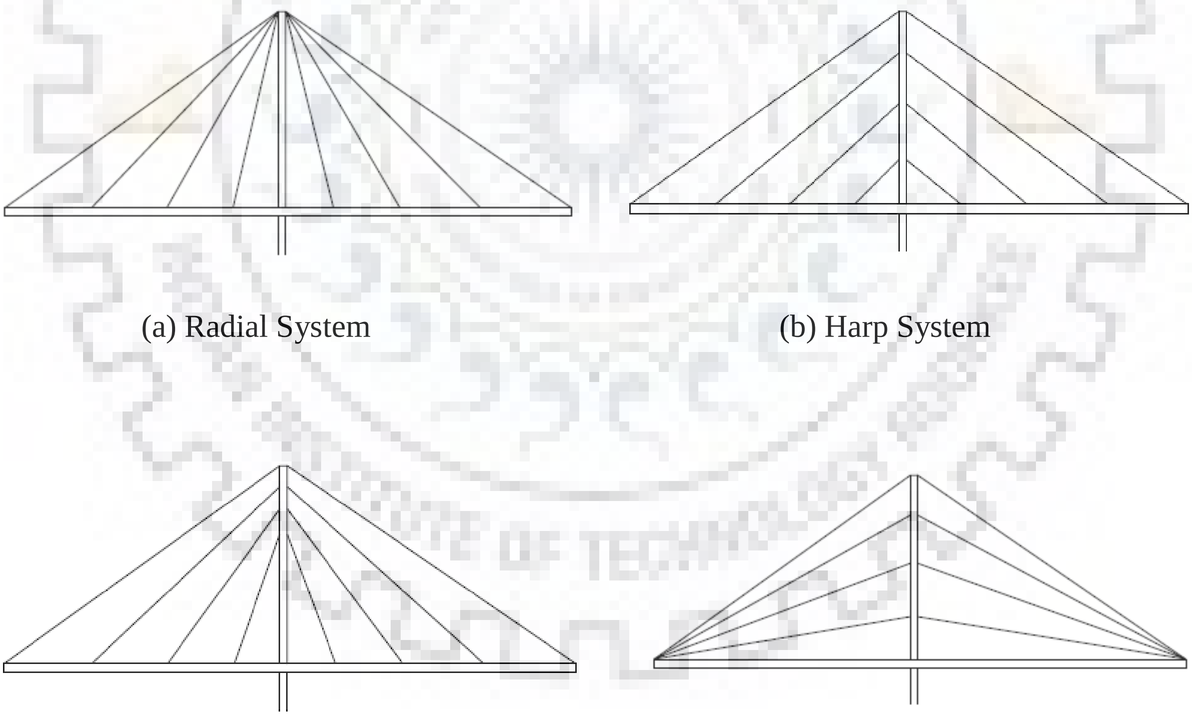

(a) Radial System (b) Harp System

(c) Fan System (d) Star System

Figure 1.1: Different arrangements of stay cables

1.4.1 Radial or Converging system- Structurally this arrangement is the best, because the inclination of the cables is maximum with the horizontal. So they carry maximum component of the load and the force in the deck is at a minimum. Because of the congestion at the top, detailing becomes complex.

1.4.2 Harp or Parallel system- It causes bending moment in the pylon. Cables are not as effective as in Radial and Fan arrangements. It is aesthetically more pleasing.

1.4.3 Fan or Intermediate system- The cable attachment points on the pylon are sufficiently spaced apart at the pylon top to avoid congestion ocuurring in radial arrangement.

1.4.4 Star system- It is aesthetically attractive but contradicts the principle that the points of attachment should be distributed along the main girder.

1.5 Spatial arrangement of the cables

In space, cables can be arranged either in one plane or in two planes. Further in two planes, the planes can be parallel to each other or may be inclined.

Joining all cables on top of the tower, in the case of two inclined cable planes, helps to prevent the dangerous torsional movement of the deck during wind oscillations.

Single plane system requires a hollow box main girder with considerable torsional rigidity in order to keep the change of cross-section deformation due to eccentric live load within allowable limits. This also requires small piers, because the size of piers is determined by the width of the main girder.

1.6 Tower types

Towers can generally take the form of-

1. Trapezoidal portal frames
2. Twin-towers
3. A-frames
4. Inverted Y-frames
5. Diamond frames
6. Single towers

1.7 Types of main girder

Main girders are generally made up of the following (Troitsky, 1988)-

1. Steel girders

2. Trusses

3. Reinforced or prestressed concrete girder

1.8 Organization of the Report

After a brief introduction, in Chapter 2 a brief review of literature related to static analysis of cable-stayed bridge is presented. Chapter 3 shows the results obtained and a detailed discussion on the results has been presented. In this chapter, firstly numerical validation has been done and then parametric studies have been carried out. The thesis has been summarised and concluded in Chapter 4.

1.9 Objective and Scope of the Study

The main objective of this study is to study the influence of various design parameters on the behaviour of cable-stayed bridge through numerical studies.

The scope of the work is:

- Numerical modelling of cable-stayed bridge and its validation, incorporating nonlinearities arising due to cable sag, beam-column, and large displacement effect.
- To study the influence of following parameters on the behaviour of cable-stayed bridge:
    - Number of cables
    - Side span to main span ratio
    - Arrangement of cables
    - Shape of pylon
    - Distribution of live load

1.10 Methodology

- To numerically validate modelling of cable with initial tension in SAP2000
- Performing parametric study of cable element with initial tension and subjected to a centrally placed load using SAP2000 software to find the percentage difference in linear and non-linear analysis, by varying the parameters, viz.,
    - angle of inclination of cable with the horizontal
    - central load on the cable
    - initial tension
    - length of cable
- Numerical validation of analysis results of cable-stayed bridges from literature
- To study the influence of following parameters on the behaviour of cable-stayed bridge of span 805 m and subjected to a uniformly distributed load of 20 kN/m distributed over the entire length of the bridge
    - Number of cables- 40, 80, 120, and 160
    - Arrangement of stay cables – Radial, Harp, and Fan
    - Side span to main span ratios- 0.3, 0.35, 0.4, 0.45, and 0.5
    - Shape of pylon- A shaped, H shaped, Diamond shaped, Inverted Y shaped, V shaped, and Portal type pylon
- To study the behaviour of the bridge under various distribution of live loads
- Finding the influence of various geometric nonlinearities involved in cable-stayed bridge, viz., Cable-sag, beam-column, and large displacement.

CHAPTER 2

LITERATURE REVIEW

2.1 Sources of Non-linearities in Cable-stayed bridges

The various sources of non-linearities involved in cable-stayed bridges which have to be considered for the analysis of cable-stayed bridges are as follows:

2.1.1 Cable sag effect-

The inclined cable stay of cable-stayed bridge is generally quite long and it is well known that a cable supported at its end and under the action of its own dead load and axial tensile force will sag into a catenary shape (Wang and Yang, 1995). In such a case, the axial stiffness of a cable will change with changing sag. When a straight cable element for a whole inclined cable stay is used in the analysis, the sag effect has to be taken into account. On the consideration of the sag non-linearity in the inclined cable stays, it is convenient to use an equivalent straight cable element with an equivalent modulus of elasticity, which can well describe the catenary action of the cable. The concept of a cable equivalent modulus of elasticity was first introduced by Ernst (1965). If the change in tension for a cable during a load increment is not large, the axial stiffness of the cable will not significantly change and the cable equivalent modulus of elasticity can be considered constant during the load increment and is given by

$$E_{eq} = \frac{E}{1 + \frac{(wH)^2 AE}{12T^3}}$$

where, E_{eq} = equivalent cable modulus of elasticity

E = effective cable material modulus of elasticity

A = cross sectional area

w = cable weight per unit length

H = horizontal projected length of the cable = L.cosα

L = inclined length of the cable

α = angle made by inclined cable with the horizontal

T = tension force in the cable

It combines both the effects of material and geometric deformation. Its value is dependent upon the weight and the tension in the cable.

When the sag effect exists and the inclined cable stay is represented by a single equivalent cable stay with one coordinate (relative axial deformation) $u_1 = \Delta L$, the stiffness matrix KE_{jk} of the cable element has the value as

$KE_{jk} = [KE] = [AE_{eq}/L]$, for $u_1 > 0$

$= [0]$, for $u_1 < 0$

where, L = cable element length

The cable stiffness vanishes and no element force exists for $u_1 < 0$, i.e., when shortening occurs.

2.1.2 Beam-column effect

Since a high pretension force exists in inclined cable stays, the towers and part of the girders are subjected to a large compression action; this means that the beam-column effect has to be taken into consideration for girders and towers of the cable-stayed bridge. In a beam-column lateral deflection and axial force are interrelated such that its bending stiffness is dependent on the element axial forces, and the presence of bending moments will affect the axial stiffness. The element bending stiffness decreases for a compressive axial force and increases for a tension force. (Wang and Yang, 1995)

2.1.3 Large displacement effect

In general, cable-stayed bridges have a larger span and less weight than that of conventional steel and reinforced concrete bridges. Large deflections may easily appear in cable-stayed bridges. Hence, the large displacement effect has to be considered in the analysis and the equilibrium equations must be set up based on the deformed position. (Wang and Yang, 1995)

Fleming (1979) discussed the various sources of non-linearity encountered in the analysis of cable-stayed bridges. He discussed the non-linear static analysis of cable-stayed bridge structures and also gave a computer program which analyses a plane cable-stayed bridge structure considering the effect of initial cable tensions, member dead weights, and distributed and concentrated live loads.

Nazmy and Abdel-Ghaffar (1990) have carried out nonlinear static analysis of three-dimensional long-span bridges under the effect of their own dead weight and a set of initial cable tensions. They considered all the sources of geometric nonlinearity.

Wang *et al.* (1993) have presented a shape finding procedure for determining the initial shape of cable-stayed bridges under the action of the dead load of girders and pretension in inclined cables. Shape iteration has been carried out by them to reduce the deflection and to smooth the bending moments in the girder.

Wang and Yang (1995) have done parametric study to find the individual influence of different sources of nonlinearity in the analysis and structural behaviour of cable stayed bridges. They first set up a finite element procedure for the nonlinear analysis of cable-stayed bridge, and then detailed parametric studies for the initial shape analysis and static deflection analysis has been carried out. The numerical results showed that in the initial shape analysis the cable sag effect is most important and the other two effects are insignificant. However, in the static deflection analysis the large deflection effect plays the key role, the beam-column effect is also significant but minor than the large deflection effect and the cable sag effect becomes the least important one.

For the analysis, they used finite element concept and the bridge is considered as an assembly of a finite number of cables, beam-column (for girder and tower) elements. The stress-strain relationship of all materials always remains within a linear elastic range during the whole nonlinear computation. Meaning thereby that only geometric nonlinearities are considered in the analysis and material behaviour is taken as linearly elastic. The cross-sectional area of the elements remains unchanged during deformation. The cable element is assumed to be perfectly flexible and possesses only tension stiffness; it is incapable of resisting compressive, shear and bending forces. For the beam element, the engineering beam theory is employed and no shear strain is considered. All cables are fixed to the tower and to the girder at their joints of attachment. They took three different types of cable stayed bridges, viz., unsymmetrical cable-stayed bridge, Symmetric harp cable-stayed bridge and Symmetric radiating cable-stayed bridge.

Agrawal, T.P. (1997) investigated the effect of number of cables and the length of central panel on the behaviour of radiating-type cable-stayed bridges. The study was carried out for double-plane bridges with 12, 20, 28, and 36 cables per plane, with side to main span ratios of 0.35, 0.40, 0.45, and 0.50, respectively. The total span considered is 360 m. The bridges were analysed by the stiffness matrix method, treating the bridges as two-dimensional structures. He has considered a uniformly distributed load of 10 kN/m over the entire length of the bridge and did linear analysis of the bridge under live load. His investigation showed that maximum cable tension decreases rapidly with the increase in the number of cables. In general, the effect of length of the central panel on the sagging moment is significant; on the hogging moment, the effect of length is not appreciable. Both the hogging and sagging moments increase with the increase in the number of cables from 12 to 36. A comparison of the weight of steel in cables and girders, as well as the total weight of steel (cables and longitudinal girders only) in the harp and radiating arrangements was also carried out. In both harp and radiating bridges, the weight of steel decreases with the increase in the number of cables.

Starossek (1996) discussed the merits and shortcomings of a modified system of cable-stayed bridge in which instead of vertical pylons, pairs of inclined pylon legs, spreading out longitudinally and connected at the top by horizontal ties (Figure 2.1), are used. Based on a comparative analysis of forces, quantities, and costs, he concluded that the alternative concept not only allows the achievement of larger maximum spans, but also can lead to an economically advantageous design- even within the span-length range of the classical cable-stayed bridge system. Other advantages are a reduced pylon height and a larger stiffness.

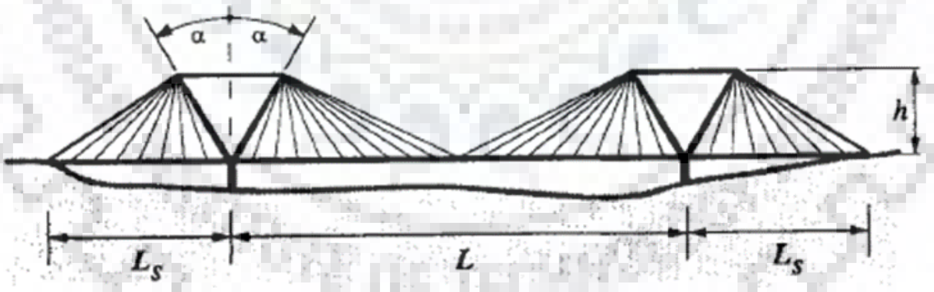

Figure 2.1: Spread pylon cable-stayed bridge (Starossek, 1996)

The horizontal force in each pair of pylon legs is balanced by horizontal ties. The system geometry entails steeper and shorter cables. The horizontal cable-force component introduced into the deck is smaller, and it changes its direction not at the pylon but within each span. Also, cable sag is reduced.

Advantages over the classical cable-stayed bridge are:

1. The compressive stresses in the deck are reduced and more equally distributed. Thus, a larger maximum span is possible.

2. The cable stiffnesses, as well as the overall system stiffness, are larger- providing advantages such as a better deformation behaviour under live loads (particularly important for railroad bridges), and an improved aeroelastic stability during and after construction.

3. The pylon height can be reduced. This may be an important feature when pylon height is limited, e.g., by environmental restrictions.

4. There are savings in cable steel.

5. Convincing visual impression conveyed by the clear and strong main lines of the system.

Disadvantages are- the more difficult construction of the inclined pylons, possibly larger pylon quantities, and additional quantities and construction difficulties related to the horizontal ties.

Wang *et al.* (2004) did analysis of cable-stayed bridge at different erection stages during construction using the cantilever method. Two computational processes have been established, viz., forward process analysis and backward process analysis.

Pedro and Reis (2010) did the nonlinear analysis of composite steel-concrete cable-stayed bridges. They considered geometrical and material nonlinear behaviour of both steel and concrete materials. They also included cable's sag and time dependent effects due to load history, creep, shrinkage and aging of concrete. They concluded that concrete time dependent effects increased deck permanent deflections reducing loads supported by the stays, the bending moments at the base of the towers are very much increased and cracking of the deck slab at mid-span cross-sections is likely to occur. Concrete time dependent effects also induce important redistribution of deck axial forces, from the concrete slab towards the steel girders, but do not affect the ultimate resistance of the deck.

CHAPTER 3

NUMERICAL STUDIES

3.1 Numerical Validation related to Cables

Some problems involving pre-tensioned cables which are available in the literature have been modelled in SAP2000 software and the results from the software are compared with the known results.

3.1.1 Cable stretched between two fixed points (Figure 3.1) (Ghali *et al.*, 2009)

Problem description: To find the vertical deflection of joint B (Δ_{BV}) under various values of force Q and plot the graph between Δ_{BV} and Q (force at joint B)

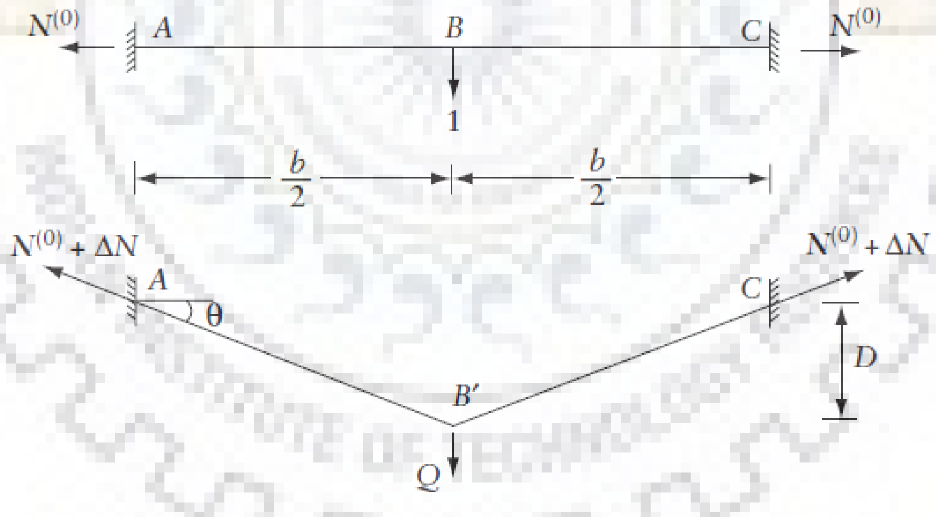

Figure 3.1: A cable stretched between two fixed points (Ghali *et al*., 2009)

Given, Area of cable (a) = 1 x 10^{-4} m^2, E = 2 x 10^8 kN/m^2, initial tension = 100 kN, initial length of cable (b) = 10 m

Application of force Q produces a displacement D and the tension in the cable becomes N.

$$N = N^{(0)} + \frac{Ea.\Delta b}{b}$$

$$\therefore N = N^{(0)} + \frac{Ea}{\frac{b}{2}}\left\{\left[\left(\frac{b}{2}\right)^2 + D^2\right]^{\frac{1}{2}} - \frac{b}{2}\right\}$$

Considering equilibrium of node B in the deflected position, $Q = 2ND\left[\left(\frac{b}{2}\right)^2 + D^2\right]^{-\frac{1}{2}}$

Table 3.1: Comparison of results from Ghali *et al.* 2009 and linear and nonlinear analysis results obtained with SAP2000

Force Q (kN)	Δ_{BV} (mm)				
	Ghali *et al.*, 2009	Linear analysis in SAP2000	Percentage difference	Nonlinear analysis in SAP2000	Percentage difference
0	0	0	0%	0	0%
4.159	100	103.98	3.98%	99.97	-0.03%
9.272	200	231.8	15.90%	199.92	-0.04%
16.287	300	407.18	35.72%	299.76	-0.08%
26.14	400	653.5	63.38%	399.58	-0.10%

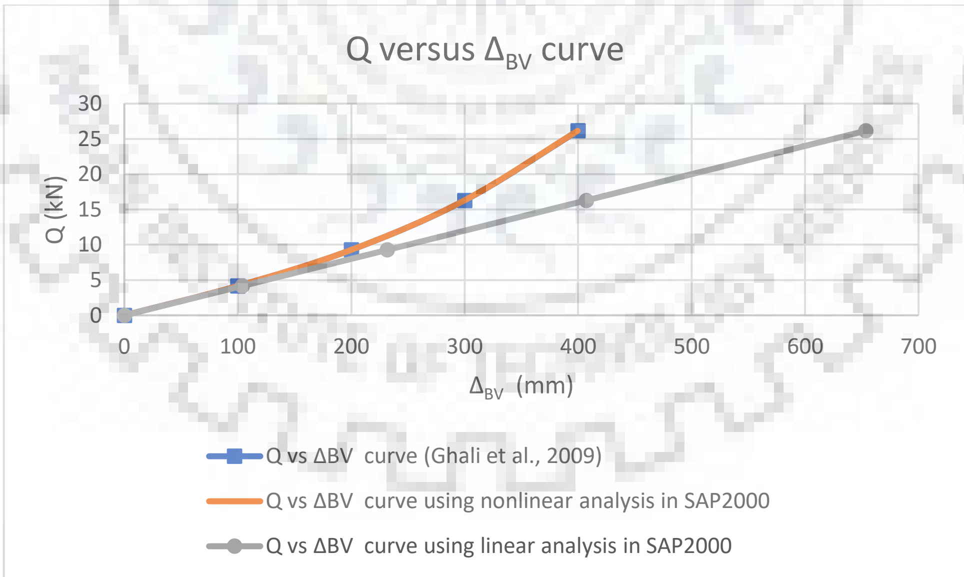

Figure 3.2: Comparison of Q vs Δ_{BV} values of linear and nonlinear analysis done using SAP2000 software with Ghali *et al.*, 2009

The results of nonlinear analysis done using the software are almost equal to the actual results. To produce the same vertical deflection, the load required increases with increase in the deflection, because the stiffness of cable increases when it is subjected to tension produced due to the load. Whereas, the linear analysis over-estimates the deflection due to load.

3.1.2 Cable subjected to multiple point loads (Figure 3.3) (Beer *et al.*, 2016)

Problem description: To find the horizontal and vertical reactions at joint A (A_H and A_V) and tension in the member 4-5 (T_{4-5}).

Given, Area of cables (a) = 0.00929 m^2, Modulus of elasticity of material of the cable (E) = 1.379 x 10^8 MPa, initial tension = 128.11 kN, l = 3.048 m, l_1 = 1.695 m, l_2 = 1.777 m, F_1 = 17.79 kN, F_2 = 26.69 kN.

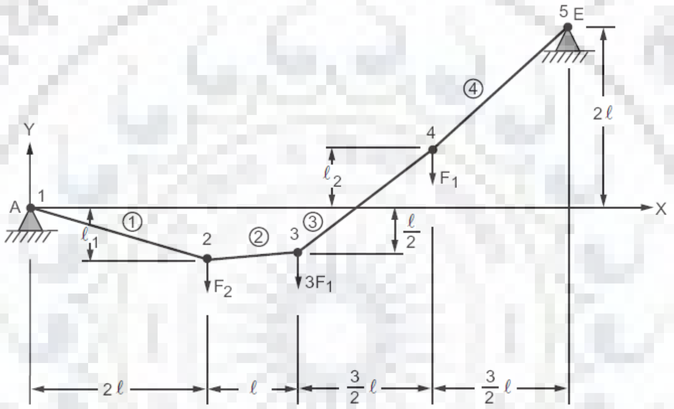

Figure 3.3: Problem model **(**Beer et al., 2016)

Table 3.2: Comparison of software results with the results of Beer *et al.*, 2016

Quantity	Beer *et al.*, 2016	SAP2000	Percentage difference
A_H	-80.068 kN	-80.046 kN	-0.03%
A_V	22.241 kN	22.246 kN	0.02%
T_{DE}	109.747 kN	110.111 kN	0.33%

3.1.3 Cable net (Figure 3.4) (SAP verification manual)

Problem description: To find the displacements for joints 1, 2, 3, and 4 in all three directions.

Given, cable cross-sectional area (a) = 1.465 cm^2, E = 82737.087 MPa, cable self-weight = 0.00146 kN/m, prestressing force in horizontal members= 24.283 kN, prestressing force in inclined members = 23.687 kN, force applied at joints 1, 2, 3, and 4 is 35.586 kN.

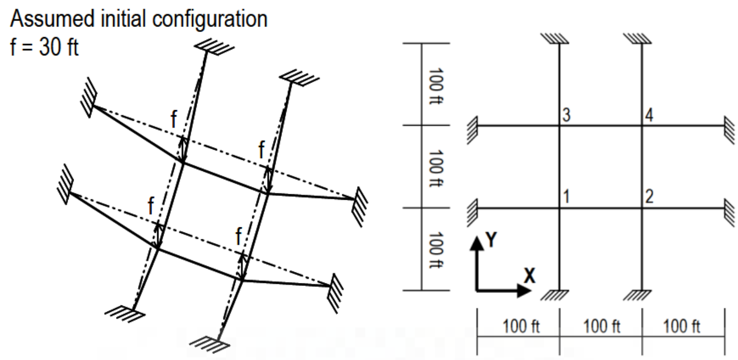

Figure 3.4: Problem from SAP verification manual

Table 3.3: Comparison of software results with the actual results

Quantity	Actual results (m)	Linear solutions in SAP2000 (m)	Percentage difference	Nonlinear solutions in SAP2000 (m)	Percentage difference
Δ_X	-0.04048	-0.07205	78%	-0.04048	0%
Δ_Y	-0.04048	-0.07205	78%	-0.04048	0%
Δ_Z	-0.45	-0.7889	75.30%	-0.44946	-0.12%

3.1.4 Cable net in the form of saddle dome (Figure 3.5) (Ghali *et al.*, 2009)

Problem description: Displacements at nodes 5,6, 7, and 11 and the forces in the segments 5-6, 6-7, 1-5, 2-6, 6-11, and 3-7.

Given, E = 2 x 10^8 kN/m^2, area of cable (a) = 5 x 10^{-4} m^2 , l = 5 m, initial tension = 300 kN.

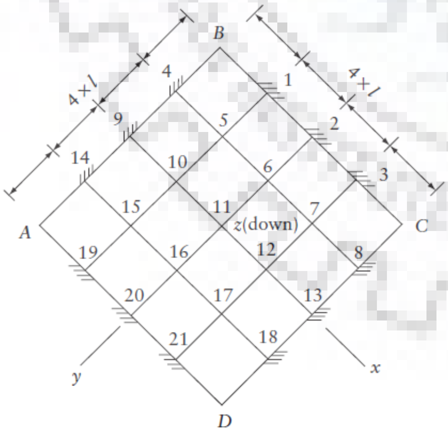

Figure 3.5: A cable net in the form of Saddle dome (Ghali et al., 2009)

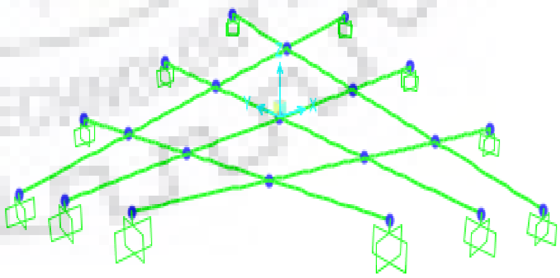

Figure 3.6: Model of the saddle dome shaped cable net in SAP2000

Table 3.4: Comparison of software results with the actual results

Quantity	Ghali *et al.*, 2009	Nonlinear analysis result from SAP2000	Percentage difference
Δ_{5X} (mm)	12.5	12.52	0.16%
Δ_{5Y} (mm)	12.5	12.52	0.16%
Δ_{5Z} (mm)	105.85	105.83	-0.02%
Δ_{6X} (mm)	16.5	16.52	0.12%
Δ_{6Y} (mm)	-0.8	-0.82	2.50%
Δ_{6Z} (mm)	134.2	134.19	-0.01%
Δ_{7X} (mm)	13.4	13.41	0.07%
Δ_{7Y} (mm)	-13.4	-13.41	0.07%
Δ_{7Z} (mm)	104.65	104.62	-0.03%
Δ_{11X} (mm)	0	0	0%
Δ_{11Y} (mm)	0	0	0%
Δ_{11Z} (mm)	173.25	173.25	0%
T_{5-6} (kN)	311	310.94	-0.02%
T_{6-7} (kN)	313	313.52	0.17%
T_{1-5} (kN)	309	308.8	-0.06%
T_{2-6} (kN)	320	320.2	0.06%
T_{6-11} (kN)	320	320.06	0.02%
T_{3-7} (kN)	316	315.82	-0.06%

3.2 Parametric study to find the significance of Cable Sag nonlinearity of stay cables

The general arrangement of the cable is shown in the figure below.

The diameter of cable (d) = 13 mm.

Cable material modulus of elasticity, E = 2 x 10^8 kN/m^2

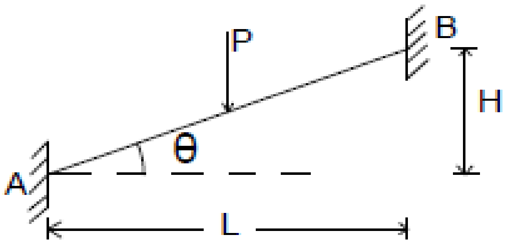

Figure 3.7: General layout of a cable on which parametric study has been performed

Here, L = horizontal projected length of the cable

H = difference of height between the two end points

θ = inclination of cable with horizontal

P = central point load applied on the cable

T = initial tension in the cable

A and B are the two end points of the cables and C is the midpoint of the cable.

For this study, 5 different horizontal projected lengths of cable have been taken, L = 30 m, 50 m, 100 m, 150 m, and 200 m. Initial tension in the cable, T = 100 kN, 150 kN, and for L=200 m T = 200 kN has been considered. Central point loads applied are, P = 5 kN, 10 kN, 15 kN, 20 kN, 25 kN, and 30 kN.

Δ_{CV} = vertical deflection at the centre of cable

In the study, the vertical deflection at the centre of the cable Δ_{CV} has been computed using both linear and nonlinear analysis using SAP2000 software for different values of central load P and for different angles of inclination of the cable with the horizontal, to find the significance of Cable sag nonlinearity of stay cables.

3.2.1 L=30 m, T=100 kN

Table 3.5: Δ_{CV} for linear and nonlinear analysis for L=30 m, T=100 kN

H (m)	θ (˚)	P = 5 kN, Δ_{CV} (m)			P = 10 kN, Δ_{CV} (m)		
		Linear analysis	Nonlinear analysis	% error in linear analysis	Linear analysis	Nonlinear analysis	% error in linear analysis
0	0	-0.375	-0.3498	7.204117	-0.75	-0.6139	22.16973

10	18.43494882	-0.3559	-0.334	6.556886	-0.7118	-0.5907	20.5011
20	33.69006753	-0.3125	-0.2971	5.18344	-0.6251	-0.5353	16.77564
30	45	-0.2662	-0.2564	3.822153	-0.5323	-0.4713	12.94292
40	53.13010235	-0.2265	-0.2204	2.767695	-0.453	-0.4125	9.818182
50	59.03624347	-0.195	-0.1911	2.040816	-0.3899	-0.3629	7.440066
60	63.43494882	-0.1702	-0.1676	1.551313	-0.3405	-0.3218	5.811063
70	66.80140949	-0.1507	-0.1491	1.073105	-0.3015	-0.2884	4.542302
H (m)	θ (˚)	P = 15 kN, Δ_{CV} (m)			P = 20 kN, Δ_{CV} (m)		
		Linear analysis	Nonlinear analysis	% error in linear analysis	Linear analysis	Nonlinear analysis	% error in linear analysis
0	0	-1.125	-0.811	38.71763	-1.5	-0.9675	55.03876
10	18.43494882	-1.0677	-0.7843	36.13413	-1.4237	-0.9385	51.69952
20	33.69006753	-0.9376	-0.7196	30.29461	-1.2502	-0.8681	44.01567
30	45	-0.7985	-0.6438	24.0292	-1.0647	-0.7847	35.68243
40	53.13010235	-0.6795	-0.572	18.79371	-0.906	-0.705	28.51064
50	59.03624347	-0.5849	-0.5099	14.70877	-0.7798	-0.635	22.80315
60	63.43494882	-0.5107	-0.4574	11.65282	-0.6809	-0.575	18.41739
70	66.80140949	-0.4522	-0.4134	9.385583	-0.603	-0.5241	15.05438
H (m)	θ (˚)	P = 25 kN, Δ_{CV} (m)			P = 30 kN, Δ_{CV} (m)		
		Linear analysis	Nonlinear analysis	% error in linear analysis	Linear analysis	Nonlinear analysis	% error in linear analysis
0	0	-1.875	-1.0978	70.79614	-2.2501	-1.21	85.95868
10	18.43494882	-1.7796	-1.0671	66.76975	-2.1355	-1.1779	81.29722
20	33.69006753	-1.5627	-0.9926	57.43502	-1.8753	-1.1	70.48182
30	45	-1.3308	-0.9038	47.24497	-1.597	-1.0073	58.54264
40	53.13010235	-1.1325	-0.8186	38.34596	-1.359	-0.9178	48.07148
50	59.03624347	-0.9748	-0.7431	31.18019	-1.1697	-0.8382	39.54903
60	63.43494882	-0.8511	-0.6782	25.49395	-1.0214	-0.7693	32.77005
70	66.80140949	-0.7537	-0.6223	21.11522	-0.9045	-0.71	27.39437

With the increase in cable inclination with the horizontal, the significance of cable sag nonlinearity decreases. With the increase in the applied load, the effect of nonlinearity is increasing.

3.2.2 L=30 m, T=150 kN

Table 3.6: Δ_{CV} for linear and nonlinear analysis for L=30 m, T=150 kN

H (m)	θ (˚)	P = 5 kN, Δ_{CV} (m)			P = 10 kN, Δ_{CV} (m)		
		Linear analysis	Nonlinear analysis	% error in linear analysis	Linear analysis	Nonlinear analysis	% error in linear analysis
0	0	-0.25	-0.2443	2.333197	-0.5	-0.4614	8.365843
10	18.43494882	-0.2373	-0.2324	2.108434	-0.4746	-0.4411	7.59465
20	33.69006753	-0.2085	-0.2052	1.608187	-0.4171	-0.3934	6.024403
30	45	-0.1778	-0.1756	1.252847	-0.3555	-0.3403	4.466647
40	53.13010235	-0.1515	-0.1502	0.865513	-0.303	-0.2935	3.236797
50	59.03624347	-0.1306	-0.1299	0.538876	-0.2613	-0.2552	2.390282
60	63.43494882	-0.1143	-0.1139	0.351185	-0.2286	-0.2247	1.735648
70	66.80140949	-0.1015	-0.1014	0.098619	-0.203	-0.2002	1.398601
H (m)	θ (˚)	P = 15 kN, Δ_{CV} (m)			P = 20 kN, Δ_{CV} (m)		
		Linear analysis	Nonlinear analysis	% error in linear analysis	Linear analysis	Nonlinear analysis	% error in linear analysis
0	0	-0.75	-0.6448	16.31514	-1	-0.7995	25.07817
10	18.43494882	-0.712	-0.6189	15.04282	-0.9493	-0.7704	23.2217
20	33.69006753	-0.6256	-0.5579	12.13479	-0.8341	-0.7005	19.07209
30	45	-0.5333	-0.4883	9.215646	-0.7111	-0.6195	14.78612
40	53.13010235	-0.4545	-0.4254	6.840621	-0.606	-0.5448	11.23348
50	59.03624347	-0.3919	-0.3726	5.179817	-0.5225	-0.481	8.627859
60	63.43494882	-0.343	-0.3299	3.9709	-0.4573	-0.4287	6.671332
70	66.80140949	-0.3045	-0.2956	3.010825	-0.406	-0.3857	5.263158
H (m)	θ (˚)	P = 25 kN, Δ_{CV} (m)			P = 30 kN, Δ_{CV} (m)		
		Linear analysis	Nonlinear analysis	% error in linear analysis	Linear analysis	Nonlinear analysis	% error in linear analysis
0	0	-1.25	-0.9323	34.07701	-1.5	-1.0484	43.07516
10	18.43494882	-1.1866	-0.9007	31.74198	-1.4239	-1.0151	40.27189
20	33.69006753	-1.0427	-0.8247	26.43385	-1.2512	-0.9345	33.88978
30	45	-0.8889	-0.7358	20.80728	-1.0666	-0.8395	27.05182
40	53.13010235	-0.7575	-0.6524	16.10975	-0.909	-0.7498	21.23233
50	59.03624347	-0.6532	-0.5804	12.54307	-0.7838	-0.6715	16.72375

60	63.43494882	-0.5716	-0.5202	9.880815	-0.6859	-0.6052	13.33443
70	66.80140949	-0.5075	-0.4708	7.795242	-0.609	-0.5502	10.68702

Here also, similar trends are observed as before. With the increase in initial tension of the cable, the significance of nonlinearity decreases.

3.2.3 L=50 m, T=100 kN

Table 3.7: Δ_{CV} for linear and nonlinear analysis for L=50 m, T=100 kN

H (m)	θ (˚)	P = 5 kN, Δ_{CV} (m)			P = 10 kN, Δ_{CV} (m)		
		Linear analysis	Nonlinear analysis	% error in linear analysis	Linear analysis	Nonlinear analysis	% error in linear analysis
0	0	-0.625	-0.5831	7.185731435	-1.2501	-1.0231	22.18746946
10	11.30993247	-0.613	-0.5731	6.962135753	-1.226	-1.0086	21.55463018
20	21.80140949	-0.5807	-0.5462	6.316367631	-1.1614	-0.969	19.85552116
30	30.96375653	-0.5367	-0.5088	5.483490566	-1.0734	-0.9129	17.58133421
40	38.65980825	-0.4893	-0.4677	4.618345093	-0.9785	-0.8494	15.19896397
50	45	-0.4436	-0.4274	3.790360318	-0.8873	-0.7856	12.94551935
60	50.19442891	-0.4023	-0.3902	3.10097386	-0.8046	-0.7254	10.91811414
70	54.46232221	-0.366	-0.3569	2.549733819	-0.7319	-0.6698	9.271424306
100	63.43494882	-0.2837	-0.2796	1.466380544	-0.5674	-0.5365	5.759552656
H (m)	θ (˚)	P = 15 kN, Δ_{CV} (m)			P = 20 kN, Δ_{CV} (m)		
		Linear analysis	Nonlinear analysis	% error in linear analysis	Linear analysis	Nonlinear analysis	% error in linear analysis
0	0	-1.8751	-1.3517	38.72160982	-2.5002	-1.6126	55.04154781
10	11.30993247	-1.839	-1.335	37.75280899	-2.452	-1.5945	53.77861399
20	21.80140949	-1.7421	-1.2891	35.1407959	-2.3228	-1.5446	50.38197592
30	30.96375653	-1.6101	-1.2237	31.57636676	-2.1468	-1.4734	45.70381431
40	38.65980825	-1.4678	-1.1491	27.73474893	-1.957	-1.3918	40.60928294
50	45	-1.3309	-1.0731	24.02385612	-1.7745	-1.3079	35.67551036
60	50.19442891	-1.2069	-0.9996	20.73829532	-1.6092	-1.2266	31.1919126
70	54.46232221	-1.0979	-0.9314	17.87631522	-1.4639	-1.1504	27.25139082
100	63.43494882	-0.8512	-0.7626	11.61814844	-1.1349	-0.9586	18.39140413

H (m)	θ (˚)	P = 25 kN, Δ_{CV} (m)			P = 30 kN, Δ_{CV} (m)		
		Linear analysis	Nonlinear analysis	% error in linear analysis	Linear analysis	Nonlinear analysis	% error in linear analysis
0	0	-3.1252	-1.8296	70.81329252	-3.7503	-2.0167	85.96222
10	11.30993247	-3.065	-1.8105	69.29025131	-3.678	-1.9967	84.20394
20	21.80140949	-2.9034	-1.7578	65.17237456	-3.4841	-1.9416	79.44479
30	30.96375653	-2.6835	-1.6825	59.49479941	-3.2202	-1.8628	72.8688
40	38.65980825	-2.4463	-1.5958	53.2961524	-2.9355	-1.7722	65.64158
50	45	-2.2182	-1.5064	47.25172597	-2.6618	-1.6789	58.54428
60	50.19442891	-2.0115	-1.4196	41.69484362	-2.4138	-1.5877	52.03124
70	54.46232221	-1.8299	-1.3379	36.77404888	-2.1958	-1.5019	46.20148
100	63.43494882	-1.4186	-1.1306	25.47320007	-1.7023	-1.2823	32.75365

3.2.4 L=50 m, T=150 kN

Table 3.8: Δ_{CV} for linear and nonlinear analysis for L=50 m, T=150 kN

H (m)	θ (˚)	P = 5 kN, Δ_{CV} (m)			P = 10 kN, Δ_{CV} (m)		
		Linear analysis	Nonlinear analysis	% error in linear analysis	Linear analysis	Nonlinear analysis	% error in linear analysis
0	0	-0.4167	-0.4072	2.333005894	-0.8334	-0.7689	8.388607101
10	11.30993247	-0.4087	-0.3997	2.251688767	-0.8174	-0.7562	8.093097064
20	21.80140949	-0.3872	-0.3796	2.002107482	-0.7744	-0.7216	7.317073171
30	30.96375653	-0.358	-0.3519	1.733447002	-0.716	-0.6733	6.341898114
40	38.65980825	-0.3265	-0.3217	1.49207336	-0.6531	-0.6197	5.389704696
50	45	-0.2963	-0.2928	1.195355191	-0.5926	-0.5673	4.459721488
60	50.19442891	-0.2689	-0.2664	0.938438438	-0.5378	-0.5187	3.68228263
70	54.46232221	-0.2449	-0.2431	0.740436035	-0.4897	-0.4754	3.007993269
100	63.43494882	-0.1905	-0.1901	0.210415571	-0.3811	-0.3746	1.735184196
H (m)	θ (˚)	P = 15 kN, Δ_{CV} (m)			P = 20 kN, Δ_{CV} (m)		
		Linear analysis	Nonlinear analysis	% error in linear analysis	Linear analysis	Nonlinear analysis	% error in linear analysis
0	0	-1.25	-1.0747	16.3115288	-1.6667	-1.3325	25.08067542
10	11.30993247	-1.226	-1.0586	15.81333837	-1.6347	-1.3146	24.34961205

20	21.80140949	-1.1617	-1.0147	14.4870405	-1.5489	-1.2645	22.4911032
30	30.96375653	-1.0741	-0.9525	12.7664042	-1.4321	-1.1937	19.97151713
40	38.65980825	-0.9796	-0.8835	10.87719298	-1.3062	-1.1136	17.29525862
50	45	-0.8889	-0.814	9.201474201	-1.1852	-1.0325	14.78934625
60	50.19442891	-0.8067	-0.7492	7.674853177	-1.0756	-0.9556	12.55755546
70	54.46232221	-0.7346	-0.69	6.463768116	-0.9794	-0.8853	10.62916525
100	63.43494882	-0.5716	-0.5501	3.908380294	-0.7621	-0.7147	6.632153351
H (m)	θ (˚)	P = 25 kN, Δ_{CV} (m)			P = 30 kN, Δ_{CV} (m)		
		Linear analysis	Nonlinear analysis	% error in linear analysis	Linear analysis	Nonlinear analysis	% error in linear analysis
0	0	-2.0834	-1.5538	34.08418072	-2.5001	-1.7474	43.07542635
10	11.30993247	-2.0434	-1.5341	33.19861808	-2.4521	-1.7266	42.01899687
20	21.80140949	-1.9361	-1.48	30.81756757	-2.3233	-1.6694	39.16976159
30	30.96375653	-1.7901	-1.4031	27.58178319	-2.1481	-1.5878	35.28781962
40	38.65980825	-1.6327	-1.3158	24.08420733	-1.9592	-1.4946	31.0852402
50	45	-1.4814	-1.2264	20.7925636	-1.7777	-1.3992	27.0511721
60	50.19442891	-1.3445	-1.1409	17.84556052	-1.6134	-1.3076	23.38635668
70	54.46232221	-1.2243	-1.0616	15.32592313	-1.4691	-1.2219	20.23078812
100	63.43494882	-0.9527	-0.8673	9.846650525	-1.1432	-1.0089	13.31152741

3.2.5 L=100 m, T=100 kN

Table 3.9: Δ_{CV} for linear and nonlinear analysis for L=100 m, T=100 kN

H (m)	θ (˚)	P = 5 kN, Δ_{CV} (m)			P = 10 kN, Δ_{CV} (m)		
		Linear analysis	Nonlinear analysis	% error in linear analysis	Linear analysis	Nonlinear analysis	% error in linear analysis
0	0	-1.2504	-1.1664	7.201646091	-2.5007	-2.0465	22.19398974
10	5.710593137	-1.2442	-1.1613	7.138551623	-2.4884	-2.0392	22.02824637
20	11.30993247	-1.2263	-1.1465	6.960313999	-2.4525	-2.0176	21.55531324
30	16.69924423	-1.198	-1.1231	6.669041047	-2.3961	-1.9832	20.81988705
40	21.80140949	-1.1616	-1.0927	6.305481834	-2.3233	-1.9382	19.86895057
50	26.56505118	-1.1194	-1.0567	5.933566764	-2.2388	-1.885	18.76923077
60	30.96375653	-1.0736	-1.0178	5.482413048	-2.1472	-1.8261	17.58392202

70	34.9920202	-1.0262	-0.9771	5.025074199	-2.0524	-1.7639	16.35580248
80	38.65980825	-0.9787	-0.9357	4.595490007	-1.9574	-1.6993	15.18860707
90	41.9872125	-0.9322	-0.8949	4.168063471	-1.8644	-1.6356	13.98875031
100	45	-0.8875	-0.8551	3.789030523	-1.7749	-1.5717	12.92867596
150	56.30993247	-0.6994	-0.6841	2.236515129	-1.3989	-1.2894	8.49232201
200	63.43494882	-0.5676	-0.5602	1.320956801	-1.1351	-1.0742	5.669335319
H (m)	θ (˚)	P = 15 kN, Δ_{CV} (m)			P = 20 kN, Δ_{CV} (m)		
		Linear analysis	Nonlinear analysis	% error in linear analysis	Linear analysis	Nonlinear analysis	% error in linear analysis
0	0	-3.7511	-2.7037	38.73950512	-5.0014	-3.2255	55.05813052
10	5.710593137	-3.7326	-2.6952	38.49065004	-4.9768	-3.2163	54.73680938
20	11.30993247	-3.6788	-2.6704	37.76213301	-4.9051	-3.1893	53.7986392
30	16.69924423	-3.5941	-2.6307	36.62143156	-4.7921	-3.1462	52.31390249
40	21.80140949	-3.4849	-2.5786	35.14697898	-4.6465	-3.0895	50.39650429
50	26.56505118	-3.3582	-2.5167	33.43664322	-4.4776	-3.0222	48.15697174
60	30.96375653	-3.2209	-2.4478	31.5834627	-4.2945	-2.9471	45.71952088
70	34.9920202	-3.0787	-2.3744	29.66223046	-4.1049	-2.867	43.1775375
80	38.65980825	-2.9361	-2.2986	27.73427304	-3.9149	-2.7839	40.62645928
90	41.9872125	-2.7966	-2.2221	25.85392197	-3.7288	-2.6999	38.10881885
100	45	-2.6624	-2.1467	24.0229189	-3.5498	-2.6162	35.68534516
150	56.30993247	-2.0983	-1.7997	16.59165416	-2.7977	-2.2307	25.41803021
200	63.43494882	-1.7027	-1.5264	11.55005241	-2.2703	-1.9184	18.34341118
H (m)	θ (˚)	P = 25 kN, Δ_{CV} (m)			P = 30 kN, Δ_{CV} (m)		
		Linear analysis	Nonlinear analysis	% error in linear analysis	Linear analysis	Nonlinear analysis	% error in linear analysis
0	0	-6.2518	-3.6595	70.83754611	-7.5022	-4.0337	85.98805067
10	5.710593137	-6.221	-3.6498	70.44769576	-7.4652	-4.0235	85.53995278
20	11.30993247	-6.1313	-3.6212	69.31680106	-7.3576	-3.9937	84.23016251
30	16.69924423	-5.9902	-3.5757	67.52523981	-7.1882	-3.9461	82.15960062
40	21.80140949	-5.8081	-3.5158	65.19995449	-6.9698	-3.8835	79.47212566
50	26.56505118	-5.597	-3.4452	62.45791246	-6.7164	-3.8091	76.32511617
60	30.96375653	-5.3681	-3.3654	59.50852796	-6.4417	-3.7259	72.8897716
70	34.9920202	-5.1311	-3.2802	56.42643741	-6.1573	-3.637	69.29612318

80	38.65980825	-4.8936	-3.192	53.30827068	-5.8723	-3.5448	65.65955766
90	41.9872125	-4.6611	-3.1025	50.23690572	-5.5933	-3.4519	62.03540079
100	45	-4.4373	-3.0134	47.25227318	-5.3247	-3.3583	58.55343477
150	56.30993247	-3.4972	-2.5996	34.52838898	-4.1966	-2.9233	43.55693908
200	63.43494882	-2.8379	-2.2623	25.44313309	-3.4054	-2.5659	32.71756499

3.2.6 L=100 m, T=150 kN

Table 3.10: Δ_{CV} for linear and nonlinear analysis for L=100 m, T=150 kN

H (m)	θ (˚)	P = 5 kN, Δ_{CV} (m)			P = 10 kN, Δ_{CV} (m)		
		Linear analysis	Nonlinear analysis	% error in linear analysis	Linear analysis	Nonlinear analysis	% error in linear analysis
0	0	-0.8334	-0.8144	2.333005894	-1.6668	-1.538	8.374512354
10	5.710593137	-0.8293	-0.8106	2.306933136	-1.6586	-1.5314	8.306125114
20	11.30993247	-0.8174	-0.7994	2.251688767	-1.6348	-1.5124	8.093097064
30	16.69924423	-0.7987	-0.7819	2.148612355	-1.5973	-1.4827	7.72914278
40	21.80140949	-0.7745	-0.7592	2.015279241	-1.549	-1.4433	7.323494769
50	26.56505118	-0.7465	-0.7328	1.869541485	-1.4929	-1.3972	6.849413112
60	30.96375653	-0.7161	-0.704	1.71875	-1.4322	-1.3467	6.348852751
70	34.9920202	-0.6846	-0.6741	1.557632399	-1.3693	-1.2932	5.884627281
80	38.65980825	-0.6531	-0.6437	1.460307597	-1.3062	-1.2396	5.372700871
90	41.9872125	-0.6223	-0.6143	1.302295295	-1.2446	-1.1865	4.896755162
100	45	-0.5926	-0.5859	1.143539853	-1.1852	-1.1348	4.441311244
150	56.30993247	-0.4681	-0.4657	0.515353232	-0.9363	-0.9118	2.686992762
200	63.43494882	-0.3811	-0.3812	-0.02623295	-0.7622	-0.7503	1.586032254
H (m)	θ (˚)	P = 15 kN, Δ_{CV} (m)			P = 20 kN, Δ_{CV} (m)		
		Linear analysis	Nonlinear analysis	% error in linear analysis	Linear analysis	Nonlinear analysis	% error in linear analysis
0	0	-2.5002	-2.1496	16.31001116	-3.3336	-2.665	25.08818011
10	5.710593137	-2.4879	-2.1413	16.1864288	-3.3173	-2.6558	24.90774908
20	11.30993247	-2.4522	-2.1173	15.8173145	-3.2696	-2.6292	24.35721893
30	16.69924423	-2.396	-2.0786	15.2698932	-3.1946	-2.5859	23.53919332
40	21.80140949	-2.3235	-2.0295	14.48632668	-3.098	-2.5291	22.49416789

50	26.56505118	-2.2394	-1.9706	13.64051558	-2.9859	-2.462	21.2794476
60	30.96375653	-2.1483	-1.9052	12.75981524	-2.8643	-2.3875	19.97068063
70	34.9920202	-2.0539	-1.8369	11.81338124	-2.7385	-2.3085	18.62681395
80	38.65980825	-1.9594	-1.7673	10.86968822	-2.6125	-2.2274	17.28921613
90	41.9872125	-1.8669	-1.6966	10.0377225	-2.4891	-2.1462	15.97707576
100	45	-1.7779	-1.6282	9.194202186	-2.3705	-2.0654	14.77195701
150	56.30993247	-1.4044	-1.3259	5.920506826	-1.8725	-1.7052	9.811165846
200	63.43494882	-1.1433	-1.1012	3.82310207	-1.5243	-1.4305	6.55714785
H (m)	θ (˚)	P = 25 kN, Δ_{CV} (m)			P = 30 kN, Δ_{CV} (m)		
		Linear analysis	Nonlinear analysis	% error in linear analysis	Linear analysis	Nonlinear analysis	% error in linear analysis
0	0	-4.167	-3.1077	34.08630177	-5.0004	-3.4949	43.07705514
10	5.710593137	-4.1466	-3.0977	33.86060626	-4.9759	-3.4843	42.80917257
20	11.30993247	-4.087	-3.0683	33.20079523	-4.9044	-3.4533	42.02067588
30	16.69924423	-3.9933	-3.0215	32.16283303	-4.792	-3.4039	40.77969388
40	21.80140949	-3.8725	-2.9601	30.823283	-4.647	-3.3389	39.17757345
50	26.56505118	-3.7323	-2.8873	29.26609635	-4.4788	-3.2617	37.31489714
60	30.96375653	-3.5804	-2.8063	27.58436375	-4.2965	-3.1758	35.28874614
70	34.9920202	-3.4232	-2.7201	25.8483144	-4.1078	-3.0842	33.18850918
80	38.65980825	-3.2656	-2.6318	24.08237708	-3.9187	-2.9895	31.08212076
90	41.9872125	-3.1114	-2.5421	22.39487038	-3.7337	-2.8938	29.02412053
100	45	-2.9631	-2.4532	20.78509702	-3.5557	-2.7988	27.04373303
150	56.30993247	-2.3407	-2.0508	14.13594695	-2.8088	-2.3643	18.80049063
200	63.43494882	-1.9054	-1.7356	9.783360221	-2.2865	-2.0189	13.25474268

3.2.7 L=150 m, T=100 kN

Table 3.11: Δ_{CV} for linear and nonlinear analysis for L=150 m, T=100 kN

H (m)	θ (˚)	P = 5 kN, Δ_{CV} (m)			P = 10 kN, Δ_{CV} (m)		
		Linear analysis	Nonlinear analysis	% error in linear analysis	Linear analysis	Nonlinear analysis	% error in linear analysis
0	0	-1.8762	-1.7501	7.205303	-3.7524	-3.0705	22.20811
30	11.30993247	-1.8401	-1.7203	6.963902	-3.6801	-3.027	21.57582

60	21.80140949	-1.7431	-1.6396	6.312515	-3.4861	-2.908	19.87964
90	30.96375653	-1.611	-1.5273	5.480259	-3.222	-2.7399	17.59553
120	38.65980825	-1.4686	-1.4043	4.578794	-2.9372	-2.5498	15.19335
150	45	-1.3317	-1.2835	3.755356	-2.6633	-2.3586	12.91868
200	53.13010235	-1.1332	-1.1044	2.607751	-2.2665	-2.065	9.757869
250	59.03624347	-0.9754	-0.9585	1.763172	-1.9507	-1.8178	7.311035
300	63.43494882	-0.8517	-0.842	1.152019	-1.7033	-1.6132	5.585172
350	66.80140949	-0.7542	-0.7505	0.493005	-1.5083	-1.4476	4.193147
H (m)	θ (˚)	P = 15 kN, Δ_{CV} (m)			P = 20 kN, Δ_{CV} (m)		
		Linear analysis	Nonlinear analysis	% error in linear analysis	Linear analysis	Nonlinear analysis	% error in linear analysis
0	0	-5.6287	-4.0563	38.76439	-7.5049	-4.8389	55.09517
30	11.30993247	-5.5202	-4.0062	37.79142	-7.3603	-4.7846	53.83313
60	21.80140949	-5.2292	-3.8686	35.17035	-6.9723	-4.635	50.42718
90	30.96375653	-4.8331	-3.6726	31.59887	-6.4441	-4.4215	45.74466
120	38.65980825	-4.4058	-3.4489	27.74508	-5.8744	-4.1768	40.64355
150	45	-3.995	-3.2211	24.02595	-5.3267	-3.9254	35.69827
200	53.13010235	-3.3997	-2.8627	18.75851	-4.533	-3.5279	28.49004
250	59.03624347	-2.9261	-2.5528	14.62316	-3.9015	-3.1787	22.73886
300	63.43494882	-2.555	-2.2916	11.49415	-3.4066	-2.8796	18.30115
350	66.80140949	-2.2625	-2.0729	9.146606	-3.0167	-2.6263	14.86502
H (m)	θ (˚)	P = 25 kN, Δ_{CV} (m)			P = 30 kN, Δ_{CV} (m)		
		Linear analysis	Nonlinear analysis	% error in linear analysis	Linear analysis	Nonlinear analysis	% error in linear analysis
0	0	-9.3811	-5.4899	70.87925	-11.257	-6.0511	86.03725
30	11.30993247	-9.2003	-5.4325	69.35665	-11.040	-5.9912	84.27694
60	21.80140949	-8.7154	-5.2744	65.23965	-10.458	-5.826	79.51253
90	30.96375653	-8.0551	-5.049	59.53852	-9.6661	-5.5897	72.92699
120	38.65980825	-7.343	-4.7888	53.33695	-8.8116	-5.318	65.69387
150	45	-6.6583	-4.5211	47.27168	-7.99	-5.0384	58.58209
200	53.13010235	-5.6662	-4.0959	38.33834	-6.7994	-4.5918	48.07701
250	59.03624347	-4.8768	-3.7191	31.1285	-5.8522	-4.1947	39.51415
300	63.43494882	-4.2583	-3.3956	25.40641	-5.11	-3.851	32.69281

350	66.80140949	-3.7709	-3.1176	20.95522	-4.525	-3.5557	27.26046

3.2.8 L=150 m, T=150 kN

Table 3.12: Δ_{CV} for linear and nonlinear analysis for L=150 m, T=150 kN

H (m)	θ (˚)	P = 5 kN, Δ_{CV} (m)			P = 10 kN, Δ_{CV} (m)		
		Linear analysis	Nonlinear analysis	% error in linear analysis	Linear analysis	Nonlinear analysis	% error in linear analysis
0	0	-1.2502	-1.2217	2.332815	-2.5005	-2.3071	8.382818
30	11.30993247	-1.2262	-1.1993	2.242975	-2.4525	-2.2688	8.096791
60	21.80140949	-1.1619	-1.139	2.010536	-2.3237	-2.1653	7.315384
90	30.96375653	-1.0742	-1.0563	1.694594	-2.1485	-2.0203	6.345592
120	38.65980825	-0.9798	-0.9658	1.449575	-1.9596	-1.8598	5.366168
150	45	-0.889	-0.8792	1.11465	-1.778	-1.7028	4.416256
200	53.13010235	-0.7576	-0.7529	0.624253	-1.5153	-1.4695	3.116706
250	59.03624347	-0.6533	-0.6521	0.184021	-1.3066	-1.2786	2.189895
300	63.43494882	-0.5717	-0.5732	-0.26169	-1.1434	-1.1269	1.464194
350	66.80140949	-0.5076	-0.5115	-0.76246	-1.0151	-1.0059	0.914604
H (m)	θ (˚)	P = 15 kN, Δ_{CV} (m)			P = 20 kN, Δ_{CV} (m)		
		Linear analysis	Nonlinear analysis	% error in linear analysis	Linear analysis	Nonlinear analysis	% error in linear analysis
0	0	-3.7507	-3.2246	16.3152	-5.001	-3.9978	25.0938
30	11.30993247	-3.6787	-3.1762	15.82079	-4.905	-3.9441	24.36297
60	21.80140949	-3.4856	-3.0446	14.48466	-4.6475	-3.794	22.49605
90	30.96375653	-3.2227	-2.8581	12.75673	-4.297	-3.5816	19.97431
120	38.65980825	-2.9394	-2.6513	10.86637	-3.9191	-3.3416	17.28214
150	45	-2.6671	-2.4429	9.177617	-3.5561	-3.0986	14.76473
200	53.13010235	-2.2729	-2.1287	6.774087	-3.0305	-2.7259	11.17429
250	59.03624347	-1.9598	-1.8656	5.049314	-2.6131	-2.4079	8.521949
300	63.43494882	-1.7151	-1.6534	3.731704	-2.2868	-2.1473	6.496531
350	66.80140949	-1.5227	-1.4829	2.68393	-2.0302	-1.9332	5.017587

H (m)	θ (˚)	P = 25 kN, Δ_{CV} (m)			P = 30 kN, Δ_{CV} (m)		
		Linear analysis	Nonlinear analysis	% error in linear analysis	Linear analysis	Nonlinear analysis	% error in linear analysis
0	0	-6.2512	-4.6618	34.09413	-7.5015	-5.2426	43.0874
30	11.30993247	-6.1312	-4.6027	33.20877	-7.3574	-5.1803	42.02652
60	21.80140949	-5.8093	-4.4405	30.82536	-6.9712	-5.0086	39.1846
90	30.96375653	-5.3712	-4.2099	27.58498	-6.4455	-4.7641	35.29313
120	38.65980825	-4.8989	-3.9482	24.07933	-5.8787	-4.4847	31.08346
150	45	-4.4451	-3.6804	20.77763	-5.3341	-4.1989	27.03565
200	53.13010235	-3.7882	-3.2641	16.05649	-4.5458	-3.7507	21.19871
250	59.03624347	-3.2664	-2.9045	12.45998	-3.9197	-3.3601	16.65427
300	63.43494882	-2.8584	-2.605	9.727447	-3.4301	-3.0299	13.20836
350	66.80140949	-2.5378	-2.3589	7.584043	-3.0453	-2.7562	10.48908

3.2.9 L=200 m, T=100 kN

Table 3.13- Δ_{CV} for linear and nonlinear analysis for L=200 m, T=100 kN

H (m)	θ (˚)	P = 5 kN, Δ_{CV} (m)			P = 10 kN, Δ_{CV} (m)		
		Linear analysis	Nonlinear analysis	% error in linear analysis	Linear analysis	Nonlinear analysis	% error in linear analysis
0	0	-2.5029	-2.3344	7.218129	-5.0058	-4.0952	22.23579
50	14.03624347	-2.4287	-2.2733	6.835877	-4.8575	-4.0059	21.25864
100	26.56505118	-2.2408	-2.1151	5.942981	-4.4815	-3.7724	18.79705
150	36.86989765	-2.0065	-1.9148	4.789012	-4.0131	-3.4652	15.8115
200	45	-1.7765	-1.7125	3.737226	-3.5529	-3.1464	12.91953
250	51.34019175	-1.5727	-1.5297	2.811009	-3.1454	-2.8487	10.41528
300	56.30993247	-1.4001	-1.3715	2.085308	-2.8001	-2.5826	8.421746
350	60.2551187	-1.256	-1.238	1.453958	-2.5121	-2.3529	6.766118
H (m)	θ (˚)	P = 15 kN, Δ_{CV} (m)			P = 20 kN, Δ_{CV} (m)		
		Linear analysis	Nonlinear analysis	% error in linear analysis	Linear analysis	Nonlinear analysis	% error in linear analysis
0	0	-7.5087	-5.4096	38.80324	-10.0116	-6.453	55.14644
50	14.03624347	-7.2862	-5.3067	37.3019	-9.715	-6.3413	53.20202

100	26.56505118	-6.7223	-5.0358	33.49021	-8.963	-6.0468	48.22716
150	36.86989765	-6.0196	-4.6762	28.72845	-8.0262	-5.6541	41.95363
200	45	-5.3294	-4.2965	24.0405	-7.1058	-5.2356	35.72083
250	51.34019175	-4.7181	-3.9329	19.96491	-6.2908	-4.8331	30.16077
300	56.30993247	-4.2002	-3.6037	16.55243	-5.6003	-4.4658	25.40418
350	60.2551187	-3.7681	-3.313	13.73679	-5.0242	-4.135	21.50423
H (m)	θ (˚)	P = 25 kN, Δ_{CV} (m)			P = 30 kN, Δ_{CV} (m)		
		Linear analysis	Nonlinear analysis	% error in linear analysis	Linear analysis	Nonlinear analysis	% error in linear analysis
0	0	-12.515	-7.321	70.93976	-15.017	-8.0693	86.10536
50	14.03624347	-12.144	-7.203	68.59225	-14.572	-7.946	83.3929
100	26.56505118	-11.204	-6.8928	62.54352	-13.445	-7.6204	76.42906
150	36.86989765	-10.033	-6.4754	54.9356	-12.039	-7.1849	67.56392
200	45	-8.8823	-6.0298	47.30671	-10.659	-6.7196	58.62105
250	51.34019175	-7.8635	-5.5996	40.42967	-9.4362	-6.2678	50.55043
300	56.30993247	-7.0003	-5.2035	34.5306	-8.4004	-5.851	43.57204
350	60.2551187	-6.2802	-4.847	29.56881	-7.5363	-5.4746	37.65937

3.2.10 L=200 m, T=150 kN

Table 3.14: Δ_{CV} for linear and nonlinear analysis for L=200 m, T=150 kN

H (m)	θ (˚)	P = 5 kN, Δ_{CV} (m)			P = 10 kN, Δ_{CV} (m)		
		Linear analysis	Nonlinear analysis	% error in linear analysis	Linear analysis	Nonlinear analysis	% error in linear analysis
0	0	-1.6672	-1.6292	2.332433096	-3.3345	-3.0766	8.382630176
50	14.03624347	-1.618	-1.5832	2.198079838	-3.2361	-2.9989	7.909566841
100	26.56505118	-1.4933	-1.4661	1.85526226	-2.9866	-2.7953	6.84363038
150	36.86989765	-1.338	-1.3191	1.432795088	-2.676	-2.5339	5.607956115
200	45	-1.1855	-1.1729	1.07426038	-2.3711	-2.2711	4.403152657
250	51.34019175	-1.0507	-1.0436	0.680337294	-2.1013	-2.0332	3.349399961
300	56.30993247	-0.9365	-0.9338	0.289141144	-1.873	-1.8262	2.5626985
350	60.2551187	-0.8414	-0.8422	-0.09498931	-1.6828	-1.6514	1.90141698

H (m)	θ (˚)	P = 15 kN, Δ_{CV} (m)			P = 20 kN, Δ_{CV} (m)		
		Linear analysis	Nonlinear analysis	% error in linear analysis	Linear analysis	Nonlinear analysis	% error in linear analysis
0	0	-5.0017	-4.2999	16.3213098	-6.669	-5.3308	25.10317401
50	14.03624347	-4.8541	-4.1993	15.59307504	-6.4721	-5.2197	23.99371611
100	26.56505118	-4.48	-3.9422	13.64212876	-5.9733	-4.9249	21.28774188
150	36.86989765	-4.014	-3.6061	11.31138904	-5.352	-4.5375	17.95041322
200	45	-3.5566	-3.2581	9.161781406	-4.7422	-4.1324	14.75655793
250	51.34019175	-3.152	-2.9382	7.276563883	-4.2026	-3.7525	11.99467022
300	56.30993247	-2.8095	-2.6545	5.839141081	-3.746	-3.4132	9.750380874
350	60.2551187	-2.5242	-2.4127	4.621378539	-3.3656	-3.1201	7.868337553
H (m)	θ (˚)	P = 25 kN, Δ_{CV} (m)			P = 30 kN, Δ_{CV} (m)		
		Linear analysis	Nonlinear analysis	% error in linear analysis	Linear analysis	Nonlinear analysis	% error in linear analysis
0	0	-8.3362	-6.2162	34.10443679	-10.003	-6.9906	43.09787429
50	14.03624347	-8.0901	-6.0948	32.73774365	-9.7082	-6.8623	41.4715183
100	26.56505118	-7.4666	-5.7756	29.27834338	-8.9599	-6.5245	37.32699824
150	36.86989765	-6.69	-5.3545	24.94163787	-8.028	-6.0755	32.13727265
200	45	-5.9277	-4.9081	20.77382286	-7.1132	-5.5994	27.03503947
250	51.34019175	-5.2533	-4.485	17.13043478	-6.3039	-5.1454	22.51525635
300	56.30993247	-4.6825	-4.1045	14.08210501	-5.619	-4.7316	18.75475526
350	60.2551187	-4.2071	-3.7694	11.61192763	-5.0485	-4.3637	15.69310448

3.2.11 L=200 m, T=200 kN

Table 3.15: Δ_{CV} for linear and nonlinear analysis for L=200 m, T=200 kN

H (m)	θ (˚)	P = 10 kN, Δ_{CV} (m)			P = 20 kN, Δ_{CV} (m)		
		Linear analysis	Nonlinear analysis	% error in linear analysis	Linear analysis	Nonlinear analysis	% error in linear analysis
0	0	-2.5004	-2.4076	3.854460874	-5.0007	-4.4252	13.00506192
50	14.03624347	-2.4268	-2.3418	3.629686566	-4.8537	-4.3197	12.36196958
100	26.56505118	-2.2406	-2.174	3.063477461	-4.4811	-4.0461	10.75109365
150	36.86989765	-2.0087	-1.9608	2.442880457	-4.0174	-3.6897	8.881480879
200	45	-1.7812	-1.7487	1.858523475	-3.5625	-3.3271	7.075230681

250	51.34019175	-1.5802	-1.5591	1.353344878	-3.1604	-2.9917	5.638934385
300	56.30993247	-1.4103	-1.3969	0.959266948	-2.8206	-2.701	4.427989633
350	60.2551187	-1.2689	-1.2621	0.538784565	-2.5379	-2.453	3.46106808
H (m)	θ (˚)	P = 30 kN, Δ_{CV} (m)			P = 40 kN, Δ_{CV} (m)		
		Linear analysis	Nonlinear analysis	% error in linear analysis	Linear analysis	Nonlinear analysis	% error in linear analysis
0	0	-7.5011	-6.0428	24.13285232	-10.002	-7.3628	35.83826805
50	14.03624347	-7.2805	-5.9149	23.0874571	-9.7074	-7.2219	34.41615087
100	26.56505118	-6.7217	-5.5804	20.45193893	-8.9623	-6.8516	30.80594314
150	36.86989765	-6.0261	-5.1412	17.21193496	-8.0348	-6.3609	26.3154585
200	45	-5.3437	-4.684	14.08411614	-7.125	-5.8441	21.91783166
250	51.34019175	-4.7406	-4.255	11.41245593	-6.3208	-5.352	18.10164425
300	56.30993247	-4.2309	-3.8714	9.286046391	-5.6411	-4.9076	14.94620588
350	60.2551187	-3.8068	-3.5415	7.491176055	-5.0757	-4.5173	12.3613663
H (m)	θ (˚)	P = 50 kN, Δ_{CV} (m)			P = 60 kN, Δ_{CV} (m)		
		Linear analysis	Nonlinear analysis	% error in linear analysis	Linear analysis	Nonlinear analysis	% error in linear analysis
0	0	-12.502	-8.4785	47.45296928	-15.002	-9.4467	58.80889623
50	14.03624347	-12.134	-8.3283	45.69840183	-14.561	-9.2892	56.75300349
100	26.56505118	-11.203	-7.9327	41.22429942	-13.443	-8.874	51.4919991
150	36.86989765	-10.044	-7.4063	35.60752332	-12.052	-8.3208	44.84424575
200	45	-8.9062	-6.8477	30.06118843	-10.688	-7.7318	38.22783828
250	51.34019175	-7.9011	-6.3132	25.15206235	-9.4813	-7.1657	32.31505645
300	56.30993247	-7.0514	-5.8275	21.002145	-8.4617	-6.6478	27.28571858
350	60.2551187	-6.3447	-5.395	17.60333642	-7.6136	-6.1863	23.07194931

3.2.12 Effect of Angle of inclination of cable with horizontal (θ) on nonlinearity

From figure 3.8, it can be concluded that as the angle of inclination of cable with the horizontal increases, the effect of nonlinearity decreases. This is because a cable stretched horizontally will have the maximum sag and a cable held vertically will have no sag. Thus, the effect of cable sag decreases with the increase in angle from the horizontal.

Similar trends have been observed for applied loads of 5, 10, 20, 25, and 30 kN.

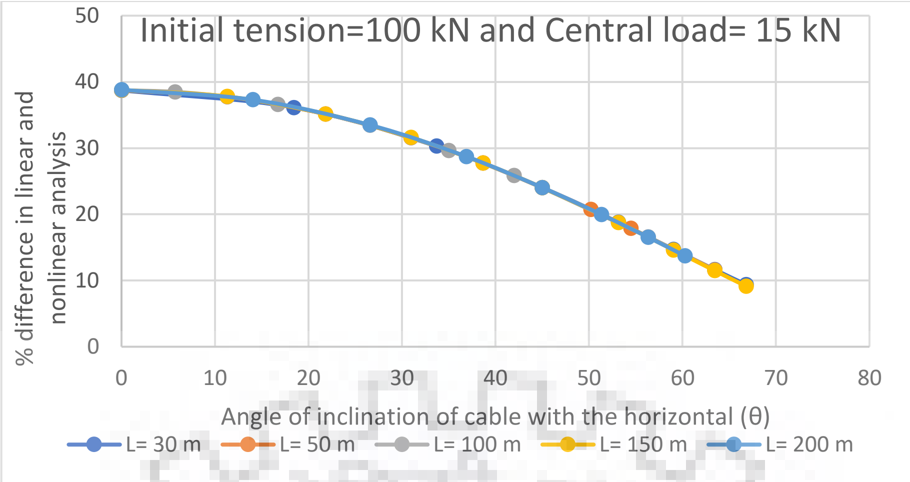

Figure 3.8: Effect of angle of inclination of cable with horizontal (θ) on nonlinearity for Initial tension of 100 kN and for applied load of 15 kN

3.2.13 Effect of Initial Tension on Nonlinearity

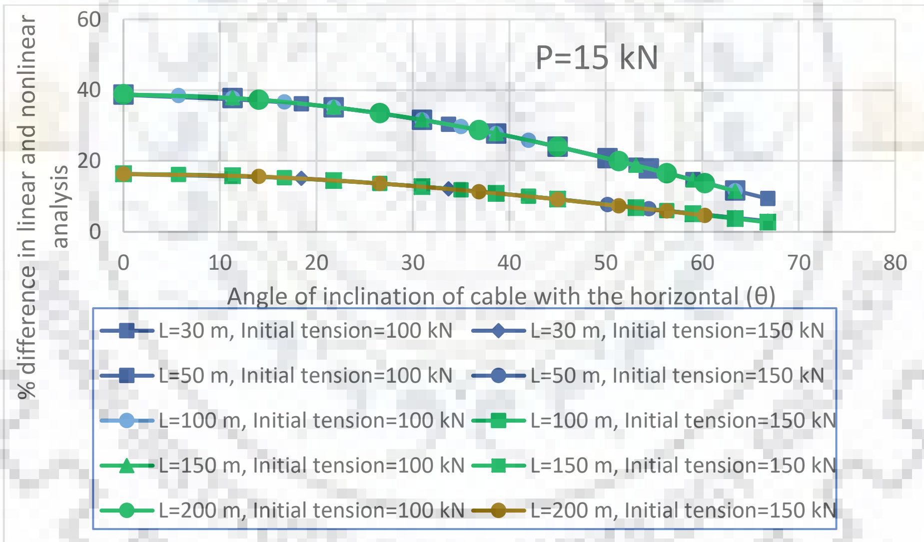

Figure 3.9: Effect of Initial Tension of cable on nonlinearity for an applied load of 15 kN

The upper set of curves in figure 3.9 correspond to an initial tension of 100 kN, and the lower set of curves correspond to an initial tension of 150 kN. It can be concluded that with the increase in initial tension from 100 to 150 kN (increase of 50 %), the effect of nonlinearity decreases by about 50 %. This is because with the increase in initial tension, the cable becomes tauter, and the cable sag reduces. Thus, the effect of Cable sag nonlinearity is decreasing.

3.2.14 Effect of Applied load on Nonlinearity

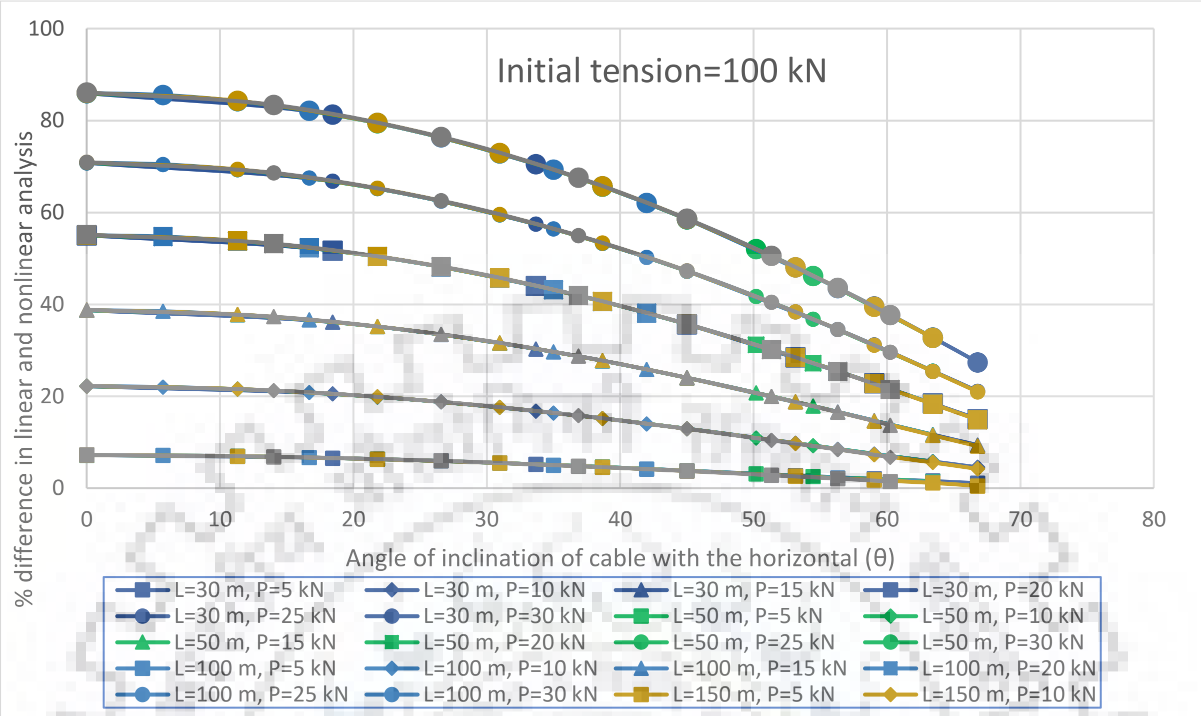

Figure 3.10: Effect of applied load on nonlinearity for an initial tension of 100 kN

From figure 3.10, it can be concluded that with the increase in the applied load, the effect of nonlinearity increases.

3.3 Numerical Validation of Cable-stayed bridge

3.3.1 Cantilever beam supported by pre-stressed cable (Kim *et al.*, 2017)

Table 3.16: Properties of the structure

	Beam	Cable
Elastic Modulus (kN/m^2)	2.1x10^8	2.1x10^8
Section area (m^2)	2	0.03
Moment of Inertia (m^4)	0.04167	-
Weight per unit volume	77	77

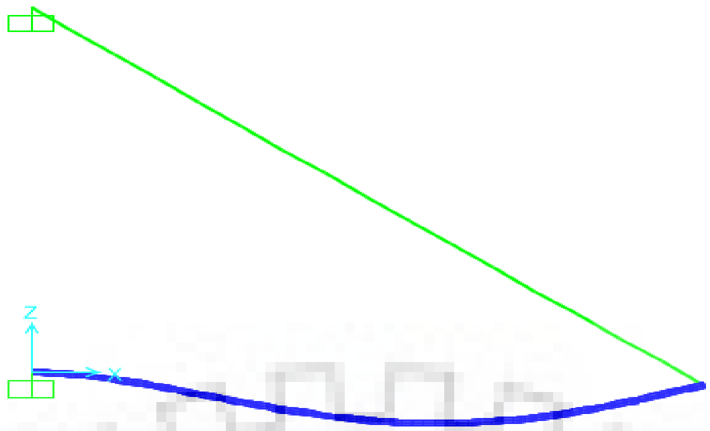

Figure 3.11: Deflected shape of the cantilever beam subjected to a UDL of 98.1 kN/m applied on the beam in SAP2000

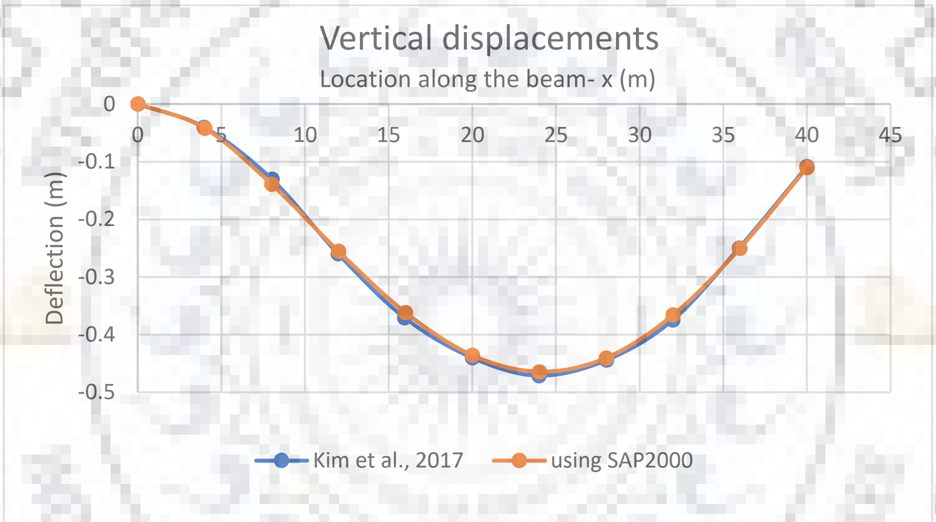

Figure 3.12: Comparison of vertical displacements along the beam

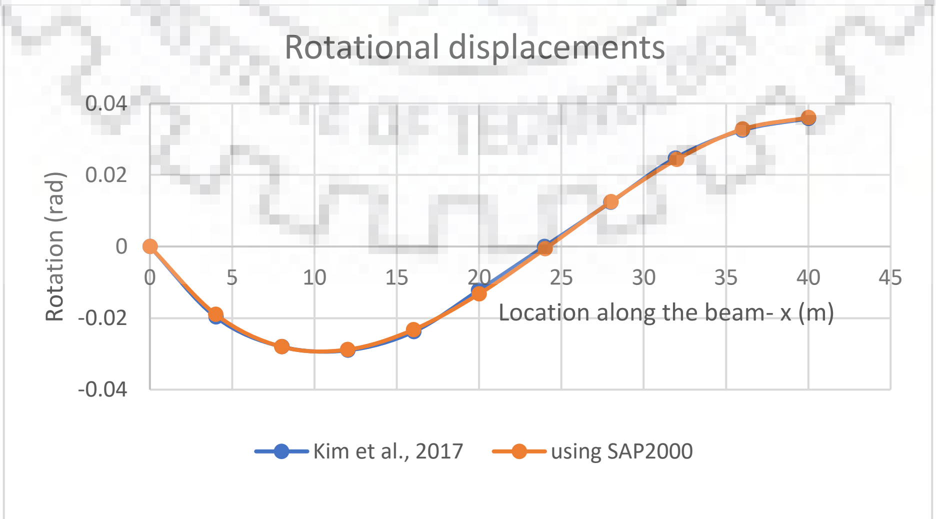

Figure 3.13: Comparison of rotational displacements along the beam

Figure 3.12 and 3.13 show that the results are almost same as obtained by Kim *et al.*, 2017.

3.3.2 Radiating type cable-stayed bridge (Agrawal, 1997)

Total length of bridge = 360 m

Live load of 10 kN/m over entire length of the bridge has been considered.

Height of pylon = 36 m

Table 3.17: Properties of the bridge

	Area of section (m^2)	Moment of Inertia of section (m^4)	Modulus of Elasticity (kN/m^2)
Girder	0.3	0.5	2×10^8
Tower	0.3	0.2	2×10^8
Total area of all cables	0.24	-	2.668×10^8

Maximum Cable Tension, Maximum Sagging moment, and Maximum Hogging moment values for side span to main span ratios of 0.35, 0.40, 0.45, and 0.50, and for 12, 20, 28, and 36 number of cables have been compared with Agrawal, 1997.

The values of maximum cable tension lies within 6% from those in the paper.

The values of sagging and hogging moments lie within 10% of the values reported in the paper.

Table 3.18: Maximum Cable Tension comparison for side to main span ratios of 0.35 and 0.4

Maximum Cable Tension (kN)						
Number of Cables	Side span to main span ratio = 0.35			Side span to main span ratio = 0.40		
	Agrawal,1997	SAP2000	Percentage difference	Agrawal, 1997	SAP2000	Percentage difference
12	820	841.26	2.592683	625	645.5	3.28
20	587.5	608.17	3.518298	443.75	463.9	4.540845
28	462.5	475.087	2.721514	343.75	361.65	5.207273
36	375	388.995	3.732	287.5	296.07	2.98087

Table 3.19: Maximum Cable Tension comparison for side to main span ratios of 0.45 and 0.5

Maximum Cable Tension (kN)						
Number of Cables	Side span to main span ratio = 0.45			Side span to main span ratio = 0.50		
	Agrawal,1997	SAP2000	Percentage difference	Agrawal, 1997	SAP2000	Percentage difference
12	578.57	580.175	0.277408	517.86	528.34	2.023713
20	371.43	368.42	0.810381	328.57	334.96	1.944791
28	264.29	269.46	1.956184	242.86	244.72	0.765873
36	214.29	216.26	0.919315	200	195.23	2.385

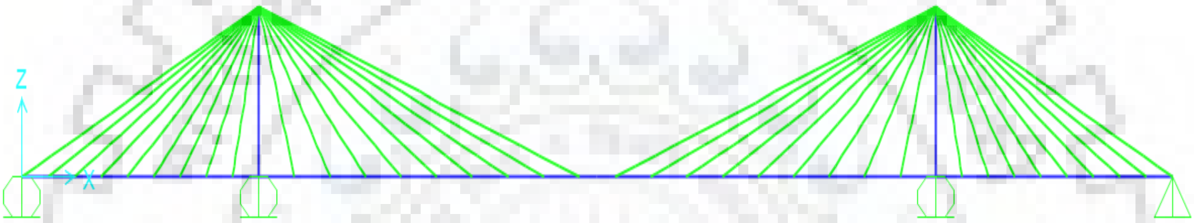

Figure 3.14: Model of the bridge for side span to main span ratio of 0.35 and number of cables – 36

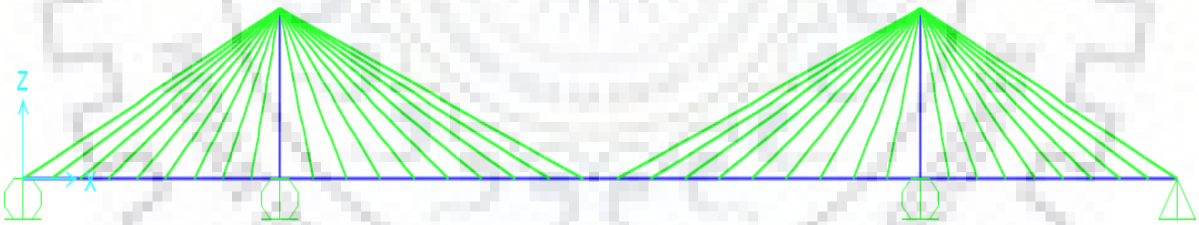

Figure 3.15: Model of the bridge for side span to main span ratio of 0.40 and number of cables – 36

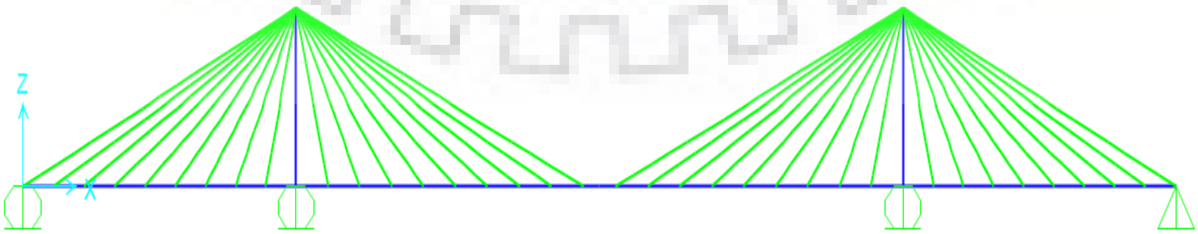

Figure 3.16: Model of the bridge for side span to main span ratio of 0.45 and number of cables – 36

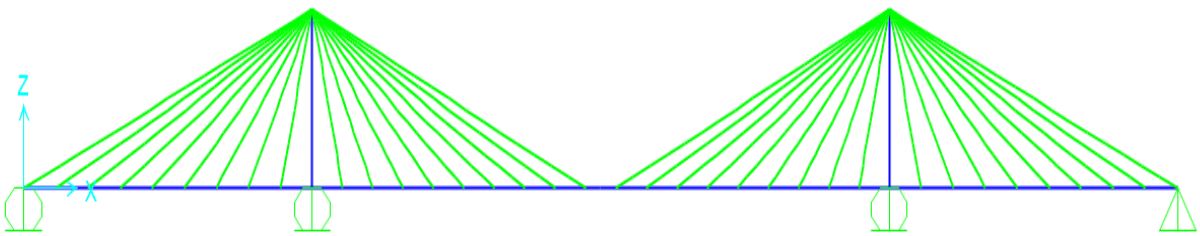

Figure 3.17: Model of the bridge for side span to main span ratio of 0.50 and number of cables – 36

Table 3.20: Maximum Sagging Moment comparison for side to main span ratios of 0.35 and 0.40

Maximum Sagging Moment (kNm)						
Number of Cables	Side span to main span ratio = 0.35			Side span to main span ratio = 0.40		
	Agrawal,1997	SAP2000	Percentage difference	Agrawal, 1997	SAP2000	Percentage difference
12	3266.67	3550.57	8.690807	2857.14	3136.274	9.769693
20	3533.33	3809.999	7.830251	3066.67	3349.433	9.220519
28	3700	3952.743	6.830878	3200	3468.265	8.383275
36	3730	4040.491	8.324147	3266.67	3542.265	8.436573

Table 3.21: Maximum Sagging Moment comparison for side to main span ratios of 0.45 and 0.50

Maximum Sagging Moment (kNm)						
Number of Cables	Side span to main span ratio = 0.45			Side span to main span ratio = 0.50		
	Agrawal,1997	SAP2000	Percentage difference	Agrawal, 1997	SAP2000	Percentage difference
12	2515.83	2751.5	9.367481	2214.29	2389.523	7.913715
20	2678.57	2915.952	8.86227	2285.71	2503.211	9.515682
28	2785.71	3010.242	8.060128	2342.86	2572.144	9.786517
36	2821.43	3069.438	8.790156	2428.57	2616.105	7.722026

Table 3.22: Maximum Hogging Moment comparison for side to main span ratios of 0.35 and 0.40

Maximum Hogging Moment (kNm)						
Number of Cables	Side span to main span ratio = 0.35			Side span to main span ratio = 0.40		
	Agrawal,1997	SAP2000	Percentage difference	Agrawal, 1997	SAP2000	Percentage difference
12	2142.86	2282.787	6.529937	2033.33	2220.755	9.217648
20	2321.43	2474.716	6.603094	2134.33	2324.396	8.905179
28	2535.71	2668.525	5.237799	2183.43	2373.647	8.711857
36	2714.29	2886.414	6.341386	2203.71	2368.627	7.483612

Table 3.23: Maximum Sagging Moment comparison for side to main span ratios of 0.45 and 0.50

Maximum Hogging Moment (kNm)						
Number of Cables	Side span to main span ratio = 0.45			Side span to main span ratio = 0.50		
	Agrawal,1997	SAP2000	Percentage difference	Agrawal, 1997	SAP2000	Percentage difference
12	2071.43	2258.645	9.037935	2142.86	2330.373	8.750572
20	2157.14	2354.902	9.167764	2157.14	2359.981	9.403256
28	2212.86	2422.04	9.452939	2178.57	2391.549	9.776087
36	2237.14	2429.99	8.620386	2214.29	2431.649	9.816171

3.3.3 Cable Tension Optimisation of Unsymmetrical cable-stayed bridge (Wang *et al.*, 1993)

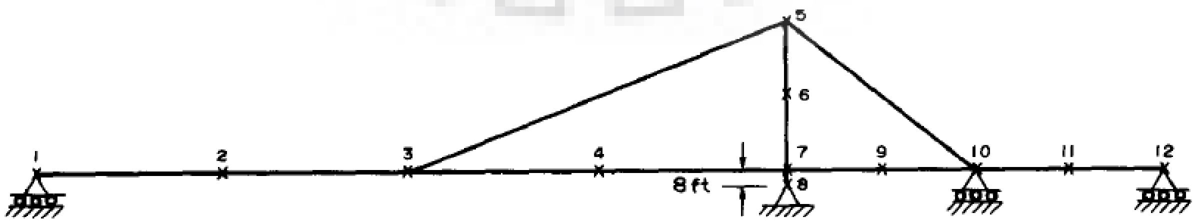

Figure 3.18: Unsymmetrical cable-stayed bridge (Wang *et al.*, 1993)

Distance between points 1-2 = 2-3 = 3-4 = 4-7 = 30.48 m

Distance between points 7-9 = 9-10 = 10-11 = 11-12 = 15.24 m

Modulus of Elasticity, E = 1.915 x 10^8 kN/m^2

Girder: I = 0.3884 m^4; A = 0.743 m^2

Tower above girder: I = 0.1726 m^4; A = 0.2787 m^2; height = 24.384 m

Tower below girder: I = 1.726 m^4; A = 0.929 m^2; height = 2.4384 m

Cable: A = 0.1022 m^2

Dead Load: Girder = 233.5 kN/m

Cable = 4.378 kN/m

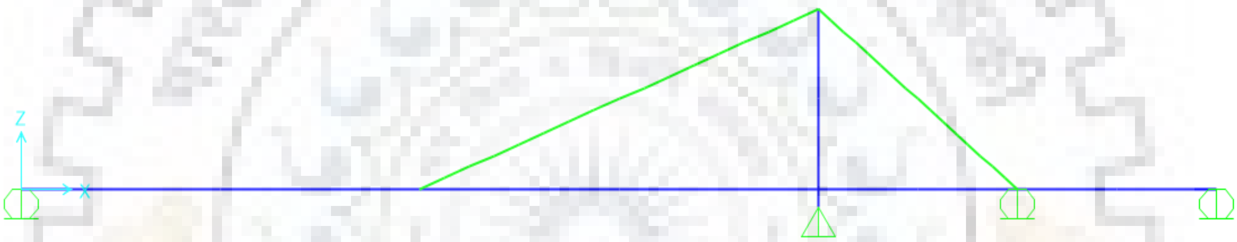

Figure 3.19: Model of the bridge in SAP2000

Table 3.24: Comparison of results of Wang *et al.*, 1993 and SAP2000

	Wang *et al.*, 1997	SAP2000	Percentage difference
Vertical deflection of node 3 (m)	.004176	.004176	0
Cable force in cable 3-5 (kN)	44526.698	44658.232	0.295404595
Cable force in cable 5-10 (kN)	53569.933	53515.22	-0.10213402
Maximum positive moment at node 2 (kNm)	60145.425	59849.504	-0.492008746
Maximum negative moment at node 3 (kNm)	96631.832	97231.782	0.620860927
Moment at node 7 (kNm)	52917.561	51023.62	-3.579041763
Shear force at the left of node 3 (kN)	8696.273	8712.153	0.182608696
Shear force at the right of node 3 (kN)	7984.558	7877.356	-1.342618384
Axial force in member 8-10 (kN)	41813.283	41824.937	0.02787234

The results of the analysis done using SAP2000 are within 5% of the results from the research paper.

Algorithm for finding Optimum Tension in cables of cable-stayed bridge under Dead load:

1. Input the geometric and physical data of the bridge

2. Input the dead load of girders and a small initial force in cable stays

3. Select control points to monitor deflection at those points. Check if the

Convergence tolerance = $\left|\frac{\text{Vertical displacement at control point}}{\text{Main span}}\right| \leq \epsilon_S \; (= 10^{-4})$

is achieved or not.

4. If convergent, then the equilibrium configuration is the desired initial shape else take the determined axial forces as initial element force and repeat step 3.

3.3.4 Cable Tension Optimisation of Symmetric Harp cable-stayed bridge (Wang *et al.*, 1993)

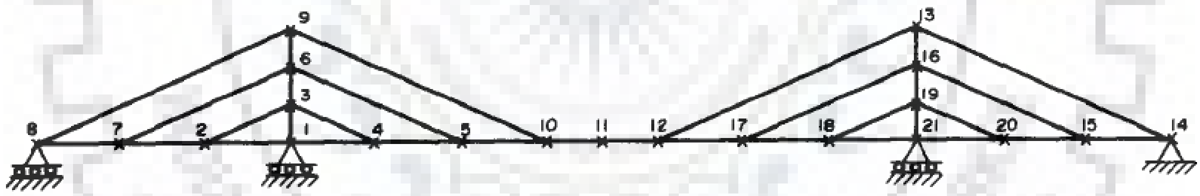

Figure 3.20: Symmetric Harp Cable-stayed bridge (Wang *et al.*, 1993)

Height of tower = 60.96 m

Distance between 8-7 = 7-2 = 2-1 = 1-4 = 4-5 = 5-10 = 45.72 m

Distance between 10-11 = 30.48 m

Modulus of Elasticity of Girder, Tower, and Cable = 2.068 x 10^8 kN/m^2

Girder: I = 1.131 m^4, A = 0.3196 m^2

Tower: I = 0.2106, 0.3452, 0.4315 m^4 (from top to bottom)

A = 0.2025, 0.2276, 0.2694 m^2

Cable: Exterior, A = 0.042 m^2, Interior, A = 0.0162 m^2

Dead Load: Girder = 87.563 kN/m

Cable: Exterior = 3.225 kN/m, Interior = 1.24 kN/m

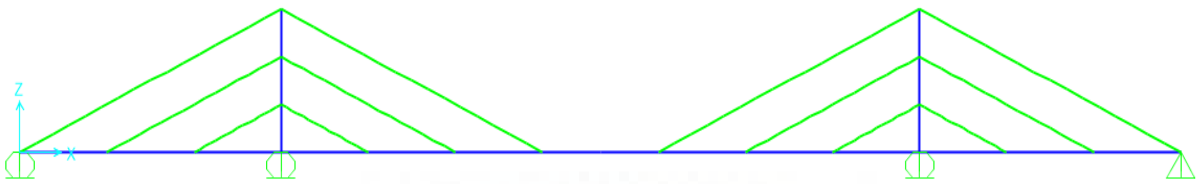

Figure 3.21: Model of the bridge in SAP2000

Table 3.25: Comparison of results of Wang *et al.*, 1993 and SAP2000

	Wang *et al.*, 1997	SAP2000	Percentage difference
Vertical deflection of node 4 (m)	0.0816	0.0816	0
Vertical deflection of node 5 (m)	0.102	0.102	0
Vertical deflection of node 10 (m)	0.090	0.090	0
Cable force in cable 8-9 (kN)	11787.787	11762.877	-0.211320755
Cable force in cable 7-6 (kN)	9554.78	9562.253	0.078212291
Cable force in cable 2-3 (kN)	9674.88	9667.453	-0.076781609
Cable force in cable 3-4 (kN)	9625.95	9505.894	-1.247227357
Cable force in cable 6-5 (kN)	9212.267	9337.262	1.356832448
Cable force in cable 9-10 (kN)	12027.99	11951.037	-0.639792899
Axial force in member 1-4 (kN)	28335.172	28145.455	-0.669544741
Maximum positive moment at node 11 (kNm)	16644.017	17807.986	6.9933203
Maximum negative moment at node 10 (kNm)	24030.511	22866.528	-4.843771158
Shear force at the left of node 1 (kN)	2268.593	2236.788	-1.401960784
Shear force at the right of node 1 (kN)	2135.146	2184.522	2.3125

As is evident from the table 3.25, the results of the analysis done using SAP2000 are within 7% of the results of the research paper.

3.3.5 Cable Tension Optimisation of Symmetric Radiating cable-stayed bridge (Wang *et al.*, 1993)

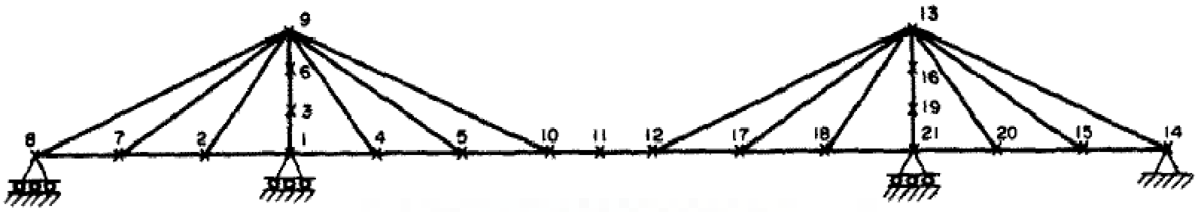

Figure 3.22: Symmetric Radiating Cable-stayed bridge (Wang *et al.*, 1993)

Height of tower = 60.96 m

Distance between 8-7 = 7-2 = 2-1 = 1-4 = 4-5 = 5-10 = 45.72 m

Distance between 10-11 = 30.48 m

Modulus of Elasticity of Girder, Tower, and Cable = 2.068 x 10^8 kN/m^2

Girder: I = 1.131 m^4, A = 0.3196 m^2

Tower: I = 0.2106, 0.3452, 0.4315 m^4 (from top to bottom)

A = 0.2025, 0.2276, 0.2694 m^2

Cable: Exterior, A = 0.042 m^2, Interior, A = 0.0162 m^2

Dead Load: Girder = 87.563 kN/m

Cable: Exterior = 3.225 kN/m, Interior = 1.24 kN/m

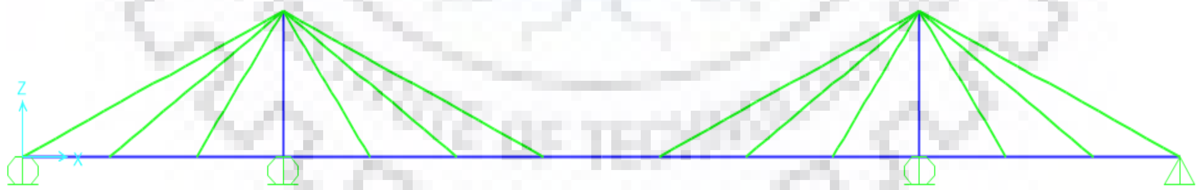

Figure 3.23: Model of the bridge in SAP2000

Table 3.26: Comparison of results of Wang *et al.*, 1993 and SAP2000

	Wang *et al.*, 1997	SAP2000	Percentage difference
Vertical deflection of node 4 (m)	0.000117	0.000117	0
Vertical deflection of node 5 (m)	0.00512	0.00512	0

Vertical deflection of node 10 (m)	0.005578	0.005578	0
Cable force in cable 8-9 (kN)	11338.517	11489.312	1.329933307
Cable force in cable 7-9 (kN)	7366.255	7144.289	-3.013285024
Cable force in cable 2-9 (kN)	5288.935	5283.598	-0.100925147
Cable force in cable 9-4 (kN)	4995.353	4886.371	-2.181656278
Cable force in cable 9-5 (kN)	6765.745	6879.175	1.6765286
Cable force in cable 9-10 (kN)	12076.922	11988.847	-0.729281768
Axial force in member 1-4 (kN)	19661.139	19613.544	-0.242081448
Maximum positive moment at node 11 (kNm)	16107.113	17328.027	7.57996633
Maximum negative moment at node 10 (kNm)	24567.415	23346.501	-4.969646799
Shear force at the left of node 1 (kN)	2072.871	2011.486	-2.961373391
Shear force at the right of node 1 (kN)	2157.387	2088.885	-3.175257732

As is evident from the table 3.26, the results of the analysis done using SAP2000 are within 8% of the results of the research paper.

3.3.6 Three-dimensional cable-stayed bridge (Nazmy and Abdel-Ghaffar, 1990)

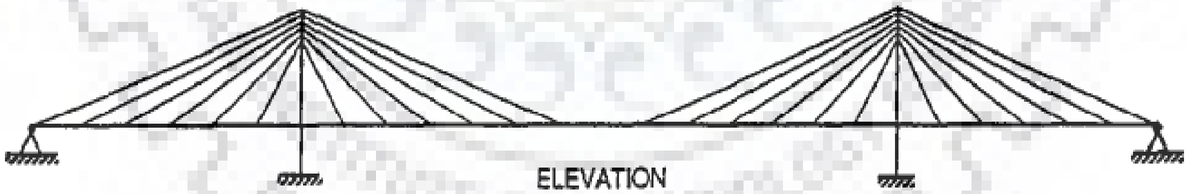

Figure 3.24: Elevation of the bridge (Nazmy and Abdel-Ghaffar, 1990)

There are 2 models with total spans of 627.888 m and 1255.776 m.

In model 1: side span length = 146.304 m, and main span length = 335.28 m

In model 2: side span length = 292.608 m, and main span length = 670.56 m

Properties of the bridge is given in table 3.27 and 3.28. The vertical displacement of centre of the bridge and horizontal displacement of the top of the pylon have been compared.

Table 3.27: Properties of model 1 (Nazmy and Abdel-Ghaffar, 1990)

	A (m^2)	I_x (m^4)	I_y (m^4)	I_z (m^4)	E (kN/m^2)	W_t (kN/m)
Girder (steel)	0.4645 0.5574 (for central part)	0.08631	21.5774	0.1295 0.6473 (for central part)	2 x 10^8	87.5634
Cross beams (steel)	0.1394 0.3252 (for central part)	0.01295 0.08631 (at towers)	5.1786	0.05179	2 x 10^8	21.8908
Tower (R.C.) above deck level	6.5032	17.2619	17.2619	8.631	2.78 x 10^7	153.2359
Tower (R.C.) below deck level	9.2903	64.7323	43.1549	43.1549	2.78 x 10^7	218.9085
Tower struts (R.C.)- Upper two struts	4.6452	1.2946	7.7679	1.2946	2.78 x 10^7	109.4542
Tower struts (R.C.)- Deck level strut	5.5742	1.7262	8.631	1.7262	2.78 x 10^7	131.3451

	Cable number	A (m^2)	Initial Tension (kN)	W_t (kN/m)	E (kN/m^2)
Cables	1, 24, 25, 48	0.01812	8674.03	1.9921	2 x 10^8
	2, 11, 14, 23, 26, 35, 38, 47	0.01161	5560.28	1.2770	2 x 10^8
	3, 10, 15, 22, 27, 34, 39, 46	0.01022	4893.04	1.1237	2 x 10^8
	4, 9, 16, 21, 28, 33, 40, 45	0.00883	4225.81	0.9705	2 x 10^8
	5, 8, 17, 20, 29, 32, 41, 44	0.00697	3336.17	0.7662	2 x 10^8
	6, 7, 18, 19, 30, 31, 42, 43	0.00567	2713.42	0.6232	2 x 10^8
	12, 13, 36, 37	0.01858	8896.44	2.0431	2 x 10^8

Table 3.28: Properties of model 2 (Nazmy and Abdel-Ghaffar, 1990)

	A (m^2)	I_x (m^4)	I_y (m^4)	I_z (m^4)	E (kN/m^2)	W_t (kN/m)
Girder (steel)	0.6968 0.8361 (for central part)	0.1036	107.8872	0.6473 3.2366 (for central part)	2×10^8	105.8058
Cross beams (steel)	0.1394 0.2787 (for central part)	0.0129 0.0863 (at towers)	5.1786	0.0518	2×10^8	21.8908
Tower (R.C.) above deck level	13.0064	34.5239	86.3097	43.1549	2.78×10^7	306.4719
Tower (R.C.) below deck level	18.5806	129.4646	215.7744	215.7744	2.78×10^7	437.8170
Tower struts (R.C.)- Upper two struts	6.5032	1.2946	7.7679	1.2946	2.78×10^7	153.2359
Tower struts (R.C.)- Deck level strut	7.4322	1.7262	8.6310	1.7262	2.78×10^7	175.1268

	Cable number	A (m^2)	Initial Tension (kN)	W_t (kN/m)	E (kN/m^2)
Cables	1, 24, 25, 48	0.03995	19127.35	4.3928	2×10^8
	2, 11, 14, 23, 26, 35, 38, 47	0.02508	12010.20	2.7582	2×10^8
	3, 10, 15, 22, 27, 34, 39, 46	0.02276	10898.14	2.5029	2×10^8
	4, 9, 16, 21, 28, 33, 40, 45	0.01951	9341.27	2.1453	2×10^8
	5, 8, 17, 20, 29, 32, 41, 44	0.01617	7739.91	1.7775	2×10^8
	6, 7, 18, 19, 30, 31, 42, 43	0.01236	5916.13	1.3587	2×10^8
	12, 13, 36, 37	0.04227	20239.41	4.6482	2×10^8

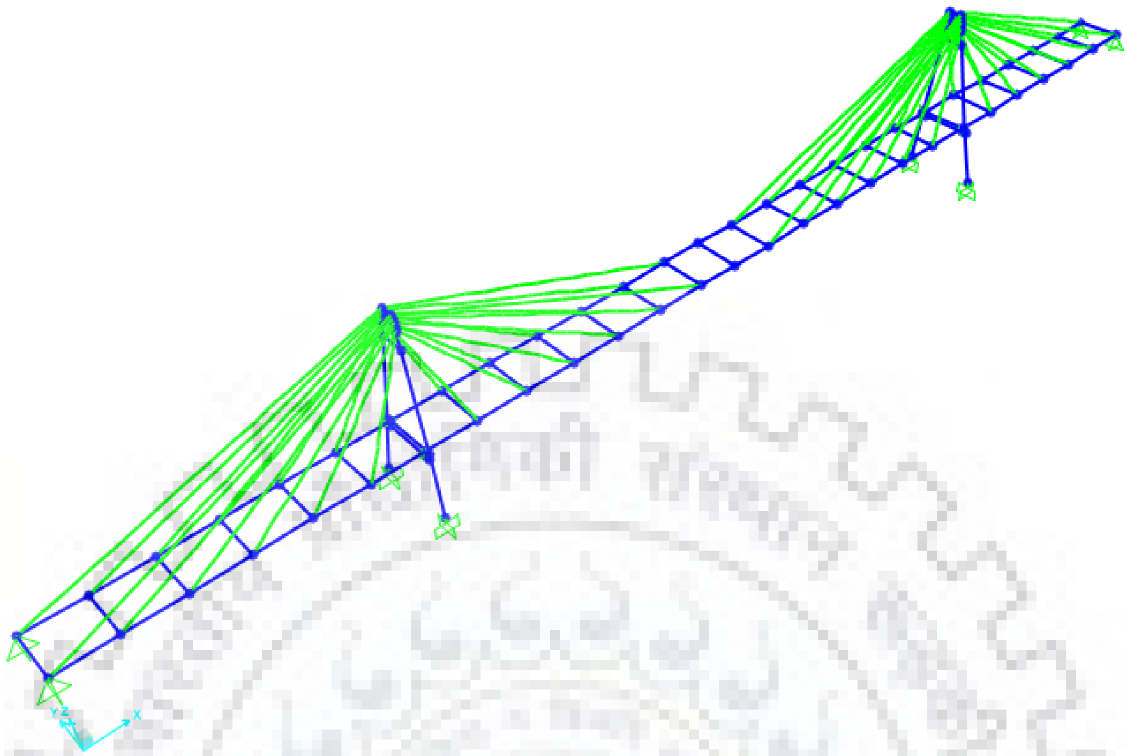

Figure 3.25: Model 1 in SAP2000

Table 3.29: Comparison of results of Model 1

Dead load multiplier	Vertical displacement of centre of the bridge (m)			Horizontal displacement of top of the pylon (m)		
	Nazmy and Abdel-Ghaffar, 1990	SAP2000	Percentage difference	Nazmy and Abdel-Ghaffar, 1990	SAP2000	Percentage difference
1	0.0762	0.077297	1.44	0.007254	0.006584	-9.2437
2	1.6764	1.693377	1.012727	0.362712	0.328971	-9.30252
3	3.048	3.176961	4.231	0.585216	0.612282	4.625
4	4.2672	4.525396	6.050714	0.862584	0.889833	3.159011
5	5.334	5.752521	7.846286	1.0668	1.149706	7.771429

The results obtained using SAP2000 are within 10% from those in the research paper.

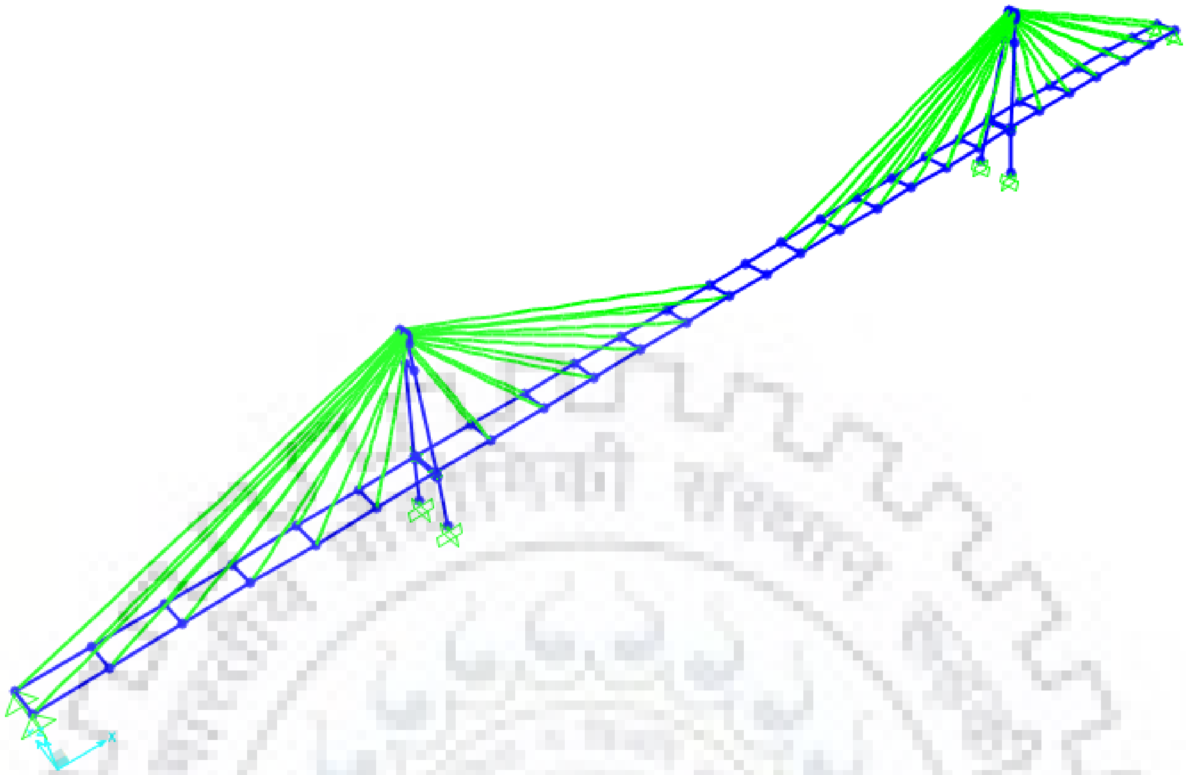

Figure 3.26: Model 2 in SAP2000

Table 3.30: Comparison of results of Model 2

Dead load multiplier	Vertical displacement of centre of the bridge (m)			Horizontal displacement of top of the pylon (m)		
	Nazmy and Abdel-Ghaffar, 1990	SAP2000	Percentage difference	Nazmy and Abdel-Ghaffar, 1990	SAP2000	Percentage difference
1	0.24384	0.265206	8.7625	0.042672	0.046299	8.5
2	3.77952	3.885529	2.804839	0.725424	0.752216	3.693277
3	6.73608	7.102328	5.437104	1.408176	1.414577	0.454545
4	9.2964	10.0118	7.69541	1.953768	2.034052	4.109204
5	11.49096	12.63542	9.959682	2.56032	2.61369	2.084524

The results obtained using SAP2000 are within 10% from those in the research paper.

3.4 Parametric Study to find the influence of Number of Cables for various Side span to Main span ratios and for different arrangements of cables on the behaviour of the bridge

Influence of number of cables, side span to main span ratio, cable arrangement, on maximum cable tension, maximum sagging moment, maximum hogging moment, deflection of centre of span of the girder, maximum compression in deck, and maximum moment in pylon have been investigated.

The influence of all the nonlinearities, viz., cable sag, beam-column effect, large displacement effect has also been investigated.

Total span of the bridge, L = 805 m

Length of central panel = 5 m

Height of pylon = 80.5 m (Total span/10)

Number of cables, n = 40, 80, 120, and 160

Side span to Main span ratio (L_S/L_M) = 0.30, 0.35, 0.40, 0.45, 0.50

Total area of all cables = 1 m^2

Arrangements of cables: Radial, Harp, and Fan

Loading on the bridge = 20 kN/m (Nowak *et al.*, 2010)

Table 3.31: Properties of the bridge

	A (m^2)	I (m^4)	E (MPa)
Girder	4.552	3.565	2.49 x 10^4
Pylon (Nazmy and Abdel-Ghaffar, 1990)	6.5	17.26	2.49 x 10^4
Cable (n = 40)	0.025 (~ 129 strands)	-	1.6 x 10^5
Cable (n = 80)	0.0125 (~ 65 strands)	-	1.6 x 10^5
Cable (n = 120)	0.00833 (~ 43 strands)	-	1.6 x 10^5
Cable (n = 160)	0.00625 (~ 32 strands)	-	1.6 x 10^5

Girder properties have been taken corresponding to AASHTO-PCI-ASBI Segmental Box girder of 10.2 m width (AASHTO-PCI-ASBI Segmental box girder standard, 1997).

3.4.1 Variation of Maximum Cable Tension

Table 3.32: Maximum cable tension for radial, harp, and fan configurations, L_S/L_M = 0.3, 0.35, 0.4, 0.45, and 0.5, number of cables- 40, 80, 120, and 160

Side span to main span ratio	Number of cables	Maximum Cable Tension (kN)				
		Cable Sag+ P-delta+ Large Displacement	Only Cable Sag	% difference between 1 &2	Cable Sag+ P-delta	% difference between 1 & 4
		1	2	3	4	5
0.3	Radial pattern					
	40	2385.90	2363.46	-0.94	2387.17	0.05
	80	1315.61	1302.36	-1.00	1316.46	0.06
	120	907.27	897.88	-1.03	907.89	0.07
	160	692.21	684.97	-1.05	692.70	0.07
	Harp pattern					
	40	2373.01	2331.16	-1.76	2374.18	0.05
	80	1315.71	1291.14	-1.87	1316.55	0.06
	120	909.39	892.07	-1.90	910.02	0.07
	160	694.68	681.33	-1.92	695.18	0.07
	Fan pattern					
	40	2400.62	2377.00	-0.98	2401.93	0.05
	80	1323.40	1308.54	-1.12	1324.33	0.07
	120	907.18	895.97	-1.24	907.93	0.08
	160	686.92	677.63	-1.35	687.56	0.09
0.35	Radial pattern					
	40	1835.52	1820.03	-0.84	1836.34	0.04
	80	1011.25	1002.09	-0.90	1011.80	0.05
	120	697.19	690.71	-0.93	697.59	0.06
	160	531.86	526.87	-0.94	532.18	0.06
	Harp pattern					
	40	1896.91	1867.48	-1.55	1897.61	0.04
	80	1051.05	1033.67	-1.65	1051.57	0.05
	120	726.34	714.09	-1.69	726.74	0.05
	160	554.82	545.34	-1.71	555.13	0.06
	Fan pattern					
	40	1851.28	1834.99	-0.88	1852.12	0.05
	80	1023.99	1013.71	-1.00	1024.60	0.06

	120	705.70	697.89	-1.11	706.18	0.07
	160	537.59	531.10	-1.21	538.01	0.08
0.4	Radial pattern					
	40	1382.60	1371.98	-0.77	1383.05	0.03
	80	760.38	754.09	-0.83	760.69	0.04
	120	523.99	519.55	-0.85	524.22	0.04
	160	399.65	396.21	-0.86	399.83	0.05
	Harp pattern					
	40	1487.46	1467.61	-1.33	1487.85	0.03
	80	822.77	810.94	-1.44	823.03	0.03
	120	568.30	559.92	-1.47	568.49	0.03
	160	433.99	427.51	-1.49	434.15	0.04
	Fan pattern					
	40	1398.25	1387.10	-0.80	1398.71	0.03
	80	775.43	768.40	-0.91	775.78	0.05
	120	537.16	531.82	-0.99	537.44	0.05
	160	411.67	407.21	-1.08	411.91	0.06
0.45	Radial pattern					
	40	979.88	973.05	-0.70	980.08	0.02
	80	537.29	533.25	-0.75	537.43	0.03
	120	369.91	367.05	-0.77	370.02	0.03
	160	282.02	279.80	-0.78	282.10	0.03
	Harp pattern					
	40	1114.50	1110.32	-0.37	1114.9	0.04
	80	613.01	605.73	-1.19	613.06	0.01
	120	422.98	417.81	-1.22	423.02	0.01
	160	322.86	318.85	-1.24	322.92	0.02
	Fan pattern					
	40	995.14	988.00	-0.72	995.35	0.02
	80	553.45	548.94	-0.81	553.60	0.03
	120	385.84	382.44	-0.88	385.97	0.03
	160	297.94	295.11	-0.95	298.05	0.04
0.5	Radial pattern					
	40	822.58	820.99	-0.19	822.51	-0.01
	80	421.16	420.34	-0.19	421.16	-0.0004
	120	282.62	282.05	-0.20	282.61	-0.0035
	160	212.89	212.46	-0.19	212.89	0
	Harp pattern					
	40	1036.26	1033.22	-0.29	1036.51	0.02
	80	529.61	528.00	-0.30	529.75	0.03
	120	355.93	354.82	-0.31	356.02	0.03
	160	268.09	267.22	-0.32	268.16	0.03
	Fan pattern					
	40	836.80	835.09	-0.20	836.75	-0.006

	80	435.31	434.40	-0.21	435.34	0.006
	120	298.29	297.62	-0.22	298.31	0.007
	160	229.59	229.05	-0.24	229.61	0.010

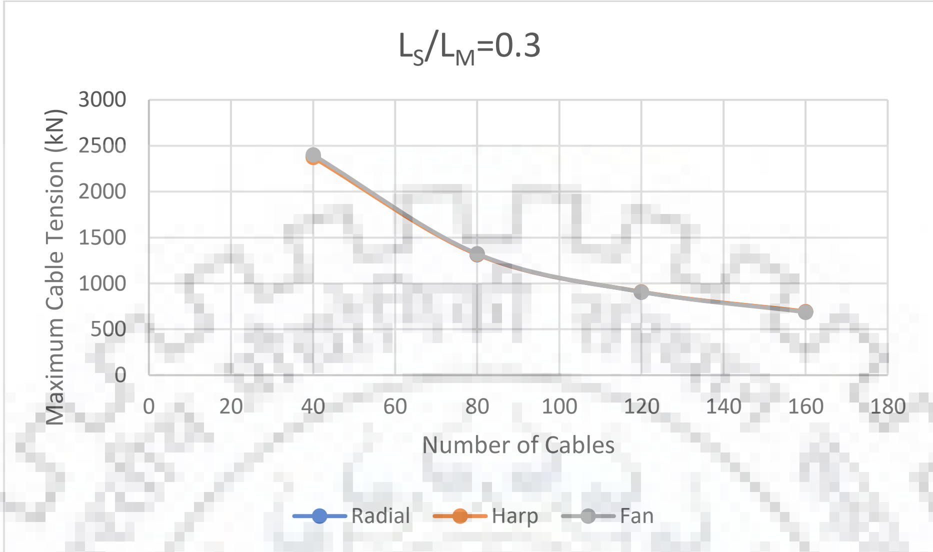

(a)

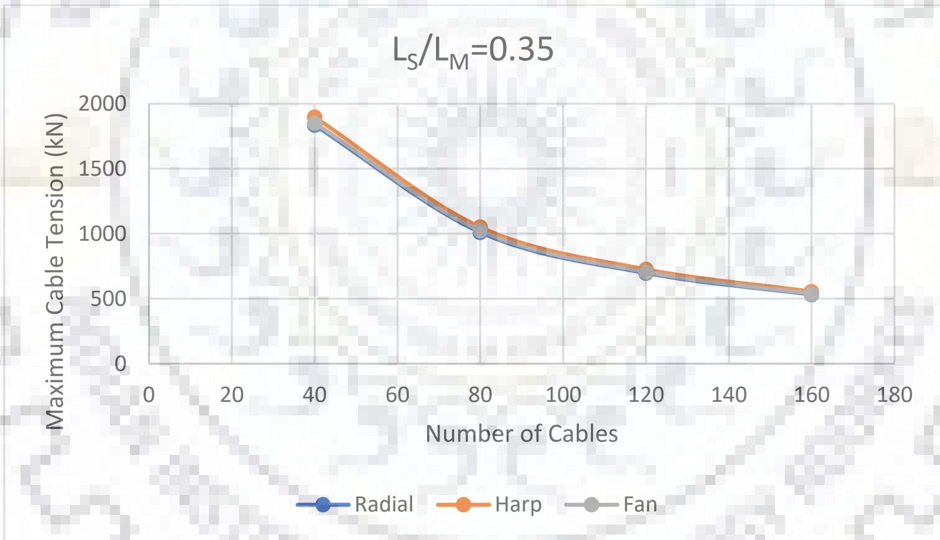

(b)

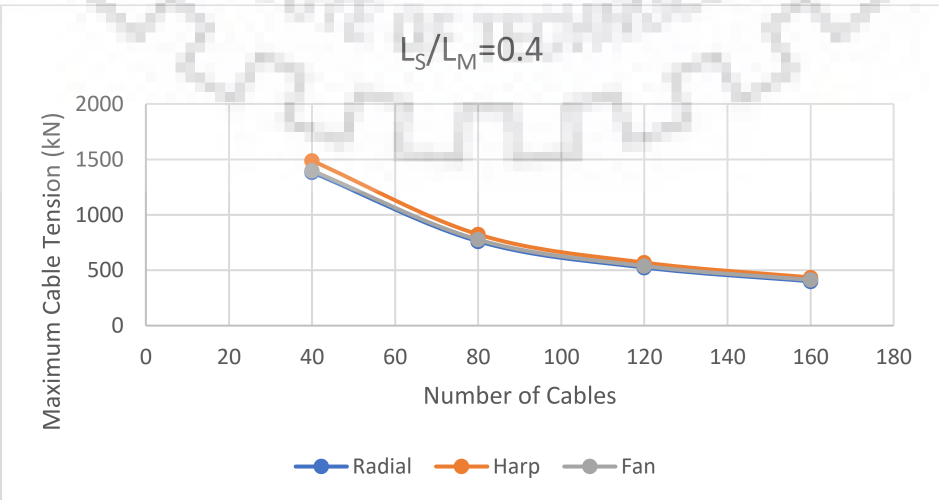

(c)

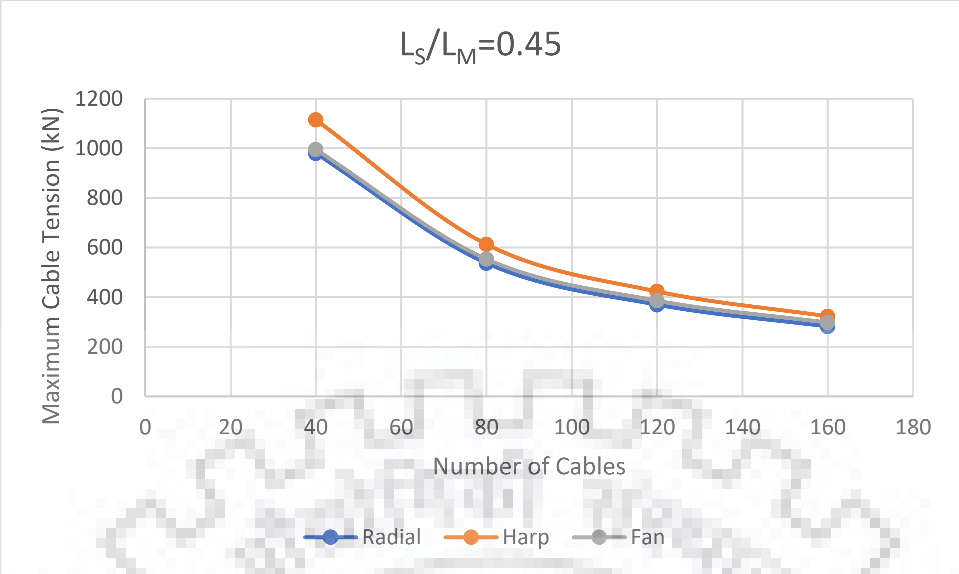

(d)

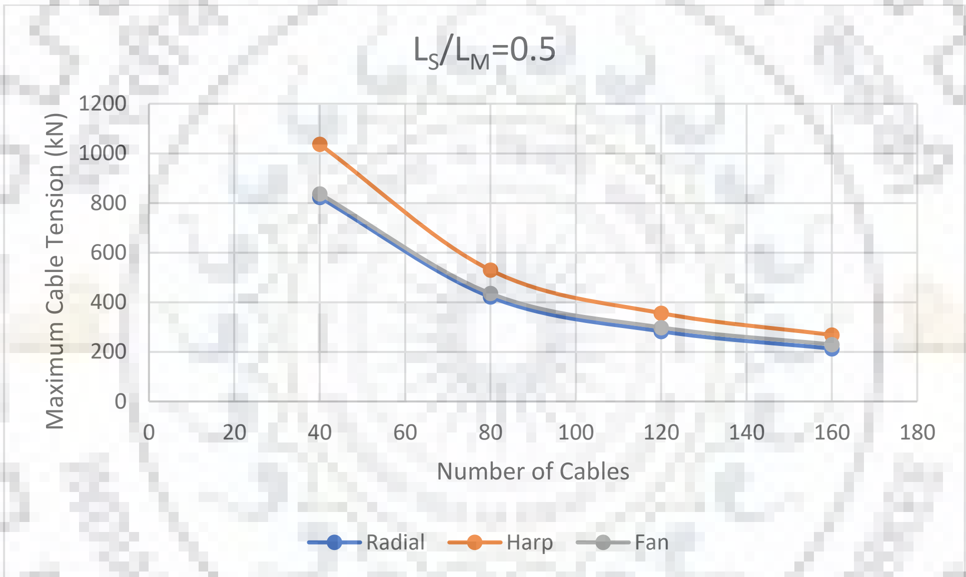

(e)

Figure 3.27: Graph showing variation of maximum cable tension with number of cables for radial, harp, and fan arrangements of the bridge for side span to main span ratios of (a) 0.3, (b) 0.35, (c) 0.4, (d) 0.45, (e) 0.5

With the increase in number of cables from 40 to 160, the maximum cable tension decreases. In the bridge with 160 cables, maximum cable tension reduces to 0.29 and 0.26 times of that in bridge with 40 cables for side span to main span ratios of 0.3 and 0.5, respectively for both radial and harp arrangement. Also, the behaviour of fan type bridge is intermediate of radial and harp configurations.

For the bridge with side span to main span ratio of 0.3, the value of maximum cable tension is almost equal for radial and harp arrangement. For side span to main span ratio of 0.35, 0.4, 0.45, and 0.5 the values are 3%, 7%, 12%, and 21%, respectively, more in harp arrangement than in radial arrangement.

The error by ignoring beam-column and large displacement nonlinearities lies within 2%. And the error by ignoring only large displacement nonlinearity lies within 0.1%.

3.4.2 Variation of Maximum Sagging Moment

Table 3.33: Maximum sagging moment for radial, harp, and fan configurations, L_S/L_M = 0.3, 0.35, 0.4, 0.45, and 0.5, number of cables- 40, 80, 120, and 160

Side span to main span ratio	Number of cables	Maximum Sagging Moment (kNm)				
		Cable Sag+ P-delta+ Large Displacement	Only Cable Sag	% difference between 1 &2	Cable Sag+ P-delta	% difference between 1 & 4
		1	2	3	4	5
0.3	Radial pattern					
	40	29756.67	29452.18	-1.02	29633.30	-0.41
	80	32638.05	32291.73	-1.06	32499.11	-0.43
	120	33807.74	33445.52	-1.07	33663.39	-0.43
	160	34402.44	34032.64	-1.07	34255.87	-0.43
	Harp pattern					
	40	20562.43	19746.85	-3.97	20398.05	-0.80
	80	19531.66	18736.72	-4.07	19351.31	-0.92
	120	19255.99	18451.00	-4.18	19070.10	-0.96
	160	19120.29	18547.77	-2.99	18931.07	-0.99
	Fan pattern					
	40	29203.40	28898.65	-1.04	29078.11	-0.43
	80	30838.21	30499.47	-1.10	30692.96	-0.47
	120	30130.63	29799.28	-1.10	29974.35	-0.52
	160	28526.52	28224.43	-1.06	28361.71	-0.58
0.35	Radial pattern					
	40	25955.63	25736.50	-0.84	25873.08	-0.32
	80	28501.42	28251.09	-0.88	28407.49	-0.33
	120	29538.93	29277.75	-0.88	29442.14	-0.33
	160	30065.65	29798.95	-0.89	29967.36	-0.33
	Harp pattern					
	40	17136.32	16659.91	-2.78	17030.95	-0.61
	80	16640.97	16338.80	-1.82	16525.06	-0.70

	120	17208.34	17178.64	-0.17	17092.92	-0.67
	160	17931.58	17906.34	-0.14	17813.14	-0.66
	Fan pattern					
	40	25568.86	25348.98	-0.86	25484.82	-0.33
	80	27211.88	26966.23	-0.90	27113.99	-0.36
	120	26870.96	26629.05	-0.90	26765.57	-0.39
	160	25756.80	25534.30	-0.86	25645.48	-0.43
0.4	Radial pattern					
	40	22426.98	22271.58	-0.69	22373.14	-0.24
	80	24657.48	24480.05	-0.72	24596.61	-0.25
	120	25577.95	25392.51	-0.73	25515.03	-0.25
	160	26044.95	25855.54	-0.73	25981.09	-0.25
	Harp pattern					
	40	14662.29	14484.34	-1.21	14600.33	-0.42
	80	15676.60	15644.17	-0.21	15607.24	-0.44
	120	16716.49	16693.34	-0.14	16643.38	-0.44
	160	17397.33	17367.75	-0.17	17322.22	-0.43
	Fan pattern					
	40	22189.11	22032.86	-0.70	22134.01	-0.25
	80	23834.39	23659.50	-0.73	23770.85	-0.27
	120	23840.54	23667.46	-0.73	23772.20	-0.29
	160	23194.59	23034.11	-0.69	23122.78	-0.31
0.45	Radial pattern					
	40	18764.13	18660.56	-0.55	18732.40	-0.17
	80	20678.83	20561.20	-0.57	20643.10	-0.17
	120	21489.66	21366.78	-0.57	21452.94	-0.17
	160	21901.37	21775.75	-0.57	21864.12	-0.17
	Harp pattern					
	40	13541.87	13492.04	-0.37	13507.86	-0.25
	80	15245.86	15226.13	-0.13	15206.59	-0.26
	120	16237.91	16208.71	-0.18	16196.41	-0.26
	160	16829.10	16795.26	-0.20	16786.30	-0.25
	Fan pattern					
	40	18805.11	18700.46	-0.56	18771.71	-0.18
	80	20445.38	20327.68	-0.58	20407.04	-0.19
	120	20795.87	20678.87	-0.56	20755.06	-0.20
	160	20617.73	20507.99	-0.53	20575.35	-0.20
0.5	Radial pattern					
	40	15636.96	15570.70	-0.42	15617.90	-0.12
	80	17249.25	17173.56	-0.44	17227.99	-0.12
	120	17960.44	17881.33	-0.44	17938.69	-0.12
	160	18321.50	18240.62	-0.44	18299.49	-0.12
	Harp pattern					
	40	13146.96	13124.62	-0.17	13126.64	-0.15

	80	14903.79	14873.06	-0.21	14880.71	-0.15
	120	15720.51	15685.60	-0.22	15696.32	-0.15
	160	16216.59	16177.90	-0.24	16191.94	-0.15
	Fan pattern					
	40	15666.90	15599.32	-0.43	15647.13	-0.13
	80	17295.06	17219.36	-0.44	17272.75	-0.13
	120	17955.14	17879.02	-0.42	17931.57	-0.13
	160	18203.40	18130.32	-0.40	18179.13	-0.13

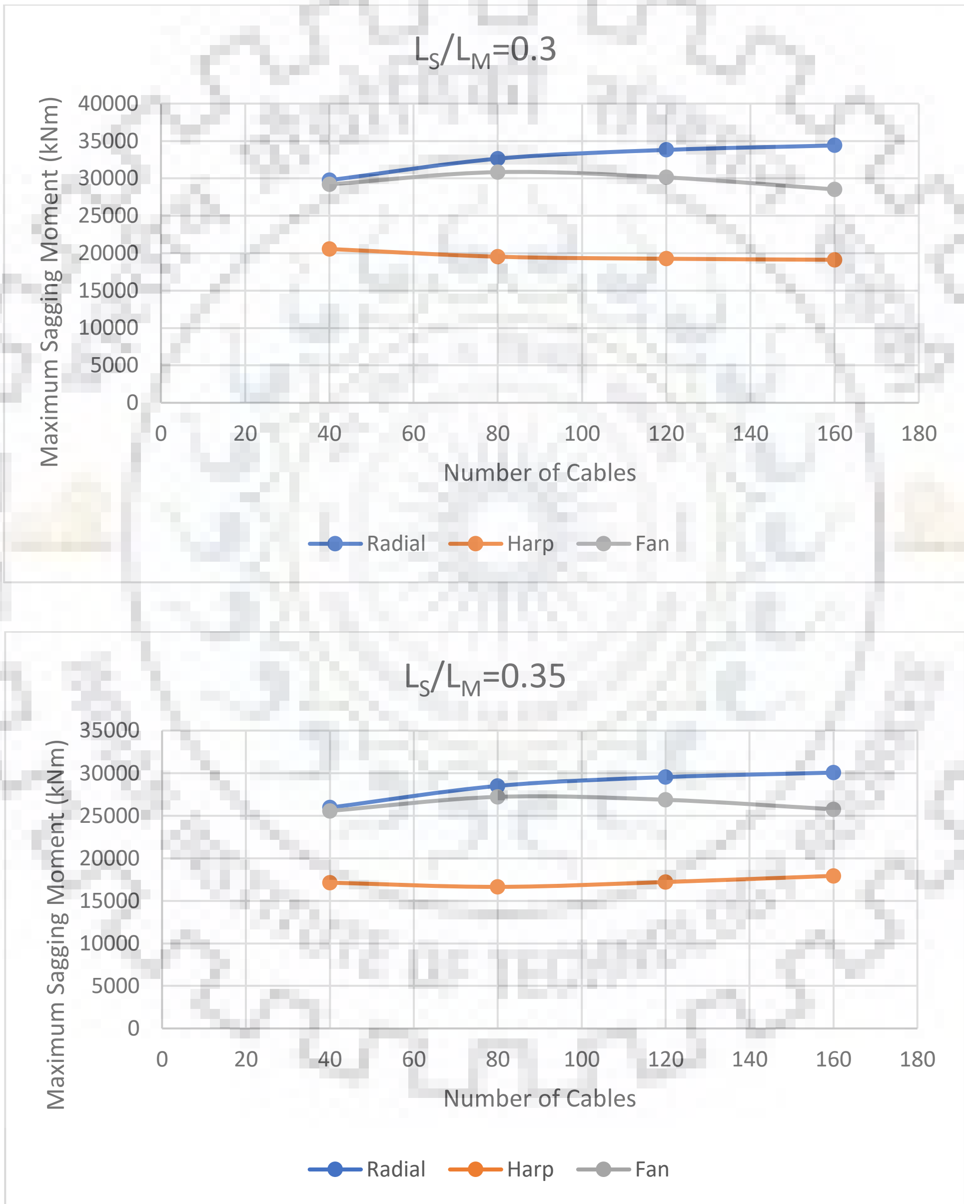

(a)

(b)

Figure 3.28: Graph showing variation of maximum sagging moment with number of cables for radial, harp, and fan arrangements of the bridge for side span to main span ratios of (a) 0.3, (b) 0.35, (c) 0.4, (d) 0.45, (e) 0.5

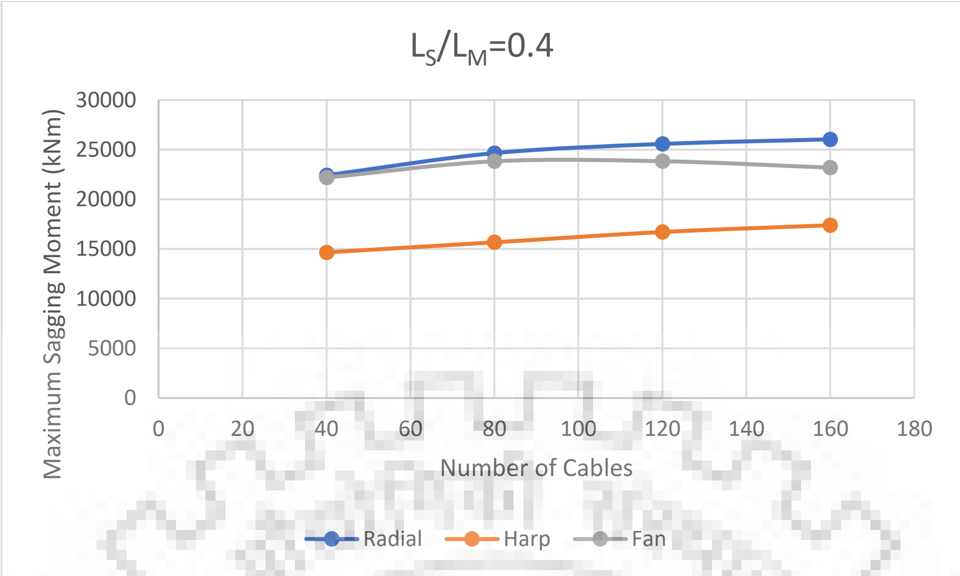

L_S/L_M=0.4
Maximum Sagging Moment (kNm)
30000
25000
20000
15000
10000
5000
0
0
20
40
60
80
100
120
140
160
180
Number of Cables
Radial
Harp
Fan

(c)

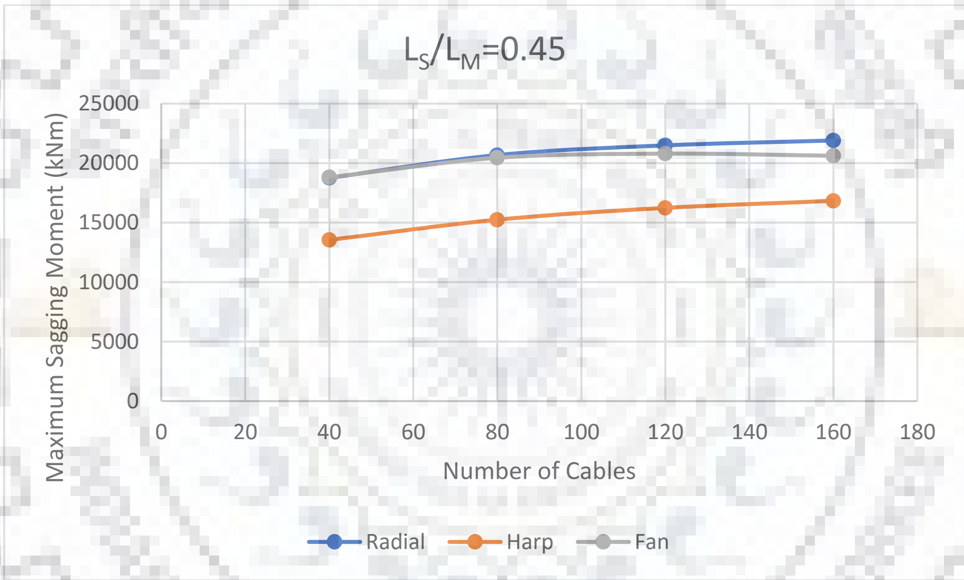

L_S/L_M=0.45
Maximum Sagging Moment (kNm)
25000
20000
15000
10000
5000
0
0
20
40
60
80
100
120
140
160
180
Number of Cables
Radial
Harp
Fan

(d)

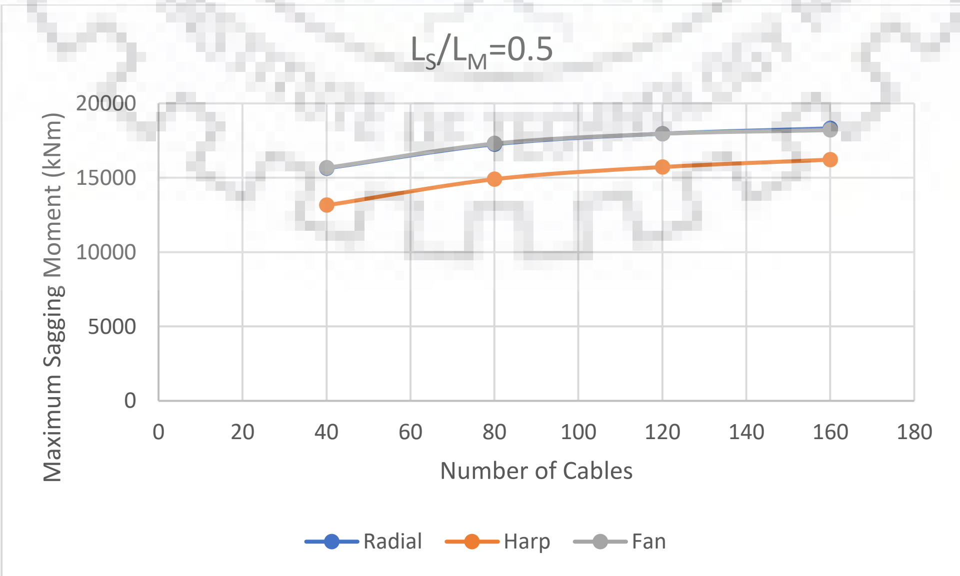

L_S/L_M=0.5
Maximum Sagging Moment (kNm)
20000
15000
10000
5000
0
0
20
40
60
80
100
120
140
160
180
Number of Cables
Radial
Harp
Fan

(e)

In general, the sagging moment increases with the increase in number of cables from 40 to 160 for both radial and harp arrangements. The fan configuration is intermediate of the two. The fan configuration with lesser number of cables resembles radial configuration, and as the number of cables increases its behaviour shifts toward harp configuration.

With the increase in side span to main span ratio from 0.3 to 0.5, the value of maximum sagging moment decreases. The maximum sagging moment in radial configuration is more than in harp configuration.

The increase in maximum sagging moment for radial configuration is 15.6% and 17.2% for side span to main span ratios of 0.3 and 0.5, respectively. For harp configuration, the increase is 4.6% and 23.3% for side span to main span ratios of 0.35 and 0.5.

The error by ignoring beam-column and large displacement nonlinearities lies within 5%. And the error by ignoring only large displacement nonlinearity lies within 1%.

3.4.3 Variation of Maximum Hogging Moment

Table 3.34: Maximum hogging moment for radial, harp, and fan configurations, L_S/L_M = 0.3, 0.35, 0.4, 0.45, and 0.5, number of cables- 40, 80, 120, and 160

Side span to main span ratio	Number of cables	Maximum Hogging Moment (kNm)				
		Cable Sag+ P-delta+ Large Displacement	Only Cable Sag	% difference between 1 &2	Cable Sag+ P-delta	% difference between 1 & 4
		1	2	3	4	5
0.3	Radial pattern					
	40	37174.14	36653.19	-1.40	37179.54	0.01
	80	41362.36	40757.58	-1.46	41370.46	0.01
	120	43098.21	42472.20	-1.45	43107.24	0.02
	160	44023.76	43377.40	-1.47	44033.59	0.02
	Harp pattern					
	40	49923.48	48309.89	-3.23	49966.68	0.09
	80	53503.23	51740.58	-3.29	53551.44	0.09
	120	54940.84	53155.56	-3.25	54983.62	0.08
	160	55725.24	53900.71	-3.27	55770.69	0.08
	Fan pattern					

	40	37385.97	36836.14	-1.47	37391.20	0.01
	80	42692.96	41987.19	-1.65	42700.62	0.02
	120	46014.18	45166.07	-1.84	46022.16	0.02
	160	48913.32	47891.50	-2.09	48922.14	0.02
0.35	Radial pattern					
	40	25436.05	25080.05	-1.40	25439.07	0.01
	80	28529.09	28113.77	-1.46	28534.14	0.02
	120	29759.25	29326.58	-1.45	29764.56	0.02
	160	30476.67	30029.70	-1.47	30482.36	0.02
	Harp pattern					
	40	32517.49	31460.79	-3.25	32543.15	0.08
	80	35302.22	34133.68	-3.31	35331.03	0.08
	120	36488.40	35299.53	-3.26	36514.91	0.07
	160	37093.94	35875.45	-3.28	37121.84	0.08
	Fan pattern					
	40	25460.05	25085.22	-1.47	25463.00	0.01
	80	29206.92	28723.83	-1.65	29210.97	0.01
	120	31464.21	30886.10	-1.84	31468.51	0.01
	160	33396.44	32702.91	-2.08	33400.80	0.01
0.4	Radial pattern					
	40	15626.17	15621.50	-0.03	15582.93	-0.28
	80	17760.52	17486.25	-1.54	17764.44	0.02
	120	18647.23	18356.94	-1.56	18651.36	0.02
	160	19124.41	18825.48	-1.56	19128.65	0.02
	Harp pattern					
	40	27828.09	27575.50	-0.91	27559.92	-0.96
	80	27574.46	27293.71	-1.02	27270.81	-1.10
	120	27488.13	27197.65	-1.06	27171.99	-1.15
	160	27443.73	27148.33	-1.08	27121.21	-1.18
	Fan pattern					
	40	16050.61	16026.41	-0.15	16005.97	-0.28
	80	17928.01	17611.81	-1.76	17931.76	0.02
	120	19359.09	18979.17	-1.96	19362.40	0.02
	160	20554.08	20103.60	-2.19	20557.15	0.01
0.45	Radial pattern					
	40	13037.02	13037.31	0.002	13009.55	-0.21
	80	12969.31	12966.26	-0.02	12936.35	-0.25
	120	12915.22	12910.71	-0.03	12880.44	-0.27
	160	12891.80	12886.38	-0.04	12855.69	-0.28
	Harp pattern					
	40	27312.23	27209.98	-0.37	27182.61	-0.47
	80	27108.75	26993.13	-0.43	26960.37	-0.55
	120	27039.56	26919.27	-0.44	26884.45	-0.57
	160	27003.90	26881.19	-0.45	26845.22	-0.59

	Fan pattern					
	40	16193.03	16186.96	-0.04	16168.47	-0.15
	80	16266.58	16239.68	-0.17	16232.29	-0.21
	120	16478.57	16429.27	-0.30	16432.48	-0.28
	160	16649.56	16588.81	-0.36	16592.85	-0.34
0.5	Radial pattern					
	40	16331.10	16337.90	0.04	16317.67	-0.08
	80	16060.14	16067.16	0.04	16046.03	-0.09
	120	15993.57	16000.71	0.04	15978.90	-0.09
	160	15964.02	15971.14	0.04	15948.94	-0.09
	Harp pattern					
	40	27444.29	27458.80	0.05	27421.64	-0.08
	80	27270.69	27287.19	0.06	27243.36	-0.10
	120	27209.86	27227.03	0.06	27180.76	-0.11
	160	27178.00	27195.53	0.06	27147.96	-0.11
	Fan pattern					
	40	16115.97	16115.81	0.00	16101.73	-0.09
	80	15740.12	15734.96	-0.03	15723.47	-0.11
	120	15658.84	15650.26	-0.05	15640.26	-0.12
	160	15765.58	15753.14	-0.08	15743.02	-0.14

In general, maximum hogging moment increases with the increase in number of cables for side span to main span ratios of 0.3 and 0.35 for harp arrangement, and for radial arrangement for side span to main span ratios of 0.3, 0.35, and 0.4. Thereafter, there is little variation in maximum hogging moment for rest of the side span to main span ratios.

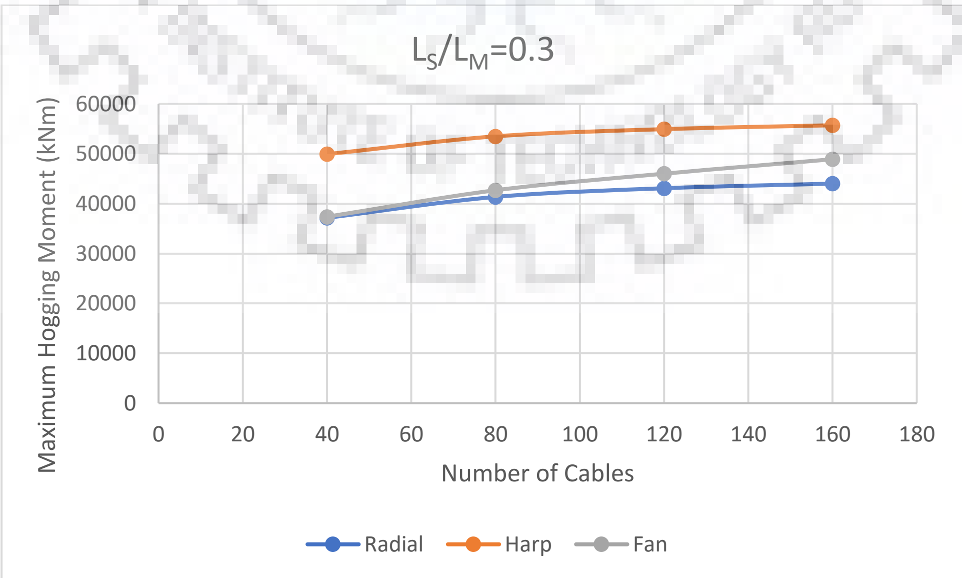

(a)

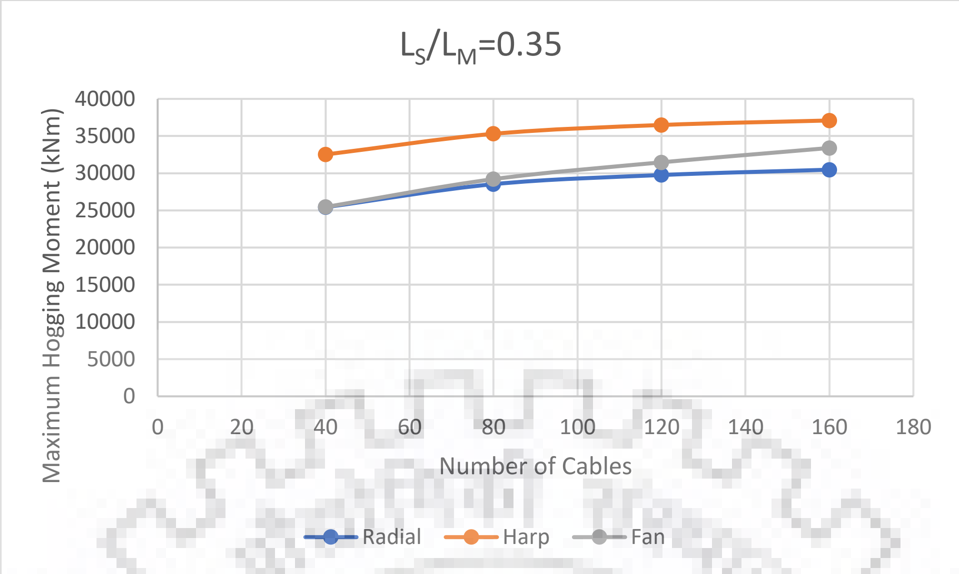

L_S/L_M=0.35
Maximum Hogging Moment (kNm)
40000
35000
30000
25000
20000
15000
10000
5000
0
0
20
40
60
80
100
120
140
160
180
Number of Cables
Radial
Harp
Fan

(b)

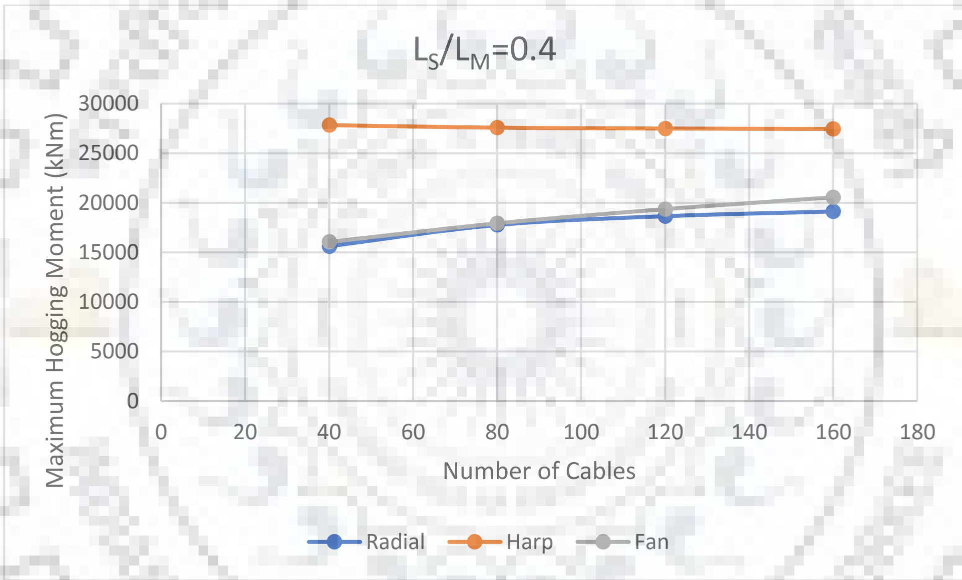

L_S/L_M=0.4
Maximum Hogging Moment (kNm)
30000
25000
20000
15000
10000
5000
0
0
20
40
60
80
100
120
140
160
180
Number of Cables
Radial
Harp
Fan

(c)

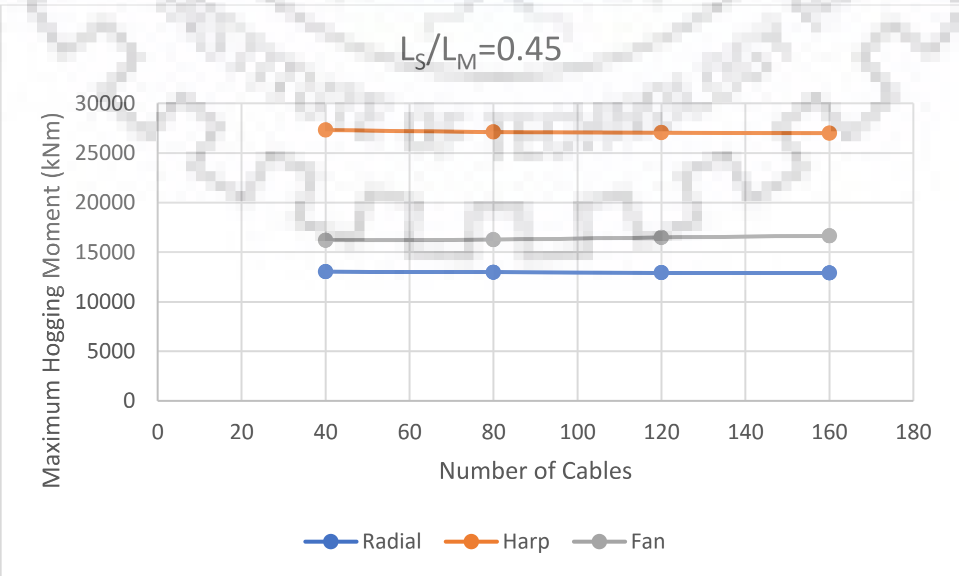

L_S/L_M=0.45
Maximum Hogging Moment (kNm)
30000
25000
20000
15000
10000
5000
0
0
20
40
60
80
100
120
140
160
180
Number of Cables
Radial
Harp
Fan

(d)

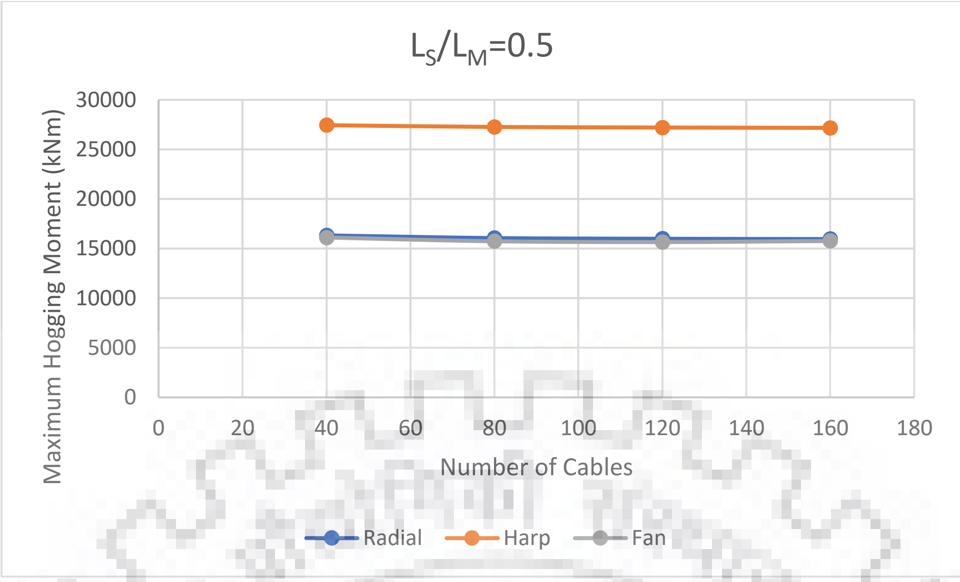

(e)

Figure 3.29: Graph showing variation of maximum hogging moment with number of cables for radial, harp, and fan arrangements of the bridge for side span to main span ratios of (a) 0.3, (b) 0.35, (c) 0.4, (d) 0.45, (e) 0.5

With the increase in side span to main span ratio from 0.3 to 0.5, the value of maximum hogging moment decreases. The maximum hogging moment in harp configuration is more than in radial configuration.

The increase in maximum hogging moment for radial configuration is 18.43%, 19.82%, and 22.39% for side span to main span ratios of 0.3, 0.35, and 0.4. And, the increase for harp configuration is 11.62% and 14.07% for side span to main span ratios of 0.3 and 0.35.

The error by ignoring beam-column and large displacement nonlinearities lie within 4%. And the error by ignoring only large displacement nonlinearity lies within 2%.

3.4.4 Variation of Deflection at Centre of Span of the Girder

Deflection at centre of span of the girder increases with the increase in the number of cables from 40 to 160 for both radial and harp arrangements. With the increase in side span to main span ratio from 0.3 to 0.5, the value of central deflection decreases, and it is more in harp than in radial arrangement.

The increase in central deflection for radial configuration is 11.3% and 9.3% for side span to main span ratios of 0.3 and 0.5, respectively. For harp configuration, the corresponding increase is 11.76% and 11.28%.

Table 3.35: Deflection at centre of span of the girder for radial, harp, and fan configurations, L_S/L_M = 0.3, 0.35, 0.4, 0.45, and 0.5, number of cables- 40, 80, 120, and 160

Side span to main span ratio	Number of cables	Deflection at centre of span of the girder (m)				
		Cable Sag+ P-delta+ Large Displacement	Only Cable Sag	% difference between 1 &2	Cable Sag+ P-delta	% difference between 1 & 4
		1	2	3	4	5
0.3	Radial pattern					
	40	-0.516247	-0.510423	-1.13	-0.51444	-0.35
	80	-0.553697	-0.546976	-1.21	-0.55162	-0.38
	120	-0.567438	-0.560362	-1.25	-0.56525	-0.39
	160	-0.57456	-0.567307	-1.26	-0.57232	-0.39
	Harp pattern					
	40	-0.681093	-0.665024	-2.36	-0.67562	-0.80
	80	-0.732742	-0.714532	-2.49	-0.72663	-0.83
	120	-0.751498	-0.73249	-2.53	-0.74516	-0.84
	160	-0.76119	-0.741765	-2.55	-0.75473	-0.85
	Fan pattern					
	40	-0.527169	-0.52093	-1.18	-0.52523	-0.37
	80	-0.581941	-0.573953	-1.37	-0.57944	-0.43
	120	-0.616888	-0.607369	-1.54	-0.61389	-0.49
	160	-0.648294	-0.637085	-1.73	-0.64471	-0.55
0.35	Radial pattern					
	40	-0.402512	-0.398736	-0.94	-0.40143	-0.27
	80	-0.431235	-0.426867	-1.01	-0.42999	-0.29
	120	-0.441775	-0.437182	-1.04	-0.44047	-0.30
	160	-0.447238	-0.442529	-1.05	-0.44590	-0.30
	Harp pattern					
	40	-0.53172	-0.521398	-1.94	-0.52855	-0.60
	80	-0.572326	-0.560531	-2.06	-0.56875	-0.62
	120	-0.58711	-0.574782	-2.10	-0.58339	-0.63
	160	-0.594759	-0.582128	-2.12	-0.59096	-0.64
	Fan pattern					
	40	-0.411153	-0.407112	-0.98	-0.40999	-0.28
	80	-0.453567	-0.448388	-1.14	-0.45208	-0.33
	120	-0.480872	-0.474685	-1.29	-0.47908	-0.37
	160	-0.505502	-0.498207	-1.44	-0.50337	-0.42
0.4	Radial pattern					
	40	-0.312806	-0.310379	-0.78	-0.31217	-0.20
	80	-0.334415	-0.331612	-0.84	-0.33369	-0.22

	120	-0.342373	-0.339422	-0.86	-0.34161	-0.22
	160	-0.346494	-0.343468	-0.87	-0.34572	-0.22
	Harp pattern					
	40	-0.411603	-0.405242	-1.55	-0.4099	-0.41
	80	-0.442942	-0.4356	-1.66	-0.44099	-0.44
	120	-0.454382	-0.446676	-1.70	-0.45234	-0.45
	160	-0.460306	-0.452409	-1.72	-0.45821	-0.46
	Fan pattern					
	40	-0.319607	-0.317014	-0.81	-0.31893	-0.21
	80	-0.351761	-0.348452	-0.94	-0.35091	-0.24
	120	-0.372499	-0.368561	-1.06	-0.37148	-0.27
	160	-0.391224	-0.386597	-1.18	-0.39002	-0.31
0.45	Radial pattern					
	40	-0.230835	-0.229384	-0.63	-0.23051	-0.14
	80	-0.24631	-0.244644	-0.68	-0.24594	-0.15
	120	-0.252015	-0.250262	-0.70	-0.25163	-0.15
	160	-0.254978	-0.253179	-0.71	-0.25458	-0.15
	Harp pattern					
	40	-0.308533	-0.304979	-1.15	-0.30770	-0.27
	80	-0.331617	-0.327476	-1.25	-0.33066	-0.29
	120	-0.34009	-0.335721	-1.28	-0.33908	-0.30
	160	-0.344483	-0.339996	-1.30	-0.34347	-0.30
	Fan pattern					
	40	-0.241756	-0.240192	-0.65	-0.24140	-0.15
	80	-0.26498	-0.262997	-0.75	-0.26453	-0.17
	120	-0.279871	-0.277538	-0.83	-0.27935	-0.19
	160	-0.293277	-0.290566	-0.92	-0.29267	-0.21
0.5	Radial pattern					
	40	-0.176238	-0.175388	-0.48	-0.17607	-0.10
	80	-0.186781	-0.185803	-0.52	-0.18659	-0.10
	120	-0.19068	-0.189652	-0.54	-0.19048	-0.10
	160	-0.192707	-0.191653	-0.55	-0.19250	-0.11
	Harp pattern					
	40	-0.226562	-0.224769	-0.79	-0.22616	-0.18
	80	-0.242928	-0.240838	-0.86	-0.24248	-0.19
	120	-0.248971	-0.246756	-0.89	-0.24850	-0.19
	160	-0.252113	-0.249832	-0.90	-0.25164	-0.19
	Fan pattern					
	40	-0.180197	-0.179289	-0.50	-0.18001	-0.10
	80	-0.196194	-0.19507	-0.57	-0.19597	-0.11
	120	-0.206324	-0.205029	-0.63	-0.20607	-0.12
	160	-0.215372	-0.2139	-0.68	-0.21508	-0.14

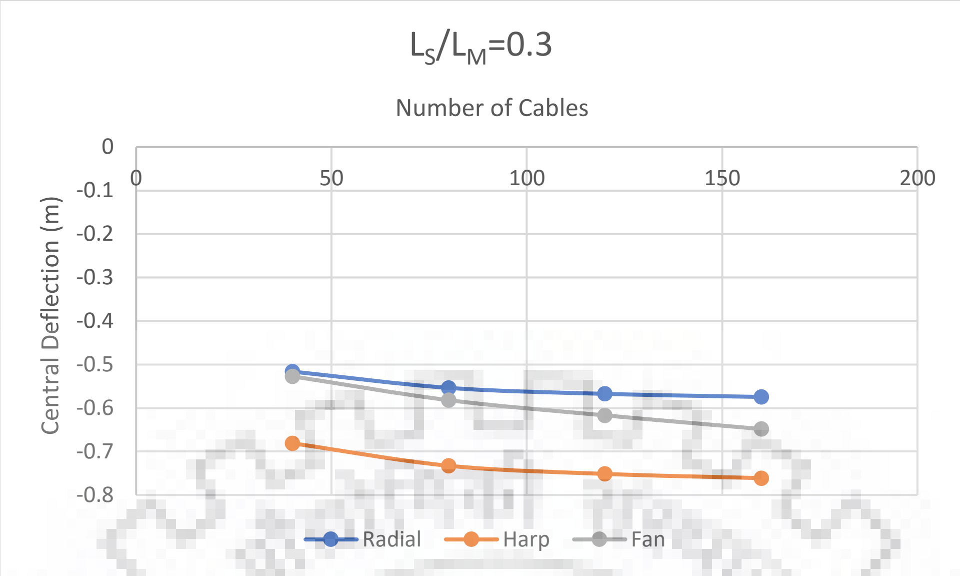

L_S/L_M=0.3
Number of Cables
Central Deflection (m)
0
-0.1
-0.2
-0.3
-0.4
-0.5
-0.6
-0.7
-0.8
0
50
100
150
200
Radial
Harp
Fan

(a)

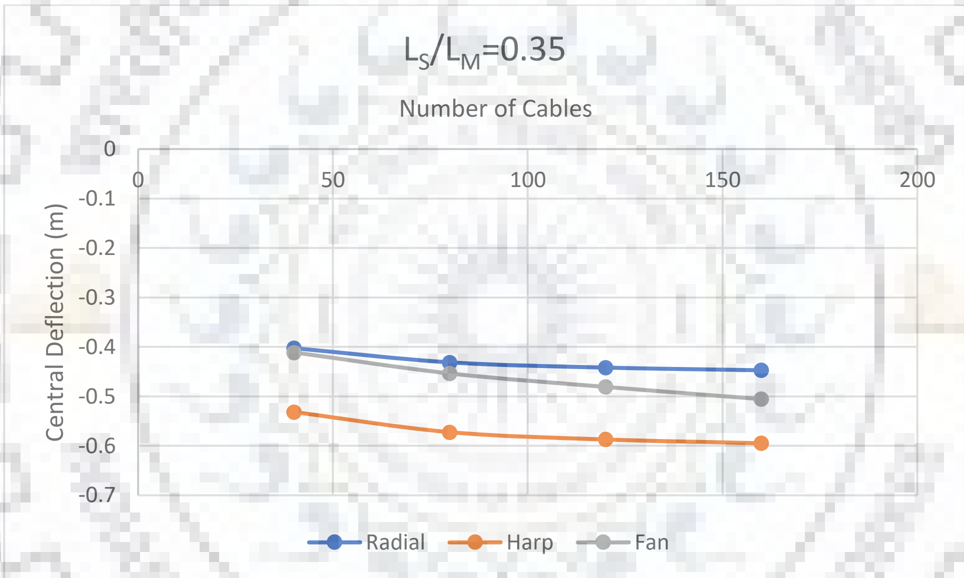

L_S/L_M=0.35
Number of Cables
Central Deflection (m)
0
-0.1
-0.2
-0.3
-0.4
-0.5
-0.6
-0.7
0
50
100
150
200
Radial
Harp
Fan

(b)

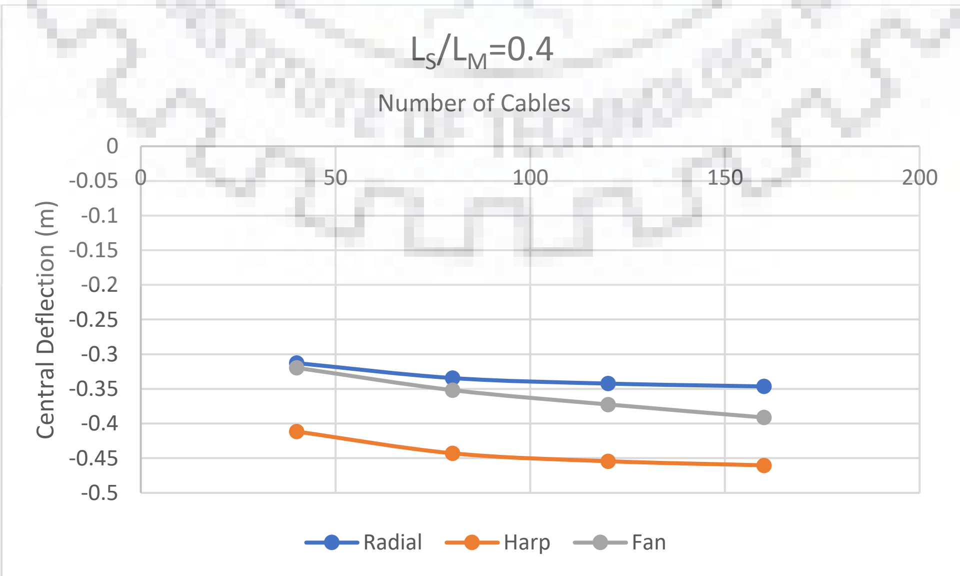

L_S/L_M=0.4
Number of Cables
Central Deflection (m)
0
-0.05
-0.1
-0.15
-0.2
-0.25
-0.3
-0.35
-0.4
-0.45
-0.5
0
50
100
150
200
Radial
Harp
Fan

(c)

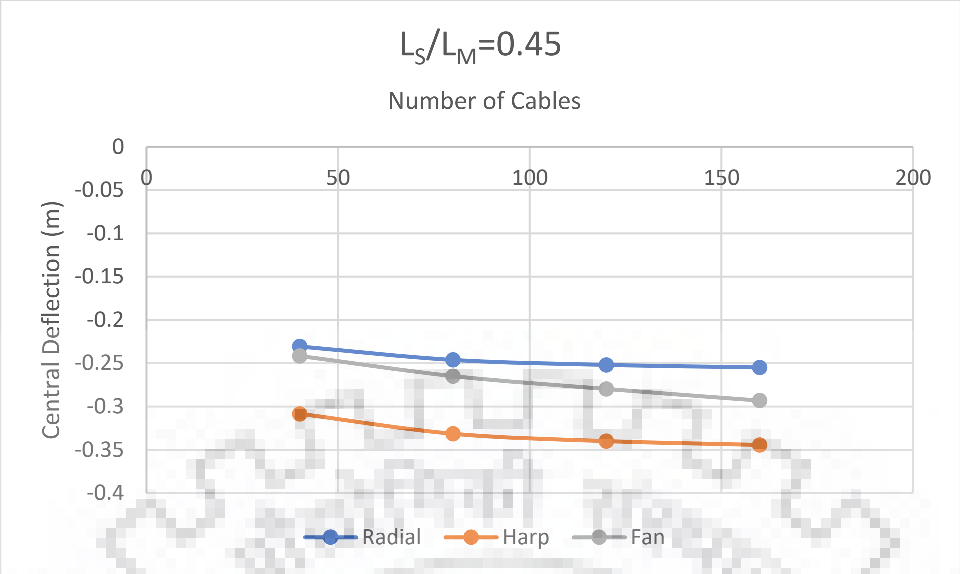

(d)

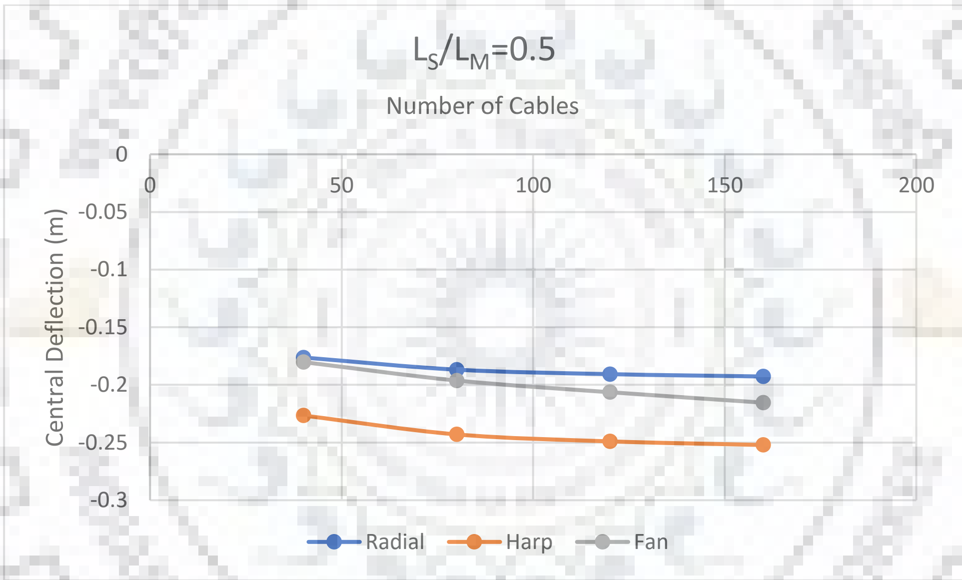

(e)

Figure 3.30: Graph showing variation of deflection at centre of span of the girder with number of cables for radial, harp, and fan arrangements of the bridge for side span to main span ratios of (a) 0.3, (b) 0.35, (c) 0.4, (d) 0.45, (e) 0.5

The central deflections for harp configurations are on an average 31.56% greater than in radial configurations.

The error by ignoring beam-column and large displacement nonlinearities lies within 3%. And the error by ignoring only large displacement nonlinearity lies within 1%.

3.4.5 Variation of Maximum Compression in Deck

Table 3.36: Maximum compression in deck for radial, harp, and fan configurations, L_S/L_M = 0.3, 0.35, 0.4, 0.45, and 0.5, number of cables- 40, 80, 120, and 160

Side span to main span ratio	Number of cables	Maximum Compression in Deck (kN)				
		Cable Sag+ P-delta+ Large Displacement	Only Cable Sag	% difference between 1 &2	Cable Sag+ P-delta	% difference between 1 & 4
		1	2	3	4	5
0.3	Radial pattern					
	40	7351.235	7308.469	-0.58	7353.1	0.03
	80	7319.53	7273.914	-0.62	7321.732	0.03
	120	7308.945	7261.972	-0.64	7311.182	0.03
	160	7303.621	7256.208	-0.65	7305.977	0.03
	Harp pattern					
	40	11998.663	11926.836	-0.60	12053.77	0.46
	80	12053.277	11986.679	-0.55	12120.96	0.56
	120	12066.264	12001.77	-0.53	12138.61	0.60
	160	12071.856	12008.489	-0.52	12146.7	0.62
	Fan pattern					
	40	7712.215	7679.996	-0.42	7715.134	0.04
	80	8124.94	8084.708	-0.50	8128.491	0.04
	120	8608.388	8560.581	-0.56	8613.901	0.06
	160	9147.606	9091.414	-0.61	9155.992	0.09
0.35	Radial pattern					
	40	6462.125	6432.305	-0.46	6463.218	0.02
	80	6431.532	6399.8	-0.49	6432.844	0.02
	120	6421.09	6388.52	-0.51	6422.388	0.02
	160	6415.678	6382.787	-0.51	6417.033	0.02
	Harp pattern					
	40	10630.792	10580.242	-0.48	10664.64	0.32
	80	10676.925	10629.356	-0.45	10718.73	0.39
	120	10687.513	10641.272	-0.43	10732.47	0.42
	160	10691.75	10646.35	-0.42	10738.60	0.44
	Fan pattern					
	40	6779.664	6757.9	-0.32	6781.865	0.03
	80	7135.461	7108.386	-0.38	7138.088	0.04
	120	7557.13	7524.776	-0.43	7560.999	0.05
	160	8034.253	7995.709	-0.48	8039.414	0.06
0.4	Radial pattern					

	40	5749.32	5728.216	-0.37	5749.981	0.01
	80	5719.637	5697.388	-0.39	5720.47	0.01
	120	5710.011	5687.141	-0.40	5710.734	0.01
	160	5704.769	5681.66	-0.41	5705.513	0.01
	Harp pattern					
	40	9532.061	9495.368	-0.38	9551.4	0.20
	80	9571.69	9536.004	-0.37	9595.336	0.25
	120	9580.256	9545.17	-0.37	9605.714	0.27
	160	9583.752	9548.973	-0.36	9610.163	0.28
	Fan pattern					
	40	6027.925	6012.795	-0.25	6029.415	0.02
	80	6334.569	6316.137	-0.29	6336.488	0.03
	120	6702.923	6680.963	-0.33	6705.551	0.04
	160	7126.81	7100.572	-0.37	7130.14	0.05
0.45	Radial pattern					
	40	5173.669	5159.287	-0.28	5174.035	0.01
	80	5146.181	5131.076	-0.29	5146.607	0.01
	120	5137.023	5121.692	-0.30	5137.537	0.01
	160	5132.41	5116.83	-0.30	5132.843	0.01
	Harp pattern					
	40	8590.871	8563.727	-0.32	8599.387	0.10
	80	8624.204	8597.312	-0.31	8634.967	0.12
	120	8631.05	8604.219	-0.31	8642.614	0.13
	160	8633.676	8606.912	-0.31	8646.02	0.14
	Fan pattern					
	40	5376.329	5366.033	-0.19	5377.295	0.02
	80	5641.007	5628.535	-0.22	5642.119	0.02
	120	5961.939	5947.121	-0.25	5963.266	0.02
	160	6336.796	6319.394	-0.27	6338.597	0.03
0.5	Radial pattern					
	40	4641.636	4632.064	-0.21	4641.815	0.00
	80	4619.674	4609.496	-0.22	4619.812	0.00
	120	4611.743	4601.337	-0.23	4611.872	0.00
	160	4607.671	4597.143	-0.23	4607.782	0.00
	Harp pattern					
	40	7842.07	7822.028	-0.26	7844.975	0.04
	80	7870.821	7850.669	-0.26	7874.54	0.05
	120	7876.16	7855.876	-0.26	7880.195	0.05
	160	7878.077	7857.726	-0.26	7882.362	0.05
	Fan pattern					
	40	4853.987	4846.951	-0.14	4854.582	0.01
	80	5083.258	5074.959	-0.16	5083.908	0.01
	120	5364.636	5354.876	-0.18	5365.309	0.01
	160	5698.437	5687.111	-0.20	5699.251	0.01

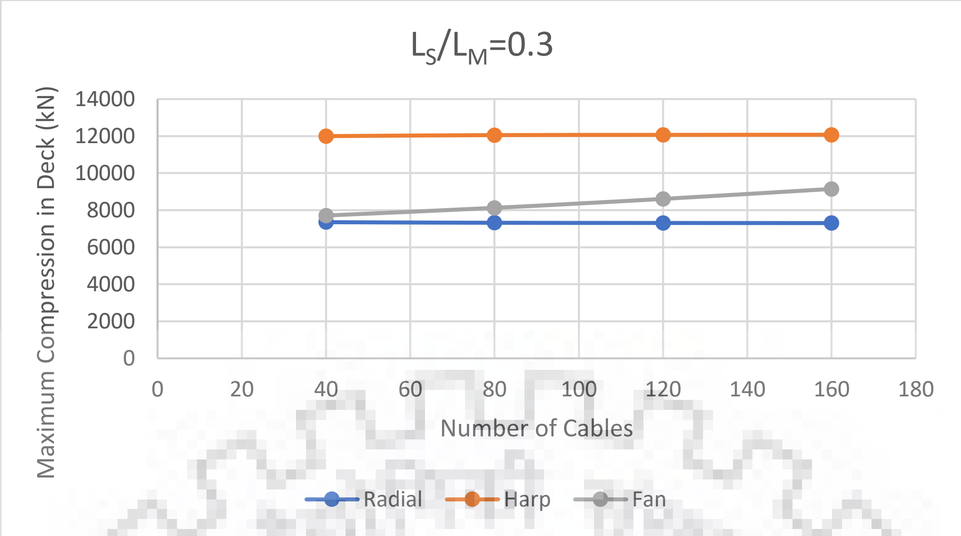
L_S/L_M=0.3
Maximum Compression in Deck (kN)
14000
12000
10000
8000
6000
4000
2000
0
0
20
40
60
80
100
120
140
160
180
Number of Cables
Radial
Harp
Fan

(a)

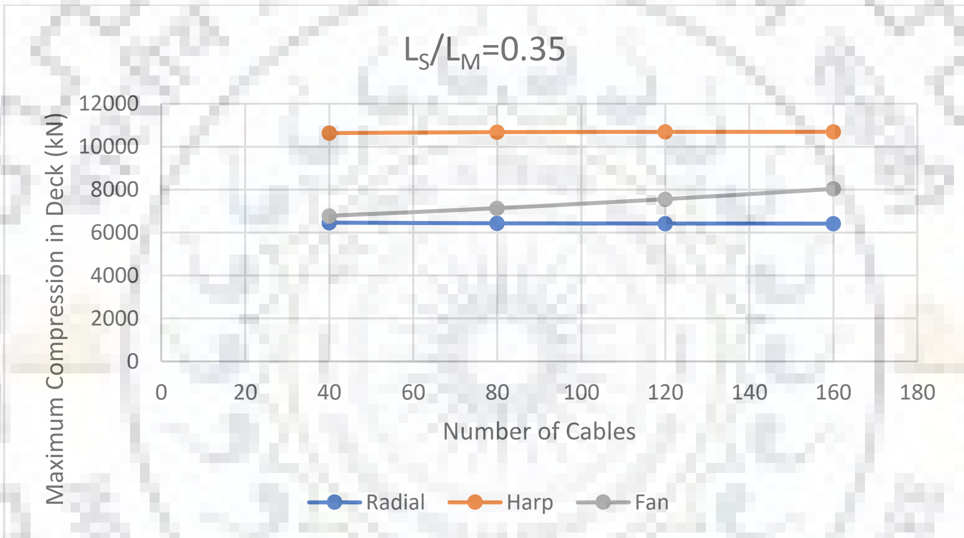
L_S/L_M=0.35
Maximum Compression in Deck (kN)
12000
10000
8000
6000
4000
2000
0
0
20
40
60
80
100
120
140
160
180
Number of Cables
Radial
Harp
Fan

(b)

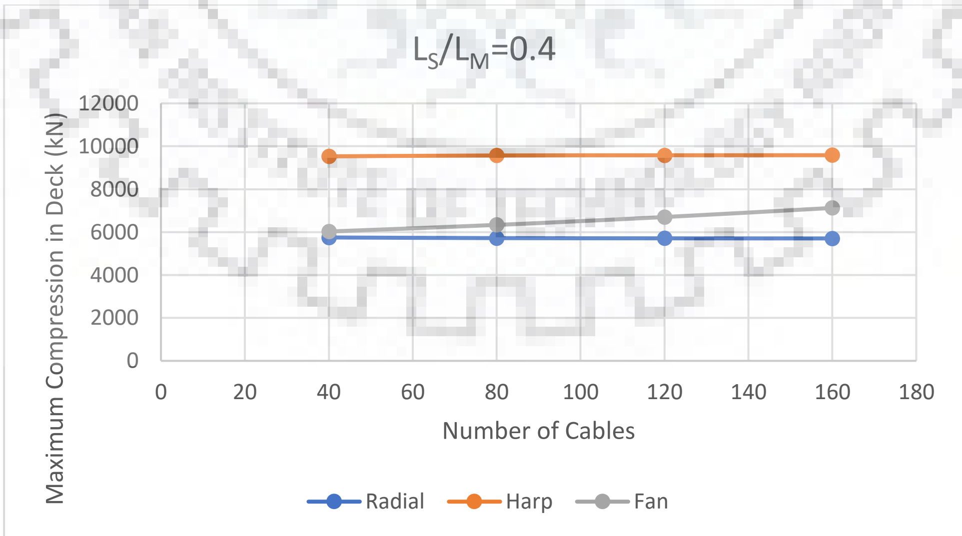
L_S/L_M=0.4
Maximum Compression in Deck (kN)
12000
10000
8000
6000
4000
2000
0
0
20
40
60
80
100
120
140
160
180
Number of Cables
Radial
Harp
Fan

(c)

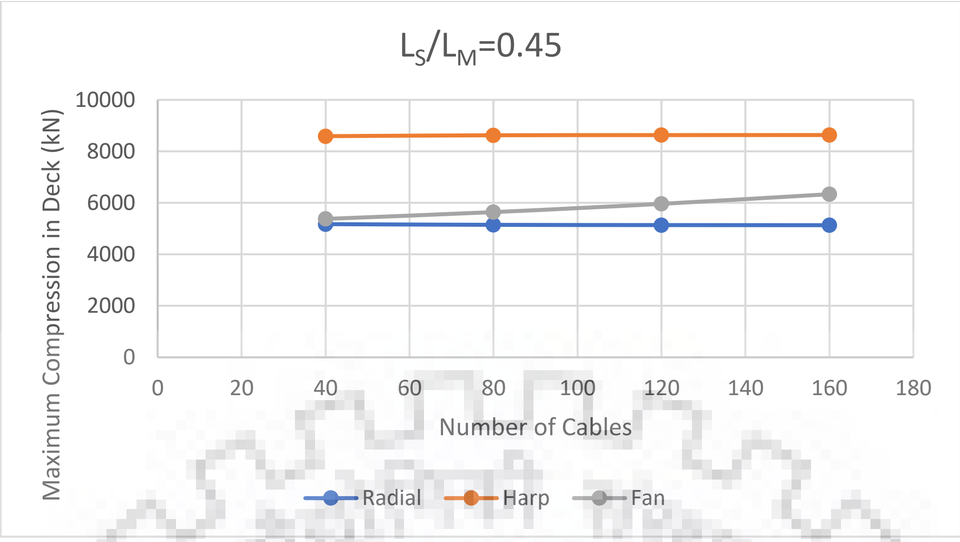

(d)

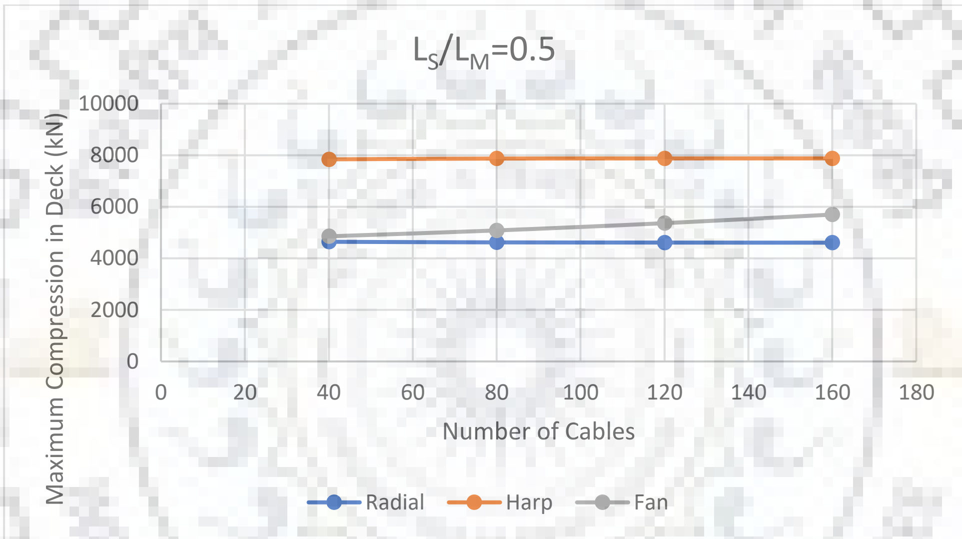

(e)

Figure 3.31: Graph showing variation of maximum compression in deck with number of cables for radial, harp, and fan arrangements of the bridge for side span to main span ratios of (a) 0.3, (b) 0.35, (c) 0.4, (d) 0.45, (e) 0.5

Maximum compression in deck is practically constant for the increase in number of cables from 40 to 160. It decreases with an increase in side span to main span ratio. For radial configuration, the value for side span to main span ratio of 0.5 is 36.89% lower than for side span to main span ratio of 0.3. For harp configuration, the corresponding value is 34.7%.

Maximum compression in deck is greater in harp configuration than in radial configuration. It is 64.58% and 70.26% greater for side span to main span ratios of 0.3 and 0.5, respectively.

The error by ignoring beam-column and large displacement nonlinearities lies within 1%. And the error by ignoring only large displacement nonlinearity lies within 0.7%.

3.4.6 Variation of Maximum Moment in Pylon

Table 3.37: Maximum moment in pylon for radial, harp, and fan configurations, L_S/L_M = 0.3, 0.35, 0.4, 0.45, and 0.5, number of cables- 40, 80, 120, and 160

Side span to main span ratio	Number of cables	Maximum Moment in Pylon (kNm)				
		Cable Sag+ P-delta+ Large Displacement	Only Cable Sag	% difference between 1 &2	Cable Sag+ P-delta	% difference between 1 & 4
		1	2	3	4	5
0.3	Radial pattern					
	40	1752.1888	1732.5742	-1.12	1747.370	-0.28
	80	1951.8909	1924.1365	-1.42	1946.45	-0.28
	120	2049.944	2011.9643	-1.85	2043.043	-0.34
	160	2097.7297	2057.4653	-1.92	2089.037	-0.41
	Harp pattern					
	40	38106.139	36748.184	-3.56	38123.76	0.05
	80	38554.960	37140.956	-3.67	38567.73	0.03
	120	38782.154	37364.382	-3.66	38798.64	0.04
	160	38888.471	37454.367	-3.69	38902.63	0.04
	Fan pattern					
	40	13484.801	13291.235	-1.44	13471.94	-0.10
	80	24701.805	24259.537	-1.79	24675.45	-0.11
	120	33397.122	32684.600	-2.13	33358.67	-0.12
	160	39189.349	38220.018	-2.47	39139.74	-0.13
0.35	Radial pattern					
	40	986.7931	980.6628	-0.62	984.9968	-0.18
	80	1082.4239	1070.37	-1.11	1078.635	-0.35
	120	1131.402	1116.7883	-1.29	1128.174	-0.29
	160	1156.8657	1142.2324	-1.26	1153.645	-0.28
	Harp pattern					
	40	27773.670	26834.545	-3.38	27785.31	0.04
	80	28307.245	27340.515	-3.42	28321.79	0.05
	120	28551.280	27558.444	-3.48	28562.91	0.04
	160	28649.640	27642.455	-3.52	28659.52	0.03
	Fan pattern					
	40	9836.4889	9696.7053	-1.42	9826.996	-0.10
	80	18109.668	17790.727	-1.76	18089.79	-0.11
	120	24509.076	24001.371	-2.07	24480.71	-0.12
	160	28768.782	28083.847	-2.38	28733.79	-0.12
0.4	Radial pattern					

	40	570.2724	564.6988	-0.98	567.8666	-0.42
	80	576.8188	572.2306	-0.80	575.9127	-0.16
	120	604.6146	598.014	-1.09	603.1406	-0.24
	160	612.793	607.0359	-0.94	611.6723	-0.18
	Harp pattern					
	40	18278.968	17672.326	-3.32	18288.61	0.05
	80	18895.393	18260.130	-3.36	18904.61	0.05
	120	19099.451	18443.845	-3.43	19106.73	0.04
	160	19185.266	18519.764	-3.47	19191.44	0.03
	Fan pattern					
	40	6516.178	6419.9325	-1.48	6509.756	-0.10
	80	12084.819	11867.295	-1.80	12071.32	-0.11
	120	16388.582	16044.757	-2.10	16368.97	-0.12
	160	19259.315	18799.497	-2.39	19235.55	-0.12
0.45	Radial pattern					
	40	301.879	297.6878	-1.39	301.096	-0.26
	80	341.4676	335.248	-1.82	339.7051	-0.52
	120	357.3665	351.9129	-1.53	356.5801	-0.22
	160	363.02	356.7623	-1.72	361.6953	-0.36
	Harp pattern					
	40	9258.8474	8941.9312	-3.42	9263.793	0.05
	80	9874.4227	9513.9349	-3.65	9876.707	0.02
	120	10035.819	9662.8786	-3.72	10036.31	0.00
	160	10135.827	9758.6675	-3.72	10139.8	0.04
	Fan pattern					
	40	3376.4697	3316.1774	-1.79	3372.332	-0.12
	80	6360.5102	6226.3284	-2.11	6351.807	-0.14
	120	8675.5429	8468.822	-2.38	8663.161	-0.14
	160	10218.083	9945.1303	-2.67	10203.40	-0.14
0.5	Radial pattern					
	40	17.6426	19.5267	10.68	18.1492	2.87
	80	11.5007	14.1192	22.77	12.0098	4.43
	120	8.7386	11.6892	33.77	9.4273	7.88
	160	7.1722	10.1585	41.64	7.8035	8.80
	Harp pattern					
	40	1697.9134	1586.1645	-6.58	1700.357	0.14
	80	2166.3977	2027.3445	-6.42	2168.077	0.08
	120	2320.6145	2179.1355	-6.10	2322.337	0.07
	160	2403.2349	2254.1022	-6.21	2405.266	0.08
	Fan pattern					
	40	663.1075	631.8573	-4.71	660.7435	-0.36
	80	1415.0836	1348.1781	-4.73	1410.280	-0.34
	120	2019.3815	1918.4562	-4.99	2012.493	-0.34
	160	2444.2027	2317.7017	-5.18	2436.352	-0.32

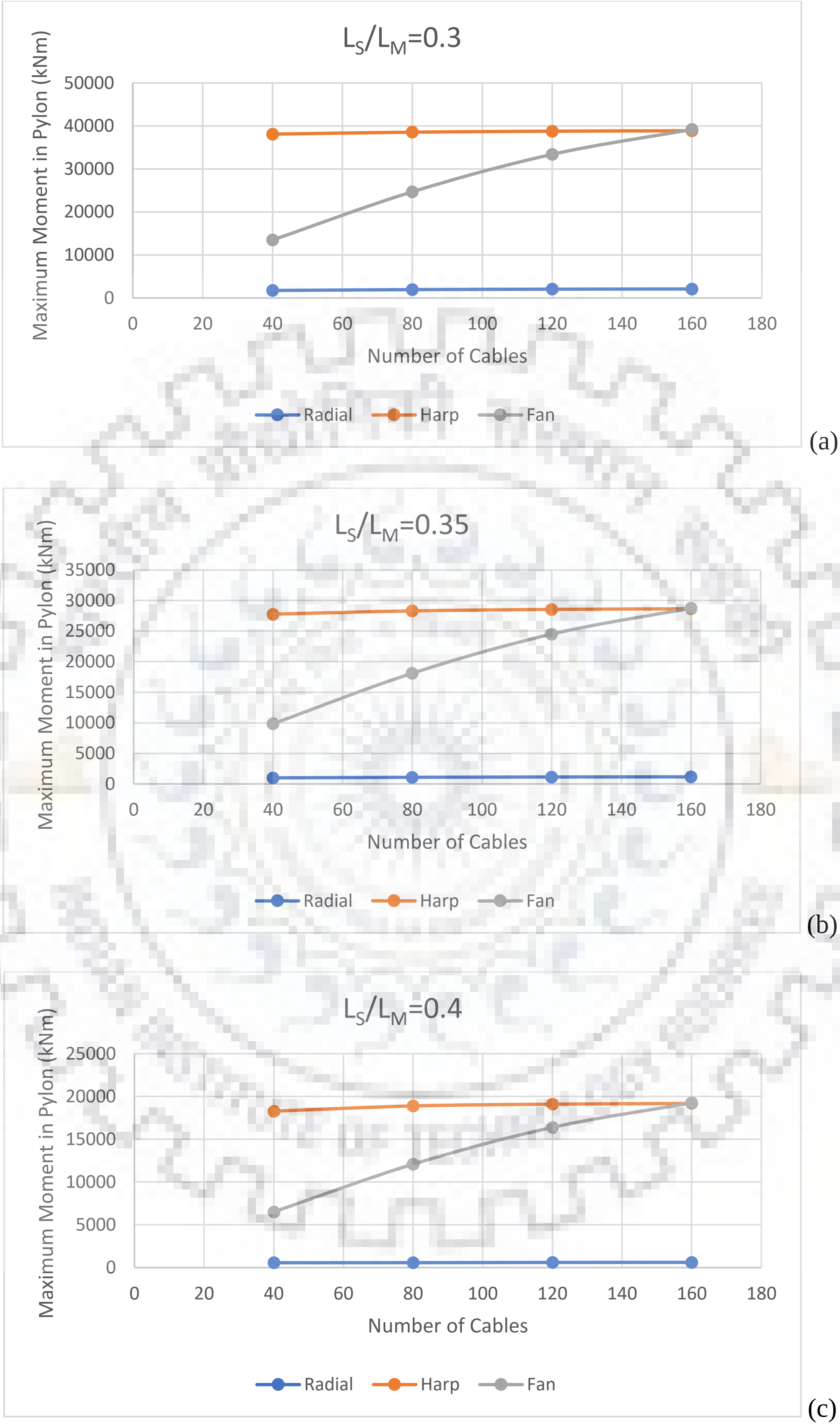

LS/LM=0.3
Maximum Moment in Pylon (kNm)
Number of Cables
Radial
Harp
Fan
(a)
LS/LM=0.35
Maximum Moment in Pylon (kNm)
Number of Cables
Radial
Harp
Fan
(b)
LS/LM=0.4
Maximum Moment in Pylon (kNm)
Number of Cables
Radial
Harp
Fan
(c)

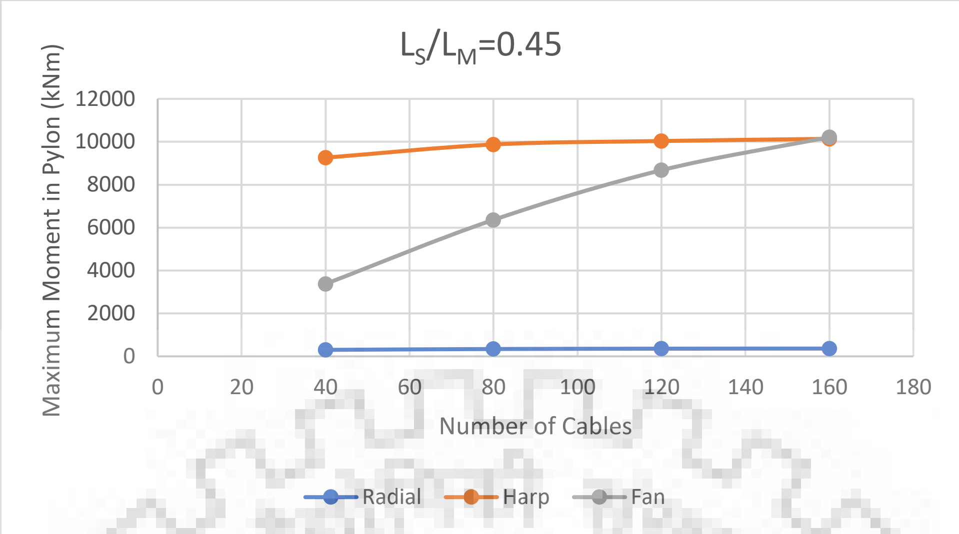

(d)

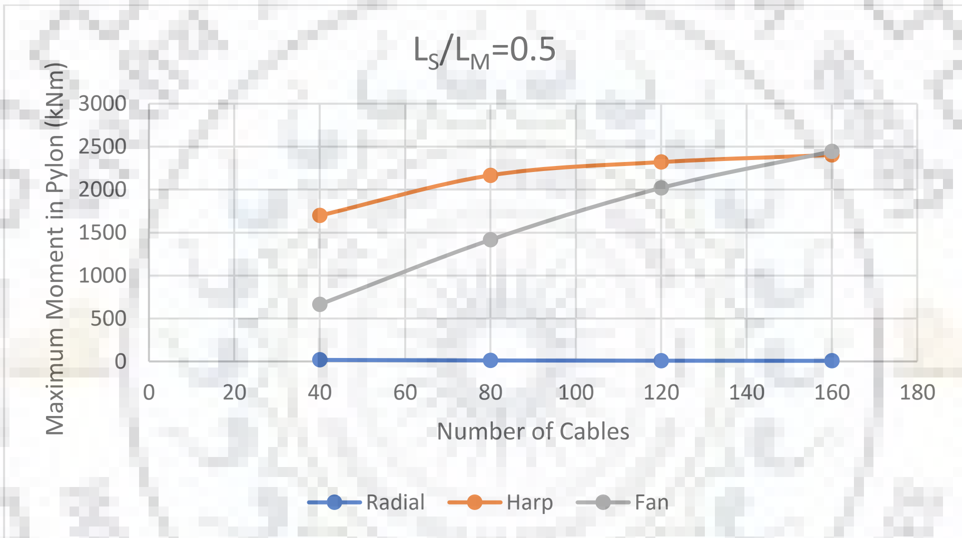

(e)

Figure 3.32: Graph showing variation of maximum moment in pylon with number of cables for radial, harp, and fan arrangements of the bridge for side span to main span ratios of (a) 0.3, (b) 0.35, (c) 0.4, (d) 0.45, (e) 0.5

In general, maximum moment in pylon increases with the increase in number of cables and decreases with the increase in side span to main span ratio. It is 21.7, 28.1, 32.1, 30.7, and 96.2 times greater in harp arrangement than in radial arrangement for side span to main span ratios of 0.3, 0.35, 0.4, 0.45, and 0.5, respectively.

The error by ignoring beam-column and large displacement nonlinearities lies within 7% for all the cases except for radial configuration and side span to main span ratio of 0.5, where the error reaches 42%. This is because of very small moments induced in this case. And the error by ignoring only large displacement nonlinearity lies within 1% for all the cases except for radial configuration and side span to main span ratio of 0.5, where the error reaches 9%.

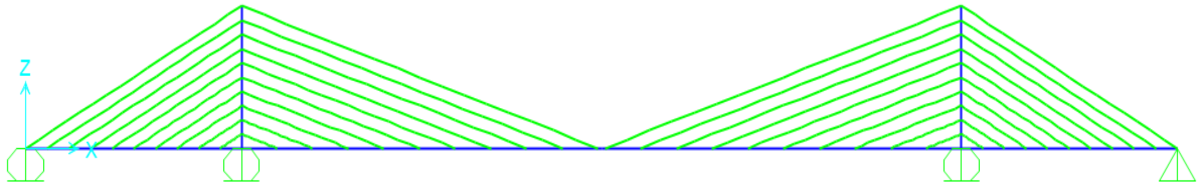

Figure 3.33: Model of harp configuration of the bridge for $L_S/L_M = 0.3$ and number of cables = 40 in SAP2000

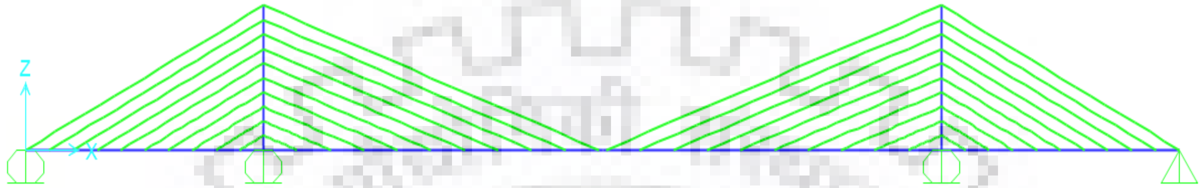

Figure 3.34: Model of harp configuration of the bridge for $L_S/L_M = 0.35$ and number of cables = 40 in SAP2000

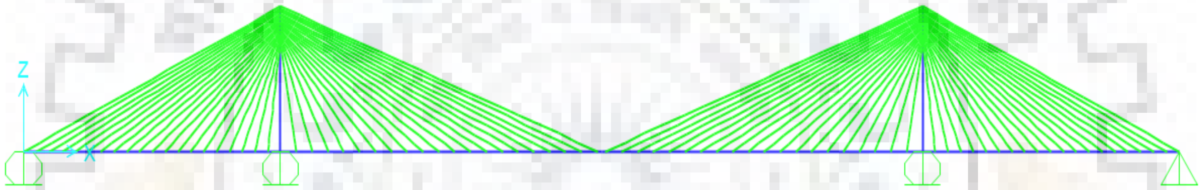

Figure 3.35: Model of fan configuration of the bridge for $L_S/L_M = 0.4$ and number of cables = 80 in SAP2000

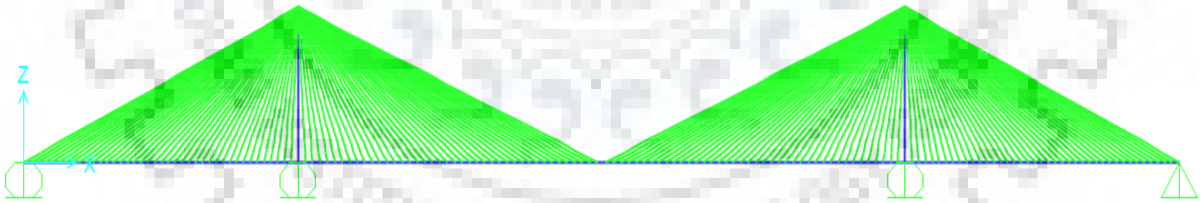

Figure 3.36: Model of radial configuration of the bridge for $L_S/L_M = 0.45$ and number of cables = 160 in SAP2000

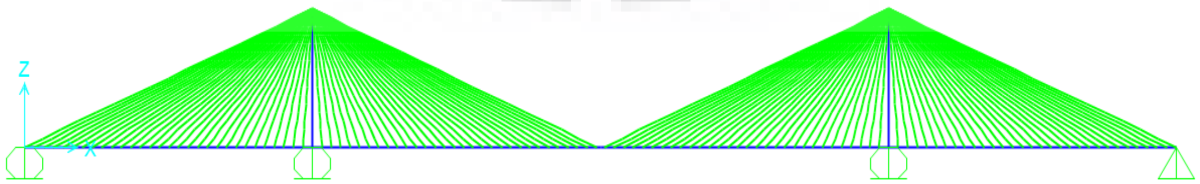

Figure 3.37: Model of radial configuration of the bridge for $L_S/L_M = 0.5$ and number of cables = 120 in SAP2000

3.5 To study the behaviour of cable-stayed bridge under various distributions of live load

The influence of various live load (20 kN/m) distribution patterns (as shown in figure 3.38) on the behaviour of cable-stayed bridge of the previous study, with side span to main span ratio of 0.5 and radial configuration has been studied to find the critical distribution of live load for forces and moments in the girder, pylon, and cables.

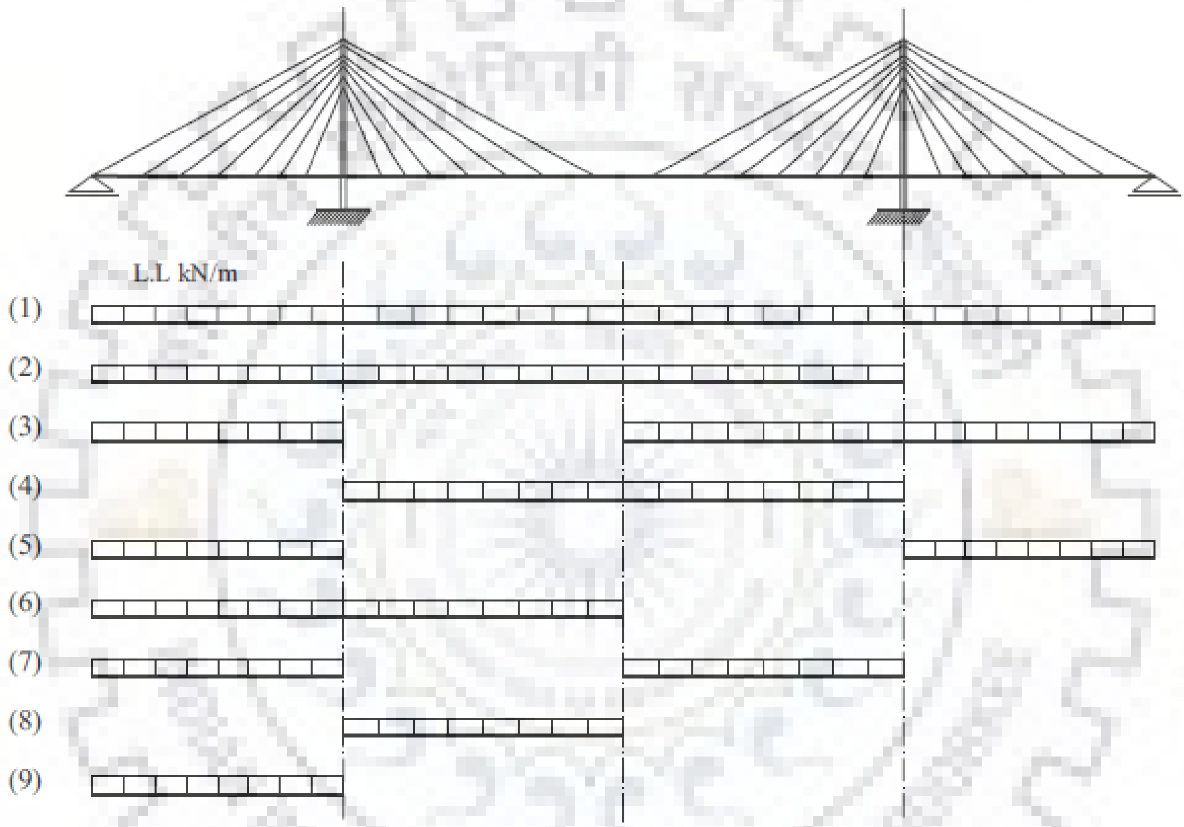

Figure 3.38: Various patterns of live load distribution (Hassan *et al.*, 2013)

Table 3.38: Maximum values of moments and forces in all the members of the bridge for different live load patterns

Number of Cables	Live load pattern	Max sagging moment	Max hogging moment	Max compression in deck	Max compression in pylon	Max moment in pylon	Max cable tension
160	1	18321.50	15964.02	4607.67	6556.70	7.17	212.89
	2	27320.35	35187.53	5342.52	7186.82	6525.58	475.52
	3	35092.61	19412.17	2745.45	4957.10	5887.69	259.65
	4	30836.08	41798.58	4758.22	6067.30	7007.81	563.27
	5	77328.42	51065.65	784.54	1846.85	12005.36	225.51

	6	14093.50	16397.31	3798.43	5855.56	390.12	188.64
	7	29343.64	22243.26	2525.78	3905.50	5772.74	303.66
	8	25867.81	28427.64	3233.58	4605.13	6064.09	385.72
	9	62374.92	34539.57	1161.71	2453.14	9483.69	241.35
120	1	17960.44	15993.57	4611.74	6555.94	8.74	282.62
	2	26935.11	34629.15	5346.49	7186.05	6478.23	622.93
	3	34943.90	19174.84	2744.35	4956.61	5861.94	341.58
	4	30367.69	41127.74	4761.34	6055.05	6952.31	737.72
	5	77237.59	51275.06	788.43	1854.81	12049.22	294.24
	6	14003.08	16408.33	3799.92	5855.36	377.73	250.89
	7	29084.52	21875.80	2526.96	3901.08	5732.06	397.62
	8	25594.41	27970.79	3236.06	4598.02	6021.35	505.23
	9	62262.90	34508.21	1165.15	2456.42	9470.57	316.55
80	1	17249.25	16060.14	4619.67	6553.15	11.50	421.16
	2	26174.53	33418.29	5354.14	7182.95	6367.64	902.37
	3	34590.67	18879.54	2740.05	4952.58	5815.58	499.60
	4	29447.59	39673.26	4767.46	6040.65	6829.64	1068.2
	5	76995.99	51827.04	798.41	1863.08	12087.93	424.59
	6	13889.07	16439.54	3802.48	5853.46	354.41	375.66
	7	28543.41	21087.14	2529.47	3892.98	5648.70	575.54
	8	25097.25	26981.27	3240.79	4590.73	5925.77	731.64
	9	61993.72	34490.16	1175.10	2463.74	9474.08	457.75
40	1	15636.96	16331.10	4641.64	6534.51	17.64	822.58
	2	23972.03	29953.83	5374.15	7159.51	6030.51	1631.2
	3	33708.57	17620.08	2730.55	4933.97	5648.31	924.03
	4	26860.40	35531.27	4784.76	5994.37	6444.25	1928.0
	5	76302.63	53419.26	830.99	1872.02	12330.57	773.37
	6	13658.15	16616.01	3806.73	5835.53	299.02	739.55
	7	27158.83	18757.04	2530.56	3855.27	5396.81	1035.4
	8	23696.47	24123.06	3253.21	4558.30	5634.44	1320.7
	9	61241.56	34334.73	1199.93	2458.41	9428.54	829.03

Maximum sagging and hogging moments in girders and maximum moment in pylon are produced for live load pattern 5, where only side spans of the bridge have been loaded and main span has been left unloaded.

Maximum compressive force in deck and pylon are produced for live load case 2, where one side span of the bridge has been left unloaded and remaining full bridge has been loaded.

Maximum cable tension is produced for live load case 4, where only the main span of the bridge has been loaded.

3.6 Parametric study to find the influence of Shape of the pylon on the behaviour of a cable-stayed bridge

The bridge validated in article 3.3.6 from Nazmy and Abdel-Ghaffar, 1990 has been taken. The properties of the model have been mentioned in article 3.3.6. The total length of the bridge is 627.888 m. A study has been carried out to find the effect of shape of pylon on the vertical deflection at the centre of span of main girder for self-weight of the bridge.

Table 3.39: Comparison of deflection at the centre of span of main girder for various shapes of pylon

Shape of the pylon	Vertical deflection at the centre of span of main girder (m)	Percentage difference from A shaped pylon
A shaped pylon	0.0773	-
H shaped pylon	0.0882	14.1
Portal type pylon	0.0760	-1.68
V shaped pylon	0.0838	8.41
Inverted Y shaped pylon	0.0884	14.36
Diamond shaped pylon	0.0796	2.98

From the table, it is evident that least deflection at centre of span occurs in the case of portal type pylon. The maximum deflection occurs in the case of Inverted Y-shaped pylon. These deflections are due to dead load only. Portal type pylon is followed by A shaped pylon, Diamond shaped pylon, V shaped pylon, H shaped pylon.

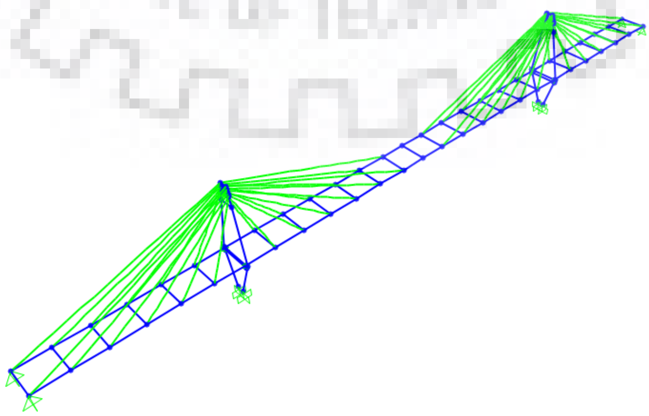

Figure 3.39: Model of the bridge with diamond shaped pylon in SAP2000

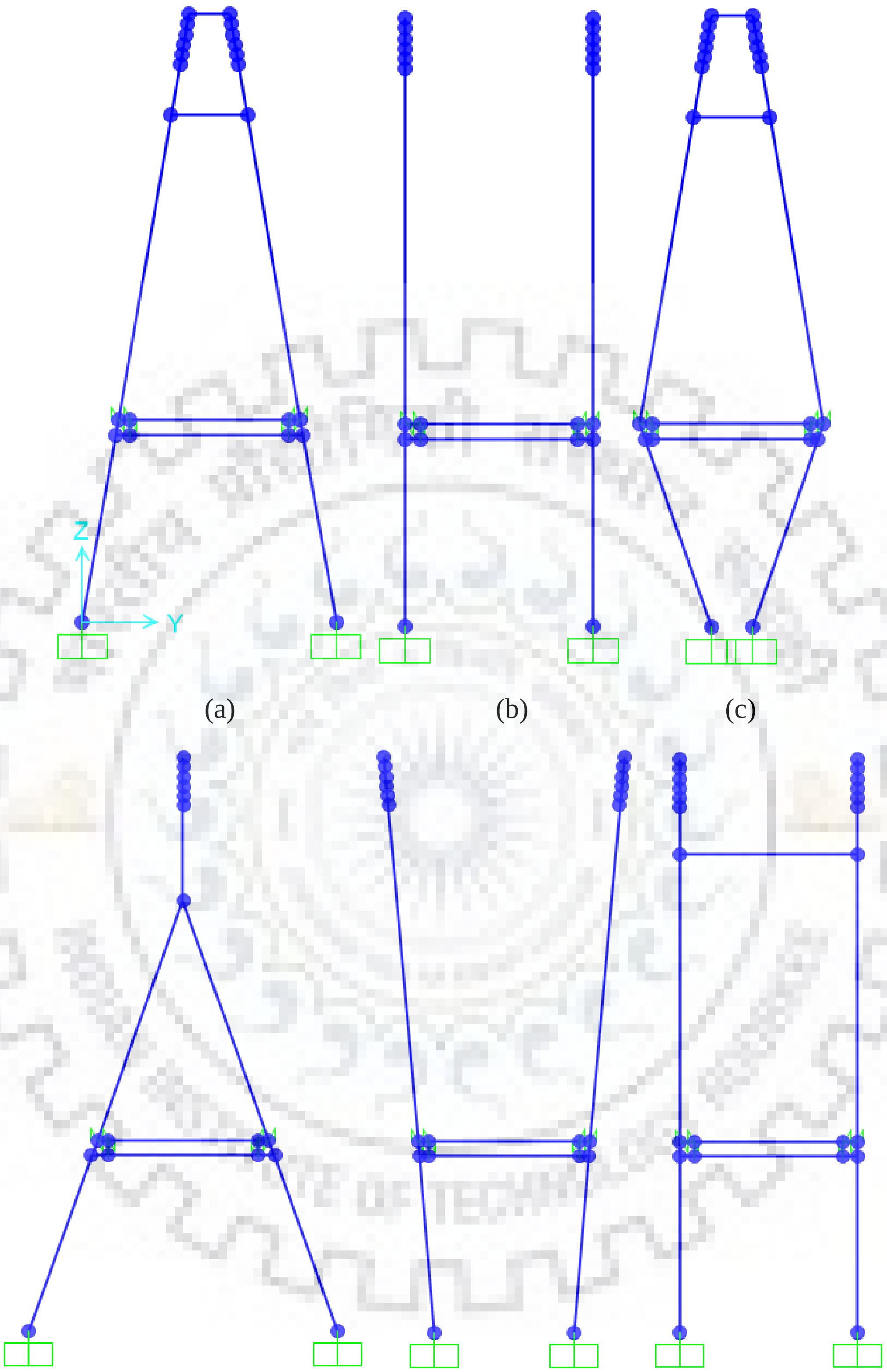

(d) (e) (f)

Figure 3.40: Various pylon shapes considered (a) A shaped pylon, (b) H shaped pylon, (c) Diamond shaped pylon, (d) Inverted Y shaped pylon, and (e) V shaped pylon (f) Portal type pylon

CHAPTER 4

SUMMARY AND CONCLUSION

- Numerical validation of cables with initial tension has been done and the results are in good agreement with the already established results.
- Parametric study to find the significance of cable sag nonlinearity of stay cables for different lengths of cable, different initial tensions, different inclination of cable with the horizontal have been carried out.
    - As the angle of inclination of cable with the horizontal increases, the effect of nonlinearity decreases.
    - With the increase in initial tension by 50%, the effect of nonlinearity decreases by about 50%.
- Numerical validation of static analysis of a cable-stayed bridge has been done.
- Numerical validation of optimisation of cable tension has been done for three different types of bridges, viz., unsymmetrical cable-stayed bridge, symmetric harp cable-stayed bridge, and symmetric radiating cable-stayed bridge.
- Numerical validation of a three-dimensional nonlinear static analysis of a cable-stayed bridge has been done for two bridges of spans- 627.888 m and 1255.776 m.
- Parametric studies have been carried out to find the influence of number of cables, side span to main span ratio, and radial, harp and fan arrangement of cables, different distributions of live load, on the behaviour of the bridge.
    - For this, 805 m long bridge with fixed length of central panel of 5 m, 80.5 m high pylon has been taken.
    - With the increase in number of cables from 40 to 160, the maximum cable tension decreases. It decreases with the increase in side span to main span ratio from 0.3 to 0.5. In general, the value of maximum cable tension is greater in harp arrangement than in radial arrangement.
    - With the increase in number of cables from 40 to 160, in general, the value of maximum sagging moment increases. It decreases with increase in side span to main span ratio from 0.3 to 0.5. The fan configuration with lesser number of cables resembles radial configuration, and as the number of cables increases, its behaviour

shifts towards harp configuration. The maximum sagging moment in radial configuration is more than in harp configuration.

- In general, maximum hogging moment increases with increase in number of cables from 40 to 160 for side span to main span ratio of 0.3 and 0.35 for harp configuration, and 0.3, 0.35, and 0.4 for radial configuration. And for other side span to main span ratios, there is little variation of maximum hogging moment. It decreases with increase in side span to main span ratio from 0.3 to 0.5. Maximum hogging moment in harp configuration is more than in radial configuration.
- Deflection at centre of span of the girder increases with the increase in number of cables from 40 to 160 and decreases with the increase in side span to main span ratio from 0.3 to 0.5. The deflection is more in harp configuration than in radial configuration.
- Maximum compression in deck is practically constant for all the number of cables. It decreases with an increase in side span to main span ratio. It is greater in harp configuration than in radial configuration.
- In general, maximum moment in pylon increases with the increase in number of cables from 40 to 160 and decreases with the increase in side span to main span ratio from 0.3 to 0.5. There is very small moment in pylon in radial configuration as compared to harp configuration, which is subjected to very high maximum moment.
- The influence of beam-column nonlinearity is more significant and the influence of large displacement nonlinearity is less important for the bridge considered in the study.
- Maximum moments in pylon and girder are obtained when only the side spans have been loaded and the main span has been left unloaded. Maximum compression in deck and pylon are obtained when one side span of the bridge has been left unloaded and remaining full bridge has been loaded. Maximum cable tension is produced when only the main span of the bridge has been loaded.

- Parametric study to find the influence of shape of pylon on the deflection at the centre of span of main girder has been carried out. Least deflection has been obtained in case of portal type pylon, which is followed by A-shaped pylon.

REFERENCES

AASHTO-PCI-ASBI Segmental Box Girder Standards: A New product for Grade Separations and Interchange Bridges. *PCI Journal (September-October, 1997)*

Agrawal, T.P. (1997). Cable-stayed bridges-Parametric study. *Journal of Bridge Engineering, Vol. 2, No. 2, ASCE, May, 1997*

Beer, F.P., Johnston, E.R.Jr., Mazurek, D.F., Cornwell, P.J., Self, B.P. (eleventh edition). (2016). *Vector Mechanics for Engineers: Statics and Dynamics*

Fleming, J.F. (1979). Nonlinear static analysis of cable-stayed bridges. *Computers and Structures, Vol. 10, pp 621-635, 1979*

Ghali, A., Neville, A.M., Brown, T.G. (sixth edition). (2009). *Structural Analysis: A Unified Classical and Matrix Approach.*

Gimsing, Niels J., Georgakis, Christos T. (third edition). (2012). *Cable Supported Bridges - concept and design.*

Hassan, M.M., Nassef, A.O., Damatty, A.A.El (2013). Optimal design of semi-fan cable-stayed bridges. *Can.J.Civil.Eng. 40: 285-297 (2013)*

Kim, Hong-Jung, Won, Deok Hee, Kang, Young-Jong, Kim, Seungjun (2017). Structural Stability of Cable-stayed bridges during Construction. *International Journal of Steel Structures 17(2): 443-469 (2017)*

Nazmy, Aly S., Abdel-Ghaffar, Ahmed M. (1990). Three-dimensional nonlinear static analysis of cable-stayed bridges. *Computers & Structures Vol. 34, No. 2, pp. 257-271, 1990*

Nowak, A.S., Lutomirska, M., Ibrahim, F.I. Sheikh (2010). The development of live load for long span bridges. *Bridge Structures 6 (2010) 79-79*

Pedro, J.J. Oliveira, Reis, A.J. (2010). Nonlinear analysis of composite steel-concrete cable-stayed bridges. *Engineering Structures 32 (2010) 2702-2716, Elsevier*

Podolny, Walter, Scalzi, John B. (second edition). (1986). *Construction and Design of Cable-Stayed Bridges.*

Starossek, Uwe (1996). Cable-stayed bridge concept for longer spans. *Journal of Bridge Engineering, Vol. 1, No. 3, ASCE, August, 1996*

Troitsky, M.S. (second edition). (1988). *Cable-stayed Bridges – theory and design.*

Wang, P.H., Tseng, T.C., Yang, C.G. (1993). Initial shape of cable-stayed bridges. *Computers & Structures Vol. 46, No. 6, pp. 1095-1106, 1993*

Wang, Pao-Hsii, Tang, Tzu-Yang, Zheng, Hou-Nong (2004). Analysis of cable-stayed bridges during construction by cantilever methods. *Computers & Structures Vol. 82, Issues 4-5, pp. 329-346, 2004*

Wang, Pao-Hsii, Yang, Chiung-Guei (1995). Parametric studies on cable-stayed bridges. *Computers & Structures Vol. 60, No. 2, Elsevier, pp. 243-260, 1996*